

**UCSF**

**UC San Francisco Electronic Theses and Dissertations**

**Title**

Elucidating the Nature of Viral Competition in Hepatitis C Virus Infection

**Permalink**

<https://escholarship.org/uc/item/4nz4s1pn>

**Author**

Webster, Brian Robert

**Publication Date**

2013

Peer reviewed|Thesis/dissertation

Elucidating the Nature of Viral Competition in Hepatitis C Virus  
Infection

by

Brian Webster

DISSERTATION

Submitted in partial satisfaction of the requirements for the degree of

DOCTOR OF PHILOSOPHY

in

Biomedical Sciences

in the

GRADUATE DIVISION

of the

UNIVERSITY OF CALIFORNIA, SAN FRANCISCO

**COPYRIGHT**

**Copyright 2013**

**by**

**Brian Webster**

## ABSTRACT

Hepatitis C virus (HCV) is a major public health threat, chronically infecting approximately 180 million people worldwide and leading to liver diseases such as cirrhosis and hepatocellular carcinoma. To date, efforts to generate a prophylactic or therapeutic vaccine have been unsuccessful. The failure of vaccine candidates, as well as the rapid emergence of drug-resistant variants, is almost entirely due to the hypervariable nature of HCV. Interestingly, while HCV is highly variable, recombination events between HCV strains are rare. This lack of recombination suggests that immune escape and drug resistance mutations are rarely transferred between strains, providing clear implications for treatment paradigms in patients infected with multiple HCV strains.

When HCV infects a host cell, that cell becomes resistant to further infection by HCV but not other viruses, such as dengue virus. This resistance, termed superinfection exclusion, acts to limit the co-occupancy of cells with multiple viral genomes, and thus prevents recombination. However, the mechanism of this block is poorly understood.

In this thesis I focus on further understanding why these recombination events are so rarely observed, through detailed investigations of the phenomena of superinfection exclusion and intracellular competition between HCV genomes during cell division. To further characterize HCV superinfection exclusion, we created a class of novel reporter HCV strains selected for their ability to infect cells already replicating HCV RNA. Importantly, the evolution of the ability to “superinfect” cells caused these viral strains to become more infectious generally, and led these

viruses to expel the HCV RNA already present in the host cells. We further identified key changes in the HCV genome that allowed the virus to overcome the superinfection block.

In addition to our work on superinfection exclusion, we identified a novel means of intracellular competition between HCV genomes co-occupying a host cell that occurs at, or shortly following, mitosis. In the setting of cellular division, we found that when two viral genomes of equivalent fitness are present within a cell, they have an equal opportunity to exclude the other. In a population of dividing cells, the competition between viral genomes proceeds apace, randomly clearing one or the other genome from cells in the span of 9–12 days. In addition to superinfection exclusion, this intracellular competition due to mitosis is likely to further limit HCV's genetic diversity and ability to recombine *in vivo*.

In sum, this thesis demonstrates that viral competition in HCV infection occurs on many more levels than was previously appreciated. This competition acts to prevent coinfection of host cells and likely explains the lack of natural recombination in HCV biology. Further, these findings shed additional light on basic aspects of HCV replication and hopefully lead in the future to novel therapies for this critical disease.

## ACKNOWLEDGMENTS

I owe a great deal of gratitude to many people in the seven-year road to this dissertation. First, I would like to thank my mentor and principal investigator, Warner. Through all my bouncing from project to project, from APOBEC to the “über-virus,” he has consistently been supportive and guided me. The freedom to explore has always been what makes science fun for me, and Warner has allowed me to do that. More than that, the reader of this thesis owes him a debt of thanks. If this thesis is comprehensible, it is thanks to his help over the years in untangling my thoughts about science in a way that makes sense on paper.

I also met a number of wonderful colleagues in Warner’s lab. Silke got me started back in the days of stem cells, and I owe her so much. I’m always going to miss that smile when I’d run up to talk about a new result or a new “color” that I was into that day. Everyone helped in some way, but Debbie, Kate, Steffi, and Brianna kept me laughing in the lab whenever things started to look a little dark.

The Gladstone Institutes and UCSF were an amazing place for my graduate studies. Eva Herker taught me what Hepatitis C actually is, and this thesis would not be possible without her; I also consider her a good friend. Melanie Ott and the rest of the HCV team, Holly, Renu, Gregory, and Dorothee, were also such key parts of my studies with the “black sheep” virus of GIVI. I would also like to thank Raul Andino and Jim McKerrow for agreeing to join my thesis committee and participate in my upcoming defense. In the early stages of my graduate career, Todd Margolis and Joanne Engel were excellent research and teaching mentors, as was the late Ben

Yen, may he rest in peace. I would also like to thank the faculty at UCSF for the enlightening classes, and my classmates in the BMS program who were great friends and colleagues. Last but certainly not least, the staff members of the BMS program, Monique and Lisa, who kept so many things running smoothly over the years.

On a personal level, there are a few people that I have met here in graduate school that I consider family more than friends, and kept me going in San Francisco. Shan and Matt, I'm so glad I could introduce you; it was so much fun living under the same roof as you two. Isa, you're the sister I never had, and you're right. Life will be considerably more boring without you around. I'd also like to thank some friends from California and beyond, Jacob, Jeff, Liz, Ray, Kristine, and Nita; I'm so glad you learned not to ask "When are you graduating?".

Lastly, I am so grateful for the love, patience, and support of my family. To my parents and my brother, none of this would have been possible without you.

## TABLE OF CONTENTS

|   |             |
|---|-------------|
| <b>TITLE PAGE</b> .....   | <b>i</b>    |
| <b>COPYRIGHT</b> .....  | <b>ii</b>   |
| <b>ABSTRACT</b> .....   | <b>iii</b>  |
| <b>ACKNOWLEDGMENTS</b> .....  | <b>v</b>    |
| <b>TABLE OF CONTENTS</b> .....  | <b>vii</b>  |
| <b>LIST OF TABLES</b> .....   | <b>xi</b>   |
| <b>LIST OF FIGURES</b> .....  | <b>xiii</b> |
| <b>ABBREVIATIONS</b> .....  | <b>xvi</b>  |
| <b>CHAPTER 1 INTRODUCTION</b> .....   | <b>1</b>    |
| Hepatitis C virus: epidemiology and treatment .....   | 2           |
| The Hepatitis C virus life cycle .....  | 5           |
| HCV model systems .....   | 10          |
| Mixed infections and recombination between HCV strains.....                                   | 11          |
| Scope of thesis .....   | 13          |
| <b>CHAPTER 2 ISOLATION AND CHARACTERIZATION OF A SUPERINFECTIOUS STRAIN OF HCV</b> .....      | <b>15</b>   |
| ABSTRACT .....  | 16          |
| INTRODUCTION .....  | 17          |
| RESULTS .....   | 19          |
| <i>Viral genomes with reporter proteins between NS5A and NS5B are highly infectious</i> ..... | 19          |
| <i>Cleaved NS5AB reporter gene localizes to the replication complex</i> .....                 | 23          |



|   |           |
|---|-----------|
| <i>Emergence of a superinfectious variant of HCV correlates with the exclusion of the primary replicon.....</i>             | 27        |
| <i>Sequence analysis of the superinfectious Jc1 strain reveals adaptive mutations and deletions .....</i>                   | 31        |
| <i>Viral adaptive mutations increase HCV superinfectivity .....</i>   | 35        |
| <i>Adaptive mutations promote superinfectivity in a non-reporter Jc1 strain .....</i>                                       | 39        |
| <i>HCV strains with a poly-U/UC deletion and the NS5A C2274R mutation overcome the post-entry superinfection block.....</i> | 41        |
| <i>Translation of superinfectious viral RNA is unaffected by poly-U/UC length or the NS5A C2274R mutation.....</i>          | 47        |
| DISCUSSION .....  | 51        |
| MATERIALS AND METHODS.....  | 57        |
| ACKNOWLEDGMENTS .....   | 67        |
| <b>CHAPTER 3 RAPID INTRACELLULAR COMPETITION BETWEEN HCV GENOMES AS A RESULT OF MITOSIS.....</b>                            | <b>68</b> |
| ABSTRACT .....  | 69        |
| INTRODUCTION.....   | 70        |
| RESULTS.....  | 71        |
| <i>Replication competence of the replicons used in the study.....</i>   | 71        |
| <i>More than one genomic strain is unstable in HCV replicon-containing cells. 75</i>  |           |
| <i>Dual-replicon cells do not exhibit higher rates of cell death.....</i>   | 80        |
| <i>Isolated dual- and single-replicon cells exhibit no difference in proliferation as assessed by CFSE dilution. ....</i>   | 83        |

|  |            |
|--|------------|
| <i>Mitosis is a key event promoting the decay of dual-replicon cells.</i> .....  | 84         |
| <i>Dual- and single-replicon cells are equally competent for proliferation.</i> .....  | 88         |
| <i>Dual-replicon cell transition through mitosis is associated with enrichment in single-replicon cells.</i> .....                     | 89         |
| <i>Mitosis is associated with a loss of fluorescence from one of the NS5A fluorophore-tagged genomes in dual-replicon cells.</i> ..... | 93         |
| <i>Decay of dual-replicon cells is biased toward the more-fit replicon.</i> .....  | 96         |
| <i>Transition of dual-replicon cells leads to explicit loss of viral genomes.</i> .....  | 101        |
| DISCUSSION .....   | 105        |
| MATERIALS AND METHODS.....   | 113        |
| ACKNOWLEDGMENTS .....  | 120        |
| <b>CHAPTER 4 CONCLUSIONS</b> .....   | <b>121</b> |
| Summary .....  | 122        |
| Significance .....   | 123        |
| <b>REFERENCES AND SUPPLEMENTAL MATERIAL</b> .....  | <b>125</b> |
| Appendix A. Supplemental Material to Chapter 2.....  | 126        |
| Appendix B. Supplemental Material to Chapter 3.....  | 139        |
| <i>Triple-replicon cells contribute to the pool of dual- and single-replicon cells over time.</i> .....                                | 142        |
| <i>Live cell counts in isolated populations of Jc1/<math>\Delta^{XFP-BSD}</math>-replicon-containing cells.</i> .....                  | 157        |
| Appendix C. References.....  | 162        |
| Appendix D. Publishing Release .....   | 171        |



## LIST OF TABLES

|   |     |
|---|-----|
| Table 2.1: Sequence analysis of point mutations in round 1 and round 9 supernatant passages of superinfectious virus. ....  | 33  |
| Table 2.2: Sequence analysis of deletions in round 1 and round 9 supernatant passages of superinfectious virus. ....  | 34  |
| <hr/>   |     |
| Supplemental Table A.1: Primers used to amplify fragments of the superinfectious virus in Rounds 1 & 9. ....  | 134 |
| Supplemental Table A.2: Primer sequences and templates used in plasmid and T7 template construction. ....   | 137 |
| Supplemental Table A.3: Primer sequences and restriction sites used in site-directed mutagenesis of pBR322 Jc1/ <sup>NS5AB-mKO2-Bsd</sup> plasmid DNA. ....             | 138 |
| Supplemental Table B.1. Statistical significance of the differences in the proportions of replicon-positive cells in dual-replicon decay experiments <sup>a</sup> ..... | 139 |
| Supplemental Table B.2. Statistical significance of differences in apoptosis rates of dual-, single-, or replicon-negative cells <sup>a</sup> .....                     | 148 |
| Supplemental Table B.3. Statistical significance of the differences in the proportions of replicon-positive cells in dual-replicon decay experiments <sup>a</sup> ..... | 153 |
| Supplemental Table B.4. Statistical significance of the differences in the proportions of replicon-positive cells in dual-replicon decay experiments <sup>a</sup> ..... | 154 |
| Supplemental Table B.5. Statistical significance of differences in apoptosis rates of dual-, single-, or replicon-negative cells <sup>a</sup> .....                     | 155 |

|   |     |
|---|-----|
| Supplemental Table B.6. Statistical significance of differences in apoptosis rates of dual-, single-, or replicon-negative cells <sup>a</sup> ..... | 156 |
| Supplemental Table B.7: Primer sequences used in plasmid construction.....  | 160 |
| Supplemental Table B.8: Probe/primer sets used in quantitative real-time PCR. ...   | 161 |

## LIST OF FIGURES

|   |    |
|---|----|
| Figure 1.1. Diversity of HBV, HIV-1, and HCV.....   | 4  |
| Figure 1.2: The Hepatitis C genome and virion.....  | 6  |
| Figure 1.3: HCV life cycle. ....  | 9  |
| Figure 2.1: Construction of highly infectious reporter HCV strains.....   | 22 |
| Figure 2.2: Cleaved reporter proteins in Jc1/ <sup>NS5AB</sup> reporter strains localize to the replication complex (RC).....   | 26 |
| Figure 2.3: Isolation of a superinfectious HCV strain. ....   | 29 |
| Figure 2.4: Contribution of identified mutations to the superinfectious phenotype...  | 37 |
| Figure 2.5: The highly infectious and superinfectious phenotype of the Mut7 and Mut6 viruses is not limited to the Jc1/ <sup>NS5AB-mKO2-Bsd</sup> reporter strain. .... | 40 |
| Figure 2.6: NS5A C2274R and $\Delta$ 3' UTR mutations increase the amount of viral protein.....   | 43 |
| Figure 2.7: NS5A C2274R and $\Delta$ 3' UTR mutations increase “supertransfection” in replicon-containing cells.....  | 45 |
| Figure 2.8: Viral RNA translation is not enhanced by the NS5A C2274R and $\Delta$ 3' UTR mutations. ....  | 49 |
| Figure 3.1: Genomic HCV constructs employed in this study and relative efficiencies of each. ....   | 73 |
| Figure 3.2: Decay of cells multiply transfected with congenic Jc1 replicon strains. .   | 78 |
| Figure 3.3: The apoptosis rate in Jc1/ $\Delta$ <sup>XFP</sup> dual- or single-replicon-containing cells is similar.....  | 81 |

|  |     |
|--|-----|
| Figure 3.4: Progression through the cell cycle is important in the dual- to single-replicon decay process.....   | 86  |
| Figure 3.5: Mitosis is associated with the decay process in dual–replicon cells. ....  | 91  |
| Figure 3.6: Loss of fluorophore-NS5A epifluorescence in dual-replicon cells after mitosis.....   | 95  |
| Figure 3.7: Bias in decay of Jc1/ $\Delta^{XFP-BSD}$ dual-replicon-containing cells. ....  | 99  |
| Figure 3.8: Explicit loss of viral RNA during the decay process.....   | 103 |
| <hr/>  |     |
| Supplemental Figure A.1: Representative flow cytometry plots indicating infection rates of viral supernatants.....   | 127 |
| Supplemental Figure A.2: Subcellular localization of the mKO2-Bsd transgene in Jc1/ $\Delta E1E2^{NS5A-GFP;NS5AB-mKO2-Bsd}$ replicon-containing cells..... | 128 |
| Supplemental Figure A.3: Flow cytometry plots of cells used in the FeOLabel magnetic bead isolation protocol.....  | 131 |
| Supplemental Figure A.4: Flow cytometry plots from superinfected cells during continuous cell passage.....   | 132 |
| Supplemental Figure A.5: Viral accumulation, infectivity, and viral spread of mutant and WT Jc1/ $^{NS5AB-mKO2-Bsd}$ strains. ....                         | 135 |
| Supplemental Figure B.1. Absolute cell counts of replicon-positive cells in dual-replicon decay experiments.....   | 140 |
| Supplemental Figure B.2: Decay of dual- and single-replicon cells in the presence and absence of triple-replicon cells.....                                | 145 |
| Supplemental Figure B.3. Sorting procedures.....   | 146 |

|   |     |
|---|-----|
| Supplemental Figure B.4: Persistence of single-replicon cells and decay of dual-replicon cells in Jc1/ $\Delta^{XFP-BSD}$ -transfected cells.....                             | 150 |
| Supplemental Figure B.5: Persistence of single-replicon cells and decay of dual-replicon cells in Jc1/ $\Delta^{XFP-BSD}$ -transfected cells.....                             | 152 |
| Supplemental Figure B.6: Jc1/ $\Delta^{XFP-BSD}$ single-replicon-positive cells that have an advantage in proliferation have a <i>disadvantage</i> in the decay process. .... | 158 |



## ABBREVIATIONS

- 7-AAD                      7-aminoactinomycin D
- ANOVA                     Analysis of variation
- APC                        Allophycocyanin
- AUC                        Area under the curve
- BSD                        Blasticidin-S-deaminase
- CFSE                       Carboxyfluorescein diacetate succinimidyl ester
- DAA                        Direct-acting antiviral
- DMEM                     Dulbecco's Modified Eagle Medium
- DMSO                      Dimethylsulfoxide
- DPBS                      Dulbecco's phosphate-buffered saline
- dsRNA                     Double-stranded RNA
- EBFP2                     Enhanced blue fluorescent protein 2
- ELISA                      Enzyme-linked immunosorbent assay
- ER                         Endoplasmic reticulum
- FACS                        Fluorescent-activated cell sorting
- FFU                         Focus-forming units
- FLuc                        Firefly luciferase
- HCV                        Hepatitis C virus
- HCVcc                     HCV cell culture (fully infectious HCV)
- HCVpp                     HCV pseudoparticles
- HEPES                     4-(2-hydroxyethyl)-1-piperazineethanesulfonic acid
- hGem                        Human Geminin

- HIV-1 Human immunodeficiency virus
- Ifn- $\alpha$  Interferon- $\alpha$
- IRES Internal ribosomal entry site
- mKO2 Monomeric Kusabira Orange 2
- MWCO Molecular weight cutoff
- PI Propidium iodide
- PMSF Phenylmethylsulfonylfluoride
- RBV Ribavirin
- RC Replication complex
- RLuc *Renilla* luciferase
- RT-PCR Reverse-transcriptase PCR
- SEM Standard error of the means
- SVR Sustained virological response
- UTR Untranslated region
- VLDL Very-low-density-lipoprotein

**CHAPTER 1**  
**INTRODUCTION**

## **Hepatitis C virus: epidemiology and treatment**

Approximately 3% of the world's population is chronically infected with Hepatitis C virus (HCV) [1]. Blood-borne transmission is the most common route of viral spread, with approximately 80% of patients failing to spontaneously clear the virus following infection. Because acute infection causes mild symptoms that do not prompt immediate testing, and because general HCV testing is not typically performed, HCV infection is often not diagnosed for many years. Over decades of chronic infection, patients can develop liver fibrosis, steatosis, and cirrhosis, and in extreme cases hepatocellular carcinoma. Based on World Health Organization estimates, HCV leads to an excess mortality of 366,000 people per year [2].

HCV is an extremely diverse virus, with six major genotypes differing in sequence by ~30-35% [3], and each major genotype containing subtypes that further differ in sequence by ~20-25%. In fact, circulating strains of HCV are more diverse than either HIV-1 or Hepatitis B virus (Figure 1.1). The genotypes are distributed geographically, whereby genotype 1 is the most common, found mainly in northern Europe and the USA, genotype 2 is endemic to the Mediterranean and Asian countries, and genotypes 3 and 4 are distributed in Europe and the Middle East, respectively. The remaining genotypes have a more restricted distribution, mainly in South Africa (genotype 5) and southeastern Asia (genotype 6). Genotypes 1, 3, and 6 are associated with intravenous drug use, while genotype 4 is associated with past medical treatments using improperly sterilized needles [4].

Until 2011, the standard treatment for chronic HCV infection was a combination of pegylated interferon- $\alpha$  (Ifn- $\alpha$ ) and ribavirin (RBV). However, this treatment leads

to a sustained virological response (SVR) in less than 50% of patients with chronic genotype-1 HCV infection [5]. An SVR is a period of aviremia for at least 24 weeks following cessation of therapy, and is considered a functional cure. In 2011, two direct-acting antiviral drugs (DAAs), boceprevir and telaprevir, were approved by the FDA and have since become part of a triple therapy with Ifn- $\alpha$  and RBV. SVR rates in patients with genotype 1 HCV now approach 80% when this triple therapy is used [6]. The goal for future drug development will be to identify combination therapies using DAAs that avoid the complications and side effects of Ifn- $\alpha$  treatment.

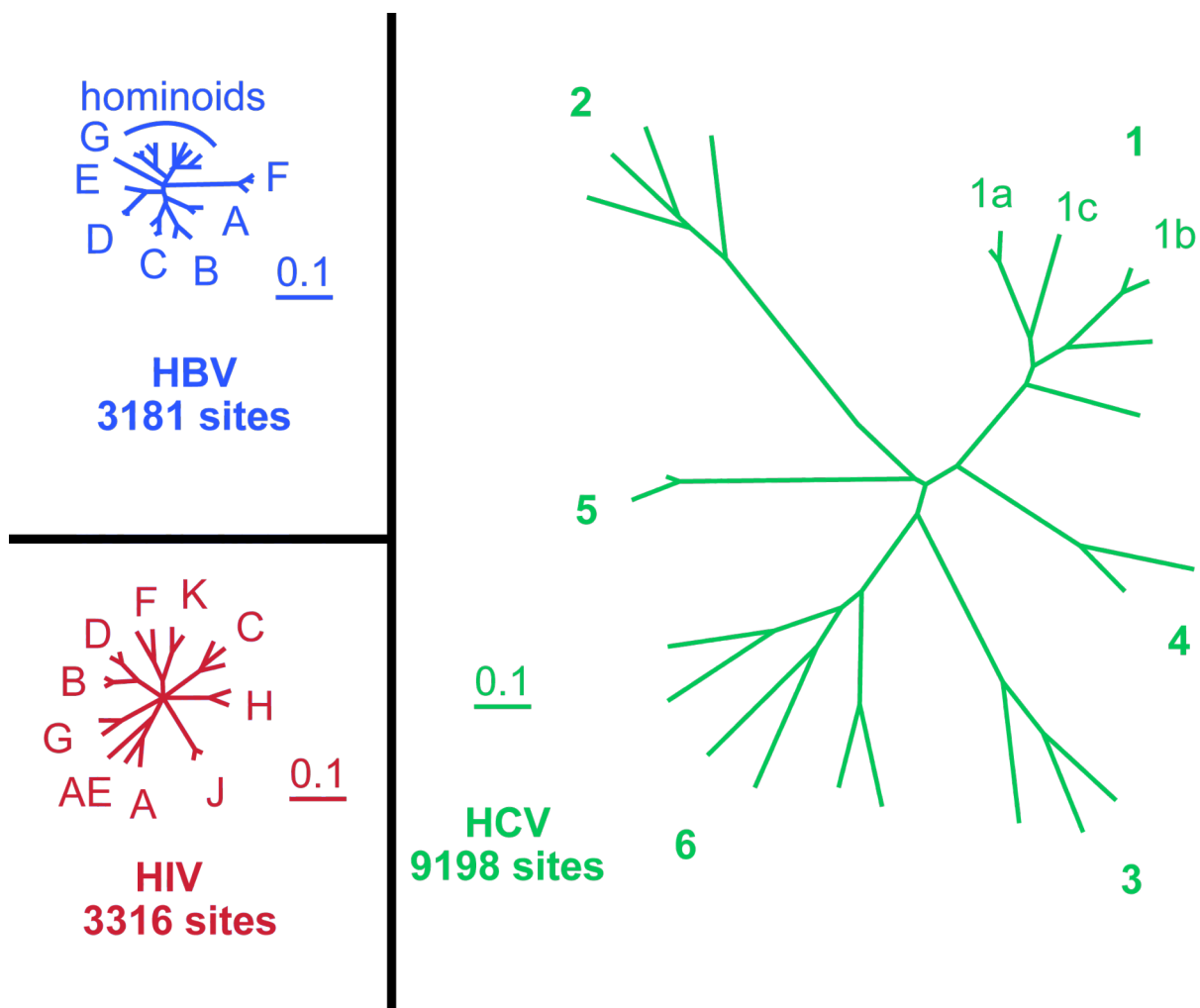


**Figure 1.1. Diversity of HBV, HIV-1, and HCV.**

Phylogenetic trees of representative strains are shown on the same scale in terms of nucleotide difference. Sites indicate the number of aligned sites for each virus.

Adapted from Mandel et al. [7].

### **The Hepatitis C virus life cycle**

Hepatitis C is a (+)-stranded enveloped ssRNA virus in the *Flavivirus* family. Within the Hepatitis C clade, six major genotypes have thus far been identified, with sequences between each major genotype varying by as much as 30% [8]. HCV's 9.6 kb genome is translated as a polyprotein (Figure 1.2A), which is cleaved into structural (C, E1, E2, p7) and nonstructural (NS2, NS3, NS4A/B, and NS5A/B) proteins by host and viral proteases [9]. All of these proteins are endoplasmic reticulum (ER)–membrane associated, through either transmembrane or membrane anchor domains or tight association with another viral protein. The HCV virion is composed of a nucleocapsid, containing the core protein and the HCV genome, surrounded by a lipid envelope containing the integral membrane E1 and E2 glycoproteins (Figure 1.2B).

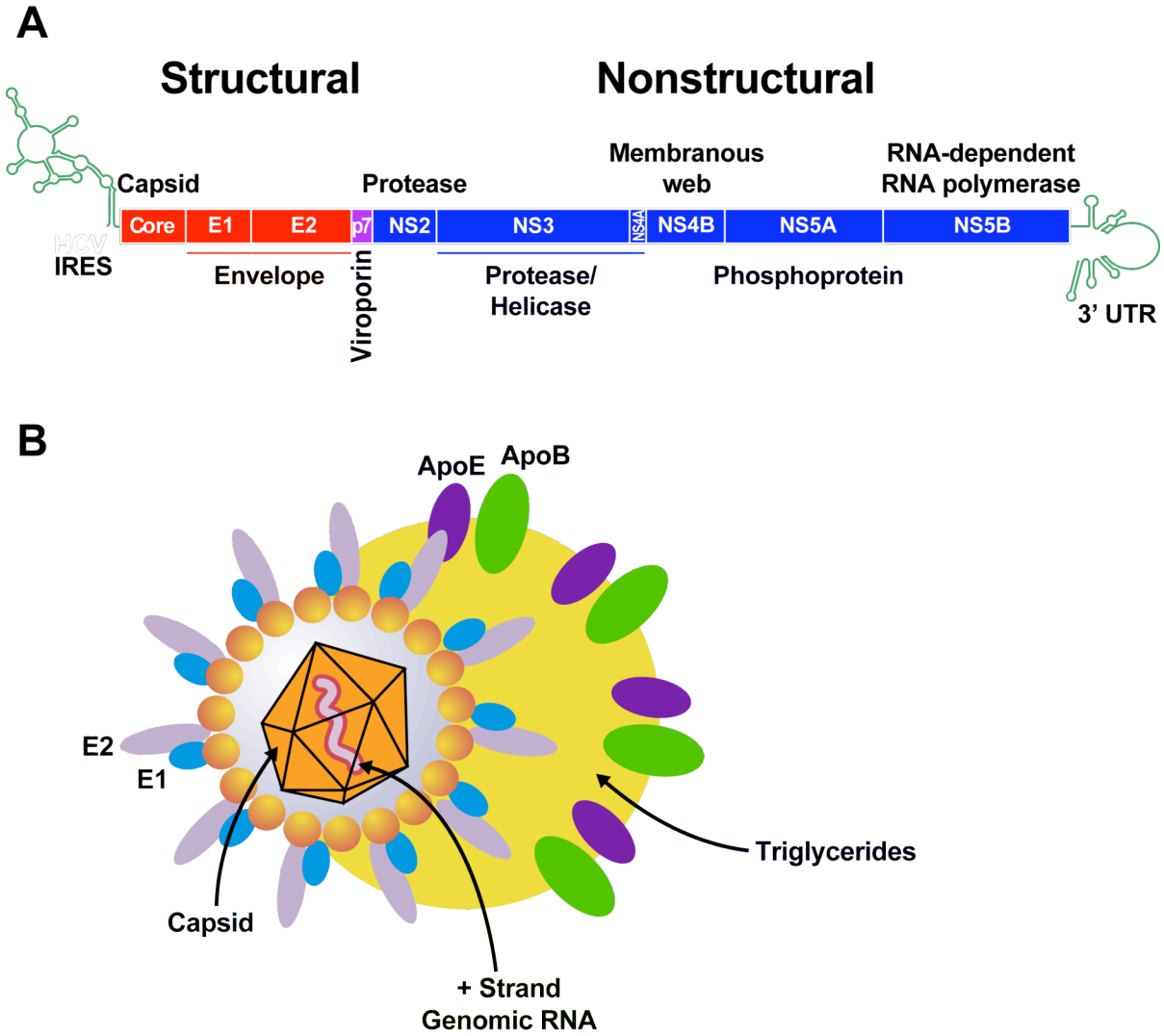


**Figure 1.2: The Hepatitis C genome and virion.**

(A) Organization of the HCV genome and polyprotein. The role of each individual viral protein is shown. (B) Structure of the HCV “lipovirion.” The individual components of the HCV virion and the associated VLDL particle are shown.



The primary cellular targets of HCV are liver hepatocytes, but infection can also occur in extrahepatic tissues, including hematopoietic cells [10]. Our understanding of the host components involved in viral entry for hepatocytes and other cells continues to evolve, but to date includes: glycosaminoglycans (including heparan sulfate), the tetraspanin CD81, the low-density lipoprotein receptor (LDL-R), another lipoprotein receptor (SR-BI), and the tight junction membrane proteins claudin-1 [11,12] and occludin [13]. In hepatocytes, HCV is internalized by receptor-mediated endocytosis (Figure 1.3). In turn, acidification of the endosome promotes virion fusion, putatively by pH-dependent conformational changes in E1 and E2 [11].

The viral genome is then uncoated and transported to the ER membrane, which functions as the primary site of HCV replication and assembly. Primary viral translation occurs as the host translation machinery is recruited to the internal ribosome entry site (IRES) sequence in the 5' UTR of the viral genome, and synthesis of nascent (+) and (-) ssRNA genomic transcripts is carried out by the viral NS5B RNA polymerase. The replication of viral RNA by nonstructural proteins occurs within an invagination of the ER membrane that is scaffolded by the viral NS4B protein, termed the “membranous web” [14,15].

Viral assembly occurs as the viral nucleocapsid buds through the ER membrane. This process requires the intracellular lipid droplets as scaffolds for production of the nucleocapsid and the host very-low-density lipoprotein (VLDL) machinery for viral budding [16]. The virion has actually been termed a “lipoviroparticle” by some, as it incorporates large quantities of triglycerides and

apolipoproteins [17]. Although controversial, virus release is thought to involve exocytosis following transit through the trans-Golgi network [18,19].

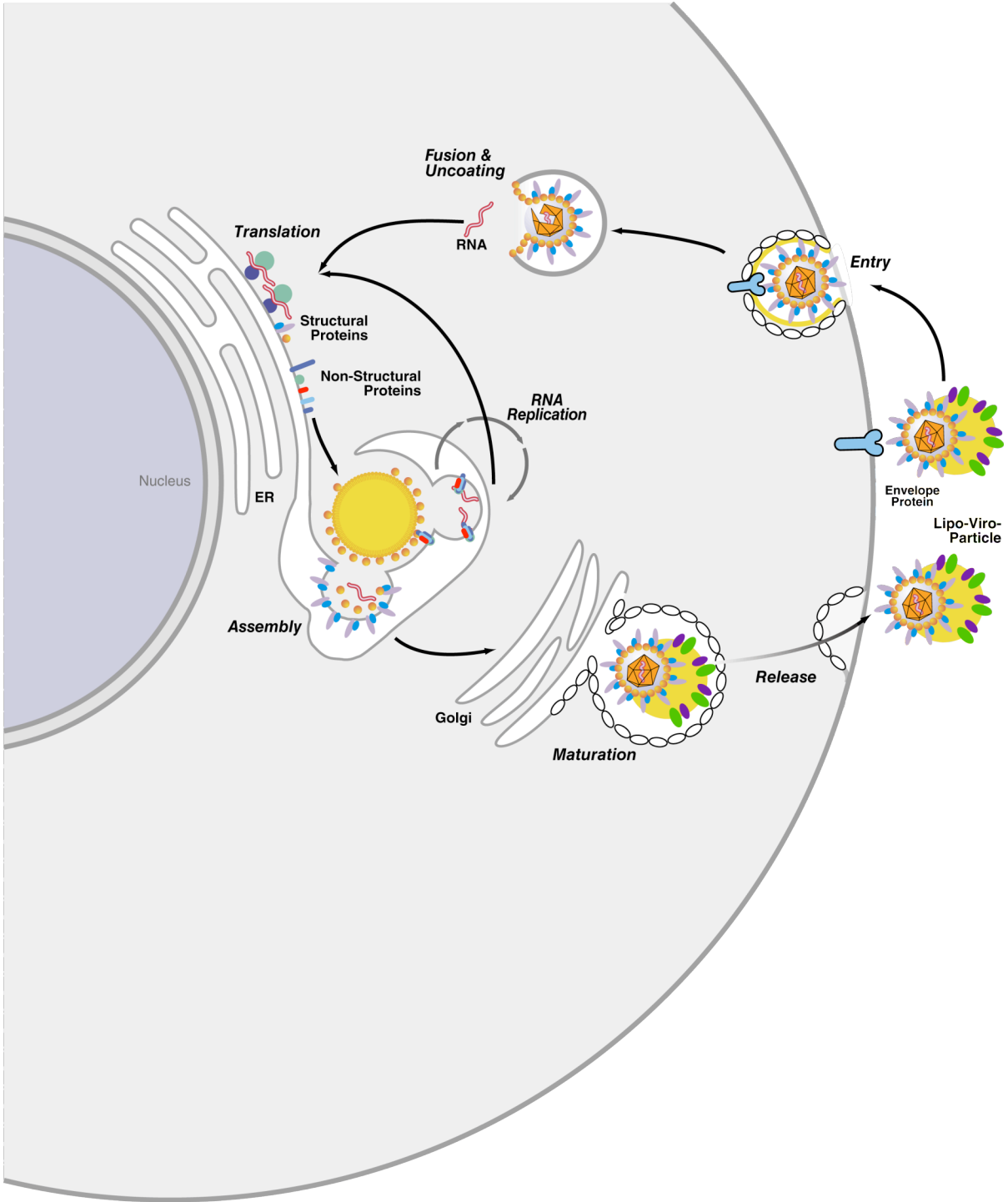


**Figure 1.3: HCV life cycle.**

Adapted from Herker et al. [20].

## HCV model systems

Historically, studies of HCV biology and pathogenesis have been hampered by the lack of defined *in vitro* systems for propagating the virus. Initial infection attempts with full-length HCV genomes in primary hepatocytes and hepatic cell lines led to only transient RNA replication but not production of infectious virions. Before 2005, there were two major model systems for HCV studies: the genomic/subgenomic replicon system and the HCV pseudoparticle (HCVpp) system. In the genomic/subgenomic replicon system, bicistronic transcripts are synthesized from plasmid clones using T7 RNA polymerase and electroporated into a hepatoma cell line, usually Huh7. The native HCV IRES directs translation of a neomycin resistance cassette, and an encephalomyocarditis virus (EMCV) IRES drives translation of full-length HCV RNA or a subset of the nonstructural genes. These genomic/subgenomic RNAs replicate autonomously in cells, and cells stably replicating HCV RNA could be isolated by G418 selection, making this system useful for studying HCV RNA replication/translation, as well as the role of nonstructural genes [21]. However, there were major problems with this system. First, the viral RNA required adaptive mutations that increased the *in vitro* fitness of the virus but reduced *in vivo* replicative capacity in chimpanzees [22]. Interestingly, the adaptive mutations clustered in three major genes: NS3 (viral protease), NS4B (putative replication scaffolding protein), and NS5A (polyfunctional protein) [14,23]. Additionally, this system was unable to produce infectious virus and only one hepatoma cell line, Huh7, supported the accumulation of high numbers of replicons, likely due to a defect in the host dsRNA-sensing innate immune response.

The HCVpp system enables the study of HCV entry by using HIV virions pseudotyped with HCV envelope glycoproteins E1 and E2. An envelope-deficient (*env*<sup>-</sup>) HIV provirus, with a reporter gene (e.g., luciferase) inserted into the *nef* open reading frame, is coexpressed in 293T cells with the HCV E1/E2 genes. Lentiviral particles with the HCV envelope are produced and harvested. These HCVpp were found to preferentially fuse to hepatocyte-derived cells, and led to the identification of cellular receptors required for HCV entry [11]. Subsequently, all putative receptors were validated by later analysis using neutralizing antibodies to antagonize or siRNA to specifically downregulate these receptors to prevent serum-derived HCV infection of hepatocyte-derived cells [24].

These two model systems were bridged in 2005, when three independent groups demonstrated complete replication *in vitro* of a genotype 2a HCV clone, JFH-1 [25,26,27]. This clone, isolated from a Japanese male patient with fulminant hepatitis [28], replicated robustly in Huh7 cells and produced infectious virions without the need for adaptive mutations, making this system more physiologically relevant [29]. The development of a cell culture–based system for HCV (HCVcc) studies therefore represented a landmark advance in HCV research, opening many new avenues of investigation.

### **Mixed infections and recombination between HCV strains**

Patients infected with more than one HCV genotype or subtype, known as mixed infections, are common [30,31]. In cohorts of injection drug users, mixed infections have been found in 3–55% of HCV-positive patients [32,33]. They can be subdivided into coinfection, in which patients are infected with multiple strains within the short

window of time before seroconversion occurs, or superinfection, in which a secondary infection occurs outside that window. Interestingly, in both patients and HCV-challenged chimpanzees, mixed infections can resolve into single infections where only one virus demonstrates viremia at later time points [34,35]. Additionally, it has been suggested that coinfection with multiple strains of HCV leads to the exacerbation of chronic HCV disease correlates [36].

Despite the prevalence of mixed infections in HCV-infected individuals, recombination between subtypes and genotypes of HCV is rare [37,38,39,40]. Although some circulating recombinant strains have been identified [41,42,43,44,45,46], one would expect much higher numbers of recombinant species in individuals infected with more than one HCV strain. The paucity of natural HCV recombinants may be ascribed to a process known as superinfection exclusion, whereby a cell productively infected with a virus becomes refractory to infection with a homologous virus. As recombination requires a single host cell to be productively infected with multiple strains, superinfection exclusion could explain why recombination in HCV is so rare. Superinfection exclusion has been described for a number of viruses of widely varying host range and methods of replication including the human immunodeficiency virus (HIV) [47], Sindbis virus [48], duck hepatitis B virus [49], citrus tristeza virus [50], and many others.

The first indication that superinfection exclusion may operate in HCV infection was provided by Evans et al. [51]. In this study, the authors showed that competition occurred between HCV replicons, where the presence of one subgenomic replicon in host cells greatly reduced the replicative capacity of a second replicon. Three

years later, after the isolation of the infectious JFH-1 strain, two studies [52,53], demonstrated conclusively that HCV superinfection exclusion occurred *in vitro*. The authors demonstrated that cells become highly resistant to secondary infections within 48 hours following a primary infection. The authors further established that HCVpp was able to infect HCVcc-infected cells, showing that superinfection exclusion was largely operating at a post-entry step. Presumably, this block occurred at the level of translation or replication of the secondary viral RNA, although the mechanism of this block remained unclear.

Understanding why recombination in HCV is rare, and the nature of superinfection exclusion, has clear implications for treating HCV infection. We are entering an age of multi-drug regimens that target multiple viral proteins. If HCV could successfully superinfect cells, drug-resistance mutations could be transferred between strains by recombination. In this case, resistance mutations would not have to arise simultaneously in one genome; recombination could transfer the mutations between genomes, drastically lowering the overall barrier to resistance [40].

### **Scope of thesis**

This thesis presents multiple projects performed during my dissertation research, with an overall concentration on the theme of viral competition in HCV infection. Chapter 2 focuses on the viral mediators of superinfection exclusion, by successfully isolating a variant of HCV that can overcome this block to replication. Chapter 3 centers on viral competition when two HCV genomes are productively replicating in a host cell, and identifies a novel, stochastic mechanism of competition that results from structural changes in the host cell during mitosis. Together, these projects

demonstrate that viral competition in HCV infection is a dynamic, complex phenomenon that occurs at multiple levels in the viral life cycle. Furthermore, this work identifies key portions of the viral life cycle where HCV may be vulnerable to interventions.

Both chapters were primarily the work of the author of this thesis, Brian Webster, who developed the hypotheses, performed the experiments, and wrote the manuscripts. The studies were performed in Warner Greene's lab, in collaboration with Melanie Ott's lab. Chapter 3 was performed in collaboration with Silke Wissing of the Greene lab and Eva Herker of the Ott lab. In each case, the collaborators provided useful intellectual contributions. Chapter 3 has been published in the *Journal of Virology* [54]. Chapter 2 has been submitted as a paper but not yet published.



**CHAPTER 2**

**ISOLATION AND CHARACTERIZATION OF A  
SUPERINFECTIOUS STRAIN OF HCV**

## ABSTRACT

Cells that are productively infected by HCV are refractory to a second infection by HCV, via a block in viral replication known as superinfection exclusion. The block occurs at a post-entry step and likely involves translation or replication of the secondary viral RNA, but the mechanism is largely unknown. To characterize HCV superinfection exclusion, we selected for an HCV variant that could overcome the block. We produced a high-titer reporter HC-J6/JFH1 (Jc1) viral genome with a fluorescent reporter inserted between NS5A and NS5B and used it to infect Huh7.5 cells containing a Jc1 replicon. With multiple passages of these infected cells, we isolated, for the first time, an HCV variant that can superinfect cells at high levels. Notably, the superinfectious virus rapidly cleared the primary Jc1 replicon from superinfected cells. Mutations in E1, p7, NS5A, and the poly-U/UC tract of the 3' UTR were important for superinfection. Furthermore, these mutations dramatically increased the infectivity of the virus in naive cells. Interestingly, viruses with a shorter poly-U/UC tract, and to a lesser extent a NS5A domain-II mutation, were most effective in overcoming the post-entry block. Neither of these changes affected viral RNA translation, indicating that the major barrier in post-entry exclusion occurs at viral RNA replication. The evolution of the ability to superinfect after less than a month in culture and the concomitant exclusion of the primary replicon suggest that superinfection exclusion dramatically affects viral fitness and dynamics *in vivo*.

## INTRODUCTION

In superinfection exclusion, a cell productively infected with a specific virus becomes resistant to infection with a homologous virus. This process has been described for viruses with a broad range of hosts, including the human immunodeficiency virus (HIV) [47], Sindbis virus [48], duck hepatitis B virus [49], and citrus tristeza virus [50]. Cells infected with or actively replicating hepatitis C virus (HCV) also become refractory to further HCV infection [52,53]. The superinfection block occurs at the level of translation or replication of the incoming secondary viral RNA [51,52,53], similar to the case of the related pestivirus bovine diarrhoea virus [55]. The exact mechanism is unclear. As HCV RNA levels quickly plateau in infected cells *in vitro*, a superinfection block at the level of RNA translation or replication suggests that access to the necessary host factor(s) is rate limiting. This has clear implications for HCV treatment. By definition, a rate-limiting host factor is critical for the replication of the virus, and may be a unique target in future therapies.

Superinfection exclusion itself also has clear implications for treating HCV infection. As viral recombination requires a host cell to be productively replicating two genomes, superinfection exclusion would be expected to effectively prevent viral recombination. If, however, HCV could successfully superinfect cells, the evolution of drug and/or vaccine resistance and transfer of these characteristics between strains would be greatly enhanced. Viral variants capable of superinfection could

result in an even greater degree of immune escape variants and drug-resistant strains within this already variable virus.

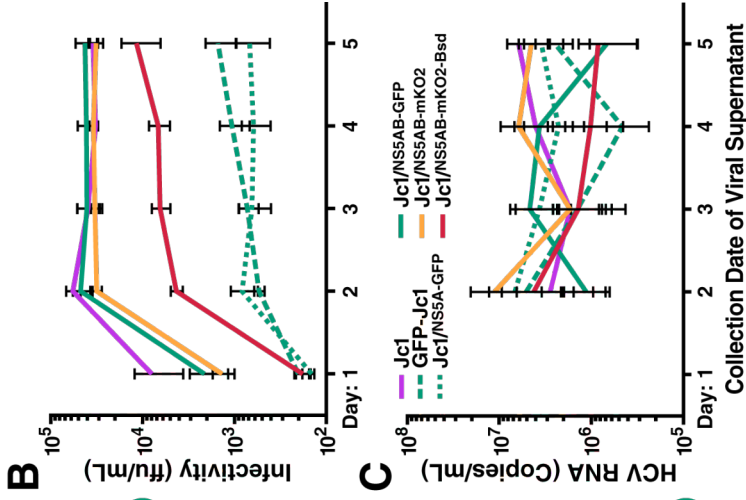
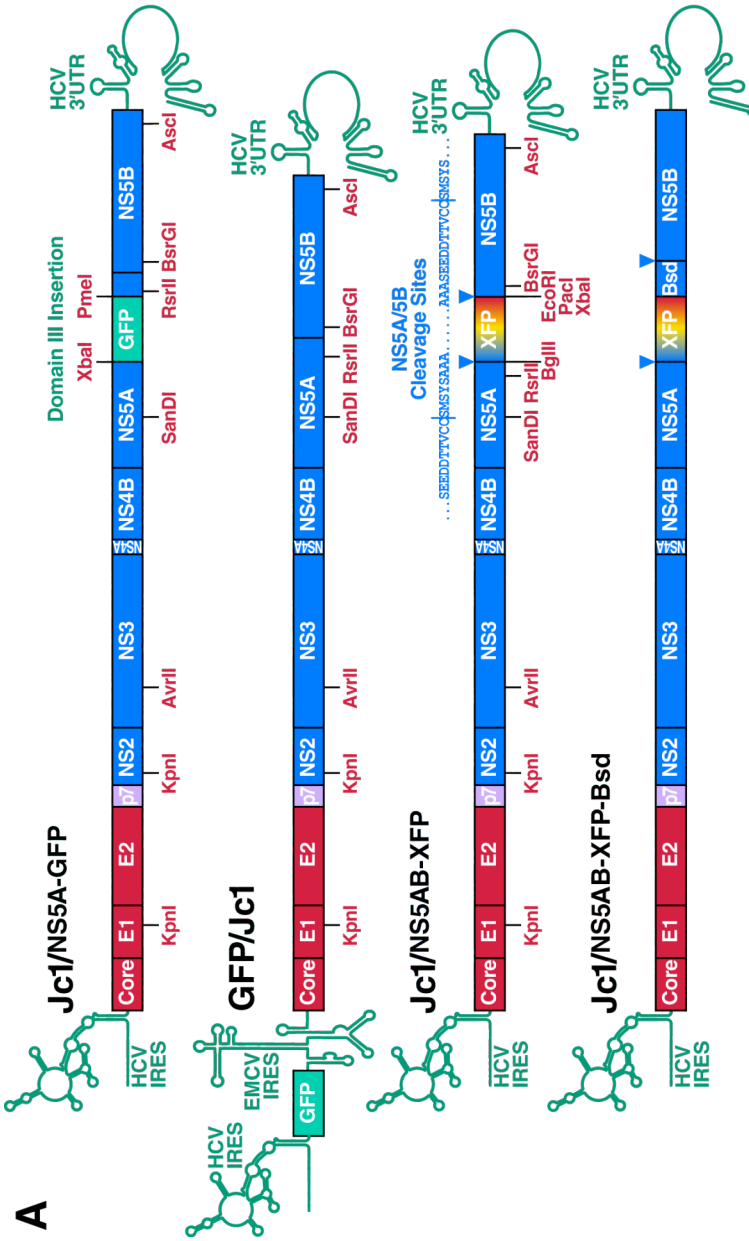
In this study, we sought to determine how various viral and host factors relate to the exclusion process, and whether HCV is capable of overcoming superinfection exclusion. To do this, we developed a new class of HCV fluorescent reporter viral genomes based on the highly infectious HC/J6–JFH1 (Jc1) chimera [56] that are significantly more infectious than existing HCV reporter strains. With this fluorescent reporter, we unambiguously distinguished multiple infections within one cell. We used these highly infectious reporter genomes to select for an HCV variant that could superinfect cells with high efficiency. By sequence analysis and characterization of the mutations in the superinfecting strain, we found that a mutation in domain II of NS5A and a deletion in the poly-U/UC region of the 3' untranslated region (UTR) are critical for HCV to overcome post-entry superinfection exclusion. We further showed that the ability to superinfect is partially restricted by the HCV genotype of the cells, and that this ability generally increases the infectivity of the virus *in vitro*.

## RESULTS

### **Viral genomes with reporter proteins between NS5A and NS5B are highly infectious**

A successful model to study HCV superinfection exclusion and viral mutations necessary to overcome the block requires that we: (1) use a highly infectious strain in the selection process and (2) be able to easily distinguish superinfected from non-superinfected cells in infected cultures. While the Jc1 chimera is highly infectious, without a fluorescent reporter, the study of superinfection is difficult. Existing Jc1 reporter strains had viral replication defects and thus were not infectious enough for our purposes. To create a more infectious Jc1 reporter strain, we used a monocistronic HCV genome with a reporter gene inserted between NS5A and NS5B (Figure 2.1A). Flanking NS5A/NS5B cleavage sites around the reporter gene allowed the viral NS3/4A protease to release the reporter from the viral polyprotein. The Jc1/<sup>NS5AB-GFP</sup> and Jc1/<sup>NS5AB-mKO2</sup> strains displayed nearly unaltered viral titers from the untagged Jc1 virus, and much higher titers than existing monocistronic (Jc1/<sup>NS5A-GFP</sup>) or bicistronic (GFP-Jc1) reporter strains (Figure 2.1B, Supplemental Figure A.1). Distinguishing infected and uninfected populations with Jc1/<sup>NS5AB-GFP</sup> and Jc1/<sup>NS5AB-mKO2</sup> was difficult by flow cytometry (Supplemental Figure A.1). However, by fusing the blasticidin resistance gene (Bsd) to mKO2 (Jc1/<sup>NS5AB-mKO2-Bsd</sup>), we obtained a brighter fluorescent signal from infected cells (Supplemental Figure A.1) while only modestly affecting viral titers (Figure 2.1B). No differences in

HCV RNA release into the cytoplasm were observed among any of the reporter or Jc1 strains (Figure 2.1C), consistent with observations that only 1/100–1/1000 secreted HCV RNAs are in infectious particles [57].



Collection Date of Viral Supernatant

**Figure 2.1: Construction of highly infectious reporter HCV strains.**

(A) Schematic diagram of HCV reporter strains. XFP represents the fluorophore tag (GFP or mKO2) and Bsd represents the blasticidin resistance gene. (B) Titers of infectious HCV particles following transfection. Huh7.5 cells were transfected with RNA transcripts of the given infectious strains, including untagged Jc1. Supernatants were collected from days 1–5 after transfection and viral titers were obtained by limiting dilution assay. Note the higher infectious titers in the Jc1<sup>NS5AB</sup> reporter strains relative to previously described reporter strains. (C) Release of HCV RNA following transfection. RNA was isolated from supernatants after transfection and HCV RNA was quantified by real-time RT-PCR.  $n=3$  independent viral preparations and quantifications; error bars indicate  $\pm$  SEM.



### **Cleaved NS5AB reporter gene localizes to the replication complex**

GFP colocalization with dsRNA, a marker for sites of active replication of HCV RNA [58], in punctate cytoplasmic structures is typical of the Jc1/<sup>NS5A-GFP</sup> HCV reporter strain, but not the bicistronic GFP-Jc1 strain (Figure 2.2A). GFP is fused to the viral replicase component NS5A in the Jc1/<sup>NS5A-GFP</sup> strain; therefore, GFP remains associated with the HCV replication complex (RC). However, in the GFP-Jc1 strain, GFP diffused throughout the cell, as it is not fused to any viral proteins. We expected that GFP from Jc1/<sup>NS5AB-GFP</sup> would diffuse similarly, as it should be soluble after polyprotein cleavage and, unlike NS5A-GFP from Jc1/<sup>NS5A-GFP</sup>, should not be tethered to the endoplasmic reticulum (ER). To our surprise, it was instead highly colocalized with dsRNA (Figure 2.2A).

We constructed a dual-fluorescent replicon, Jc1/ $\Delta$ E1E2<sup>NS5A-GFP;NS5AB-mKO2-Bsd</sup>, to further explore this unexpected result (Supplemental Figure A.2A). The NS5A-GFP and mKO2-Bsd reporters had a high degree of colocalization in live cells (Supplemental Figure A.2B & C), suggesting that the mKO2-Bsd reporter protein localizes in or adjacent to the RC. To ensure that this colocalization did not result from incomplete cleavage of the mKO2-Bsd reporter from either NS5A-GFP or NS5B, we performed iodixanol fractionation of lysates from Jc1/ $\Delta$ E1E2<sup>NS5A-GFP;NS5AB-mKO2-Bsd</sup> replicon-containing cells (Figure 2.2B, Supplemental Figure A.2D). While an incomplete cleavage product corresponding to NS5A-GFP-mKO2-Bsd (\*, Figure 2.2B) was observed, approximately 45% of the total mKO2-Bsd was fully cleaved from the HCV polyprotein (\*\*, Figure 2.2B). Interestingly, even the fully cleaved mKO2-Bsd protein cofractionated with the ER marker calreticulin and the HCV RC

marker NS5A-GFP, suggesting that the soluble mKO2-Bsd protein remains associated with the HCV RC.

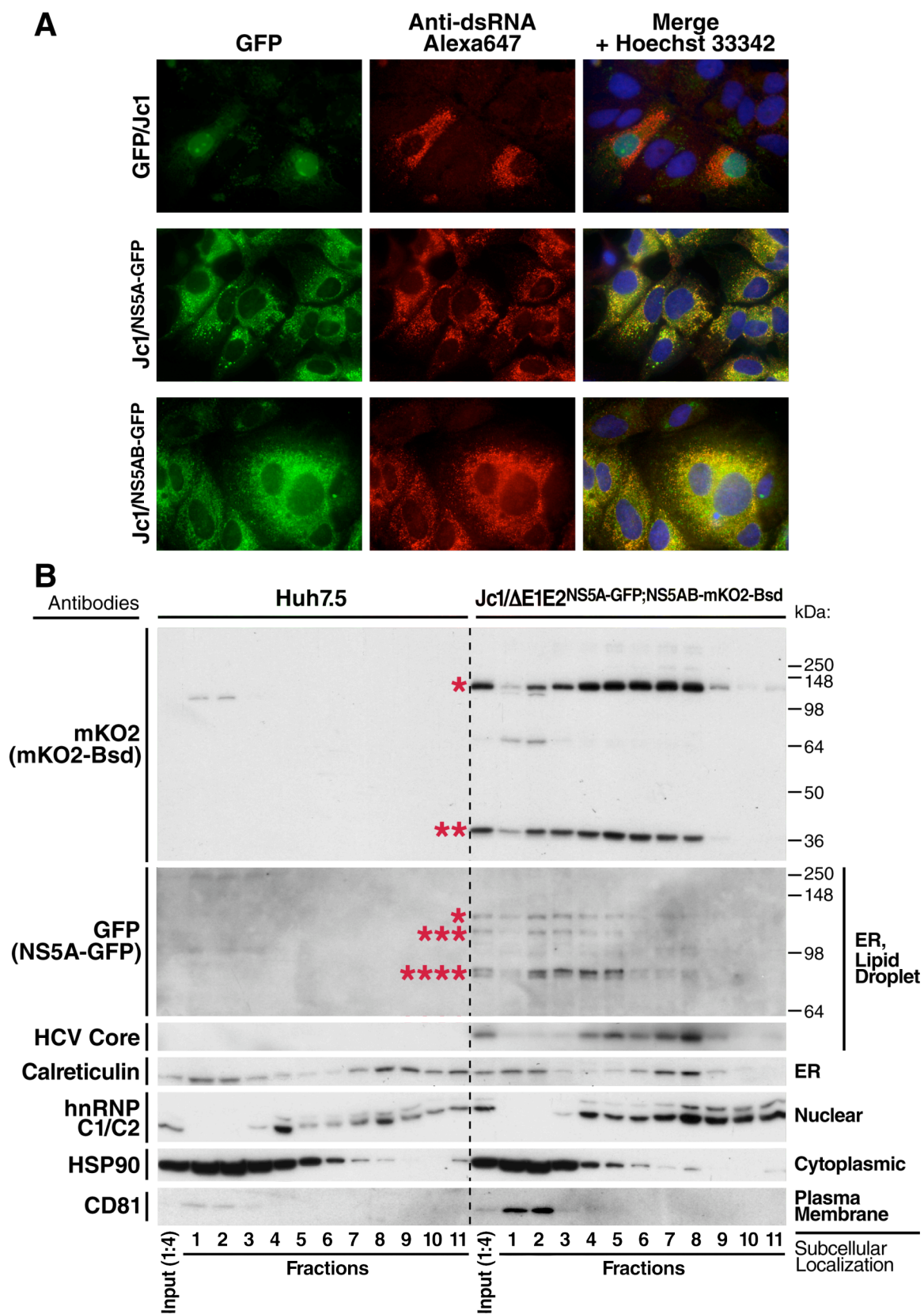


**Figure 2.2: Cleaved reporter proteins in Jc1/<sup>NS5AB</sup> reporter strains localize to the replication complex (RC).**

(A) Localization of GFP in various reporter strains. Huh7.5 cells were transfected with the indicated viral RNA transcripts; 2 days later, the cells were stained for dsRNA (HCV replication sites) and DNA (Hoescht 33342) and imaged by epifluorescence microscopy. Note that GFP in the Jc1/<sup>NS5AB-GFP</sup> reporter strain displays significant colocalization with dsRNA. (B) Iodixanol gradient fractionation of Huh7.5 and Jc1/ $\Delta$ E1E2<sup>NS5A-GFP;NS5AB-mKO2-Bsd</sup> replicon-containing cells. Cell lysates were fractionated over a discontinuous iodixanol (4%, 8%, 12%, 20%, 30%, and 35%) gradient. A total of 11 fractions were collected from the top (low density, soluble proteins) to the bottom (high density, ER and nuclear-rich). The fractions were then analyzed by western blot for mKO2, GFP, HCV core, Calreticulin, hnRNP C1/C2, HSP90, and CD81. \*: uncleaved NS5A-GFP-mKO2-Bsd (apparent MW 130 kDa, calculated MW 119 kDa), \*\*: cleaved mKO2-Bsd (38 kDa, 42 kDa), \*\*\*: uncleaved NS4B-NS5A-GFP (110 kDa, 105 kDa), \*\*\*\*: cleaved NS5A-GFP (84/87 kDa, 77 kDa).

## **Emergence of a superinfectious variant of HCV correlates with the exclusion of the primary replicon**

To select for a superinfectious strain of HCV, we first attempted to superinfect Jc1/ $\Delta$ E1E2<sup>NS5A-GFP-Bsd</sup> polyclonal replicon cells (Figure 2.3A) with Jc1/<sup>NS5AB-mKO2-Bsd</sup> viral supernatants. We elected to use the Jc1/<sup>NS5AB-mKO2-Bsd</sup> virus due to the brighter fluorescent signal in infected cells. However, only a very small number of replicon cells were superinfected, and the Jc1/<sup>NS5AB-mKO2-Bsd</sup> secondary infection was quickly eliminated from cultures (data not shown). We therefore decided on a somewhat unorthodox strategy of using replicon-negative 7.5-H2B-EBFP2 cells [54] (Figure 2.3B, Supplemental Figure A.3) to act as a reservoir of virus that could spread into Jc1/ $\Delta$ E1E2<sup>NS5A-GFP-Bsd</sup> replicon cells. The histone H2B-EBFP2 transgene would serve as a marker for “replicon-negative” cells, and by gradually decreasing the ratio of naive:replicon cells, we expected to gradually increase the selection pressure to superinfect. A similar strategy was used to isolate protease inhibitor-resistant HCV strains [59].

Rather than simply passage viral supernatants onto new cultures, we preserved the most efficient method of infection or cell-to-cell spread. To do this, cells in the primary Jc1/<sup>NS5AB-mKO2-Bsd</sup>-transfected culture were labeled with paramagnetic FeOLabel beads and mixed with the secondary untransfected culture. After allowing the infection to spread into the secondary culture, we removed the cells from the primary culture by magnetic selection (Figure 2.3B, Supplemental Figure A.3).

After the first round of this viral “passage” between cultures, the naive 7.5-H2B-EBFP2 cells were gradually eliminated from the culture, likely due to HCV infection-

induced death from the Jc1/<sup>NS5AB-mKO2-Bsd</sup> virus. Further, a low but stable superinfection was established in the replicon-containing cells (Figure 2.3C). By simply continuing to passage the cells in this culture, we observed the emergence of a Jc1/<sup>NS5AB-mKO2-Bsd</sup> variant that superinfected with high efficiency beginning 31 days after magnetic separation, as measured by the mKO2-positive percentage of replicon (GFP)-positive cells. Remarkably, emergence of the superinfecting strain correlated with the disappearance of replicon-positive cells in the culture (Figure 2.3C, Supplemental Figure A.4), suggesting that the secondary virus was excluding active replication of the primary replicon.

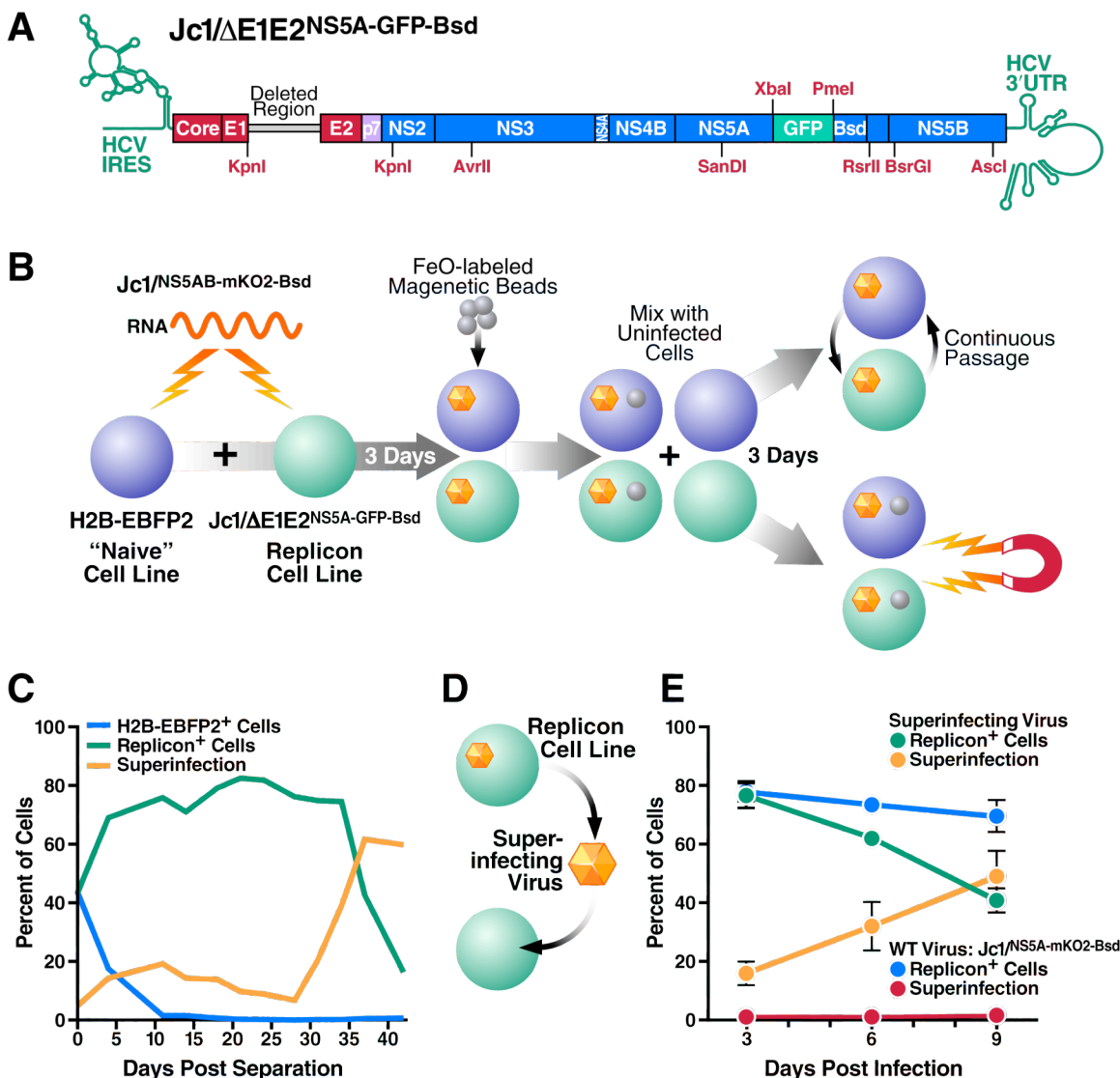


**Figure 2.3: Isolation of a superinfectious HCV strain.**

(A) Schematic diagram of the  $Jc1/\Delta E1E2^{NS5A-GFP}$  replicon construct. (B) Diagram of the strategy used to isolate the superinfectious  $Jc1/NS5AB-mKO2-Bsd$  reporter strain. Briefly, a 1:1 mixture of HCV-naïve EBFP2-tagged cells (H2B-EBFP2) and polyclonal  $Jc1/\Delta E1E2^{NS5A-GFP}$  replicon-containing cells were transfected with  $Jc1/NS5AB-mKO2-Bsd$  RNA. Three days later, these cells were labeled with FeO-label magnetic beads and mixed with unlabeled H2B-EBFP2 and  $Jc1/\Delta E1E2^{NS5A-GFP}$  cells

to allow the secondary Jc1/<sup>NS5AB-mKO2-Bsd</sup> virus to spread into the unlabeled cells. The magnetically labeled cells were removed 3 days later, and the Jc1/<sup>NS5AB-mKO2-Bsd</sup> infected culture was continuously passaged. (C) Emergence of a superinfectious Jc1/<sup>NS5AB-mKO2-Bsd</sup> strain during continuous passage. The blue line indicates the percentage of H2B-EBFP2 “naive” cells determined by flow cytometry; these cells were quickly eliminated from the culture, likely by the Jc1/<sup>NS5AB-mKO2-Bsd</sup> virus. The orange line indicates the percentage of Jc1/ $\Delta$ E1E2<sup>NS5A-GFP</sup> replicon-containing cells superinfected with Jc1/<sup>NS5AB-mKO2-Bsd</sup>. Note that emergence of the superinfectious strain at ~27 days post-separation correlates with elimination of the Jc1/ $\Delta$ E1E2<sup>NS5A-GFP</sup> replicon (green line) from the culture. (D) Serial passage of viral supernatants over replicon-containing cultures to further select for a superinfectious phenotype. (E) Viral supernatants passaged for 10 rounds display high superinfection rates and the ability to exclude the primary Jc1/ $\Delta$ E1E2<sup>NS5A-GFP</sup> replicon.  $n=3$  independent experiments; error bars indicate  $\pm$  SEM.



## Sequence analysis of the superinfectious Jc1 strain reveals adaptive mutations and deletions

We hypothesized that the superinfectious Jc1 strain acquired novel mutations that correlate with superinfectivity. The sequence of the superinfectious strain's genome was analyzed by isolating RNA from viral supernatants from the continuously passaged culture 42 days after magnetic separation. The RNA was reverse transcribed and PCR amplified in eight segments spanning the entire Jc1/<sup>NS5AB-mKO2-Bsd</sup> genome. The primers used for amplification are given in Supplemental Table A.1, where the extreme terminal regions of the 5' & 3' UTRs were not amplified. We then cloned the PCR products into pCR4 Topo and sequenced them to determine which mutations had been acquired by the superinfectious strain ("Round 1", Table 2.1). Importantly, few of the clones had sequences derived from the Jc1/ $\Delta$ E1E2<sup>NS5A-GFP-Bsd</sup> replicon, which would have manifested as a deletion in E1/E2 or a GFP-Bsd insertion in NS5A domain III. No clones had NS5A-GFP-Bsd sequence, and only 2/16 clones had the  $\Delta$ E1E2 sequence.

We hypothesized that further selection pressure for superinfectivity would lead to fixation of the mutations acquired in round 1, as well as the acquisition of further adaptive mutations. The superinfectious virus could now be directly passaged over Jc1/ $\Delta$ E1E2<sup>NS5A-GFP-Bsd</sup> replicon cells, by serial passage of viral supernatants (Figure 2.3D & E). This was not possible with wild-type (WT) Jc1/<sup>NS5AB-mKO2-Bsd</sup>, as the secondary virus would not persist due to superinfection exclusion. The superinfectious virus was passaged for nine rounds over Jc1/ $\Delta$ E1E2<sup>NS5A-GFP-Bsd</sup> replicon cells to provide further selection pressure for the ability to superinfect. The

viral RNA was again sequenced, expanding the sequenced region to the full extent of the 5' and 3'UTRs (Supplemental Table A.1). Again, only one of seven clones had the  $\Delta E1E2$  sequence, and none had NS5A-GFP-Bsd sequence.

Point mutations present in at least 50% of clones sequenced in either round 1 or 9 are shown in Table 2.1. We observed seven nonsynonymous mutations leading to an amino acid change and three silent mutations in the viral coding sequence. The distribution of deletions in the various clones analyzed is shown in Table 2.2. In round 1, deletions spanning much of the mKO2-Bsd region were observed in four of 18 clones. In passaging viral supernatants, cultures were selected for high numbers of GFP+:mKO2+ cells, whereas blasticidin was not used for selection. Correspondingly, in round 9, 5/5 clones had deletions in the Bsd gene, but no clones had deletions in mKO2. A specific deletion of 24 nucleotides (nt) in the poly-U/UC region of the 3' UTR was observed in all clones analyzed.

| HCV Gene               | HC/J6 Derived Sequence |      |      |        |      | JFH-1 Derived Sequence |       |        |      |      |      |                 |
|------------------------|------------------------|------|------|--------|------|------------------------|-------|--------|------|------|------|-----------------|
|                        | E1                     | E1   | E2   | E2     | p7   | NS3                    | NS4A  | NS5A   | NS5A | NS5A | Bsd  | 3'UTR Poly-U/UC |
| Nucleotide Number      |                        |      |      |        |      |                        |       |        |      |      |      |                 |
| Jc1/NS5AB-mKO2-Bsd     | 1087                   | 1343 | 1571 | 1637   | 2607 | 5030                   | 5412  | 7159   | 7160 | 7649 | 8525 | 10701           |
| H77 ref                | 1088                   | 1344 | 1572 | 1638   | 2596 | 5019                   | 5401  | 7160   | 7161 | 7586 | N/A  | N/A             |
| Construct Nucleotide   | G                      | G    | A    | T      | T    | G                      | A     | G      | T    | G    | T    | C               |
| Mutant Prevalence*     |                        |      |      |        |      |                        |       |        |      |      |      |                 |
| Round 1                | •                      | T/g  | •    | •      | T/c  | •                      | T     | A/g    | C/t  | •    | C    | T               |
| Round 9                | A/g                    | T    | G    | C/T    | C/t  | A                      | T     | A      | C    | A/G  | C    | T               |
| Round 1 Distribution** |                        |      |      |        |      |                        |       |        |      |      |      |                 |
| Mutant                 | •                      | 6/8  | •    | •      | 3/7  | •                      | 10/10 | 7/11   | 7/11 | •    | 7/7  | 9/9             |
| Round 9 Distribution   |                        |      |      |        |      |                        |       |        |      |      |      |                 |
| Mutant                 | 8/10                   | 4/4  | 6/6  | 3/6    | 8/12 | 6/6                    | 6/6   | 6/6    | 6/6  | 3/6  | 5/5  | 4/4             |
| Amino Acid Number      |                        |      |      |        |      |                        |       |        |      |      |      |                 |
| Jc1/NS5AB-mKO2-Bsd     | 249                    | 335  | 411  | 433    | 756  | 1564                   | 1691  | 2273   | 2274 | 2437 | 2729 | N/A             |
| H77 ref                | 249                    | 335  | 411  | 433    | 752  | 1560                   | 1687  | 2273   | 2274 | 2415 | N/A  | N/A             |
| Amino Acid Change      | Silent                 | A→S  | I→V  | Silent | V→A  | A→T                    | H→L   | Silent | C→R  | D→N  | Y→H  | N/A             |

**Table 2.1: Sequence analysis of point mutations in round 1 and round 9 supernatant passages of superinfectious virus.**

RNA was isolated, reverse transcribed, cloned, and sequenced from the superinfectious Jc1/<sup>NS5AB-mKO2-Bsd</sup> strain 41 days after continuous passage of superinfected cells (round 1), and after 9 rounds of passage of viral supernatants over replicon-containing cells (round 9). The nucleotide and amino acid positions of mutations present in ≥50% of the sequenced clones are given for the Jc1/<sup>NS5AB-mKO2-Bsd</sup> strain and H77 reference sequence (AF009606), where possible.

\*: Mutant prevalence in sequenced clones is given as follows: X/X (50/50 distribution), X/x (major/minor nucleotide), X (fixed mutation), • (mutation not observed).

\*\* : Mutant distribution is given as the number of sequenced clones with/without the mutation. For the poly-U/UC mutation, a number of round 1 & 9 clones had a deletion in this region, and do not contribute to these numbers.

| Clone  | mKO2-Bsd Deletion |                         | Poly-U/UC Deletion |             | Poly-U Tract Lengths |             |             |             |             |             |             |             |             |             |             |             |             |             |             |             |             |             |             |             |             |             |             |             |             |             |             |             |             |             |    |
|--------|-------------------|-------------------------|--------------------|-------------|----------------------|-------------|-------------|-------------|-------------|-------------|-------------|-------------|-------------|-------------|-------------|-------------|-------------|-------------|-------------|-------------|-------------|-------------|-------------|-------------|-------------|-------------|-------------|-------------|-------------|-------------|-------------|-------------|-------------|-------------|----|
|        | Round 1           | Round 9                 | Round 1            | Round 9     | Round 1              | Round 9     |             |             |             |             |             |             |             |             |             |             |             |             |             |             |             |             |             |             |             |             |             |             |             |             |             |             |             |             |    |
| 1      | 7733-8623         | 8586-8798               | 10716-10739        | 10716-10739 | 40                   | 63          |             |             |             |             |             |             |             |             |             |             |             |             |             |             |             |             |             |             |             |             |             |             |             |             |             |             |             |             |    |
| 2      |                   | 8586-8795               |                    |             | 41                   | 45          |             |             |             |             |             |             |             |             |             |             |             |             |             |             |             |             |             |             |             |             |             |             |             |             |             |             |             |             |    |
| 3      | 7677-8822         | 8586-8795               |                    |             | 10716-10739          | 10716-10739 | 65          | 50          |             |             |             |             |             |             |             |             |             |             |             |             |             |             |             |             |             |             |             |             |             |             |             |             |             |             |    |
| 4      |                   | 8589-8798               |                    |             |                      |             | 41          | 45          |             |             |             |             |             |             |             |             |             |             |             |             |             |             |             |             |             |             |             |             |             |             |             |             |             |             |    |
| 5      | No Deletion       | 8589-8798               |                    |             |                      |             | 10716-10739 | 10716-10739 | 45          | 36          |             |             |             |             |             |             |             |             |             |             |             |             |             |             |             |             |             |             |             |             |             |             |             |             |    |
| 6      |                   | 8525-8562,<br>8584-8799 |                    |             |                      |             |             |             | 10716-10739 | 10716-10739 |             |             |             |             |             |             |             |             |             |             |             |             |             |             |             |             |             |             |             |             |             |             |             |             |    |
| 7      |                   | •                       |                    |             |                      |             |             |             |             |             | 10716-10739 | 10716-10739 | 39          | 35          |             |             |             |             |             |             |             |             |             |             |             |             |             |             |             |             |             |             |             |             |    |
| 8      |                   | •                       |                    |             |                      |             |             |             |             |             |             |             | 10716-10739 | 10716-10739 | 50          | •           |             |             |             |             |             |             |             |             |             |             |             |             |             |             |             |             |             |             |    |
| 9      |                   | •                       |                    |             |                      |             |             |             |             |             |             |             |             |             | 10716-10739 | 10716-10739 | 54          | •           |             |             |             |             |             |             |             |             |             |             |             |             |             |             |             |             |    |
| 10     |                   | •                       |                    |             |                      |             |             |             |             |             |             |             |             |             |             |             | 10716-10739 | 10716-10739 | 50          | •           |             |             |             |             |             |             |             |             |             |             |             |             |             |             |    |
| 11     |                   | •                       |                    |             |                      |             |             |             |             |             |             |             |             |             |             |             |             |             | 10716-10739 | 10716-10739 | 41          | •           |             |             |             |             |             |             |             |             |             |             |             |             |    |
| 12     |                   | •                       |                    |             |                      |             |             |             |             |             |             |             |             |             |             |             |             |             |             |             | 10716-10739 | 10716-10739 | 52          | •           |             |             |             |             |             |             |             |             |             |             |    |
| 13     |                   | •                       |                    |             |                      |             |             |             |             |             |             |             |             |             |             |             |             |             |             |             |             |             | 10716-10739 | 10716-10739 | 50          | •           |             |             |             |             |             |             |             |             |    |
| 14     |                   | •                       |                    |             |                      |             |             |             |             |             |             |             |             |             |             |             |             |             |             |             |             |             |             |             | 10716-10739 | 10716-10739 | 63          | •           |             |             |             |             |             |             |    |
| 15     |                   | •                       |                    |             |                      |             |             |             |             |             |             |             |             |             |             |             |             |             |             |             |             |             |             |             |             |             | 10716-10739 | 10716-10739 | 65          | •           |             |             |             |             |    |
| 16     |                   | •                       |                    |             |                      |             |             |             |             |             |             |             |             |             |             |             |             |             |             |             |             |             |             |             |             |             |             |             | 10716-10739 | 10716-10739 | •           | •           |             |             |    |
| 17     |                   | •                       |                    |             |                      |             |             |             |             |             |             |             |             |             |             |             |             |             |             |             |             |             |             |             |             |             |             |             |             |             | 10716-10739 | 10716-10739 | •           | •           |    |
| 18     |                   | •                       |                    |             |                      |             |             |             |             |             |             |             |             |             |             |             |             |             |             |             |             |             |             |             |             |             |             |             |             |             |             |             | 10716-10739 | 10716-10739 | •  |
| Median |                   |                         |                    |             |                      |             |             |             |             |             |             |             |             |             |             |             |             |             |             |             |             |             |             |             |             |             |             |             |             |             |             |             |             |             | 50 |

**Table 2.2: Sequence analysis of deletions in round 1 and round 9 supernatant passages of superinfectious virus.**

RNA was isolated, reverse transcribed, cloned, and sequenced from the superinfectious Jc1/<sup>NS5AB-mKO2-Bsd</sup> strain 41 days after continuous passage of superinfected cells (round 1), and after 9 rounds of passage of viral supernatants over replicon-containing cells (round 9). The nucleotide positions of deletions are given for the Jc1/<sup>NS5AB-mKO2-Bsd</sup> strain from each clone sequenced. A consistent 24-nt deletion of the 10716-10733 region was observed in every clone sequenced; however, the preceding poly-U tract varied in length according to each clone. The lengths of the poly-U tract are given in the third column for each clone, as well as the median length.

•: not a sequenced clone.

### **Viral adaptive mutations increase HCV superinfectivity**

How do these point mutations and poly-U/UC deletion affect superinfectivity? To examine this, we introduced the seven amino acid substitutions in the viral coding sequence and a 21-nt deletion in the poly-U/UC into the parental Jc1/<sup>NS5AB-mKO2-Bsd</sup> construct (the observed deletions in mKO2-Bsd were not introduced). Our initial studies showed that the NS5A D2437N mutation in the protease cleavage site between NS5A and mKO2-Bsd was detrimental to superinfectivity (data not shown). This is not surprising, as this is a change from a highly conserved—but not essential [60]—acidic residue in the P6 position of the NS5A/mKO2-Bsd cleavage site. Correspondingly, this mutation was analyzed separately. The mutant and parental WT Jc1/<sup>NS5AB-mKO2-Bsd</sup> viruses were used to superinfect Jc1/ $\Delta$ E1E2<sup>NS5A-GFP-Bsd</sup> replicon cells. Viral input was normalized as the amount of HCV core per infection, which did not appreciably vary across the mutant strains following viral production (Supplemental Figure A.5B). The Mut7 virus, carrying the poly-U/UC deletion and 6/7 of the amino acid substitutions, was ~15-fold as superinfectious as the WT strain (Figure 2.4B). Note that viral genomes including the NS5A D2437N mutation in the context of the Mut7 mutations have a defect superinfectivity.

We next analyzed the contribution of the Mut7 mutations to superinfectivity, by reverting each of the mutations to WT, and used the resulting viruses to infect Jc1/ $\Delta$ E1E2<sup>NS5A-GFP-Bsd</sup> replicon cells. The E1 A335S, p7 V756A, and NS5A C2274R mutations appeared to be the most important (Figure 2.4B, Supplemental Figure A.5C), as their reversion to WT caused a decrease in superinfectivity. To ensure that the superinfectious phenotype of these viruses was not limited to the same

polyclonal Jc1/ $\Delta$ E1E2<sup>NS5A-GFP-Bsd</sup> replicon cell line used for initial selection of the virus, infections were also carried out in a separately transfected and isolated monoclonal Jc1/ $\Delta$ E1E2<sup>NS5A-GFP-Bsd</sup> replicon cell line. No difference in superinfection was observed between the polyclonal and monoclonal replicon cell lines.

The various mutant strains of Jc1/<sup>NS5AB-mKO2-Bsd</sup> were then used to infect naive Huh7.5 cells. Interestingly, mutant viral strains with higher superinfectivity in replicon cells had higher infectivity in naive Huh7.5 cells (Figure 2.4B & C), as well as higher viral titers in supernatants not normalized by HCV core (Supplemental Figure A.5A). Furthermore, when the viruses were used to infect the Con1 SGR/<sup>NS5A-GFP</sup> genotype 1b replicon cell line (Figure 2.4A & D), higher superinfectivity in Jc1/ $\Delta$ E1E2<sup>NS5A-GFP-Bsd</sup> replicon cells correlated with higher superinfectivity in Con1 SGR/<sup>NS5A-GFP</sup> replicon cells. However, superinfectivity was generally lower in the Con1 SGR/<sup>NS5A-GFP</sup> replicon cells, suggesting that the superinfectious virus may have evolved to specifically superinfect cells replicating genotype 2a HCV RNA.

We were intrigued that reverting either the NS3 A1564T or the NS4A H1691L mutation led to an increase in superinfectivity (Figure 2.4B). We therefore reverted both mutations together to the WT sequence and superinfected Jc1/ $\Delta$ E1E2<sup>NS5A-GFP-Bsd</sup> replicon cells with this virus (Figure 2.4E). Surprisingly, reverting both mutations did not lead to a further increase in superinfectivity; instead, superinfectivity was lower than in the single revertants. We therefore conclude that the NS3 A1564T and NS4A H1691L mutations increase superinfectivity in isolation, but not in conjunction.

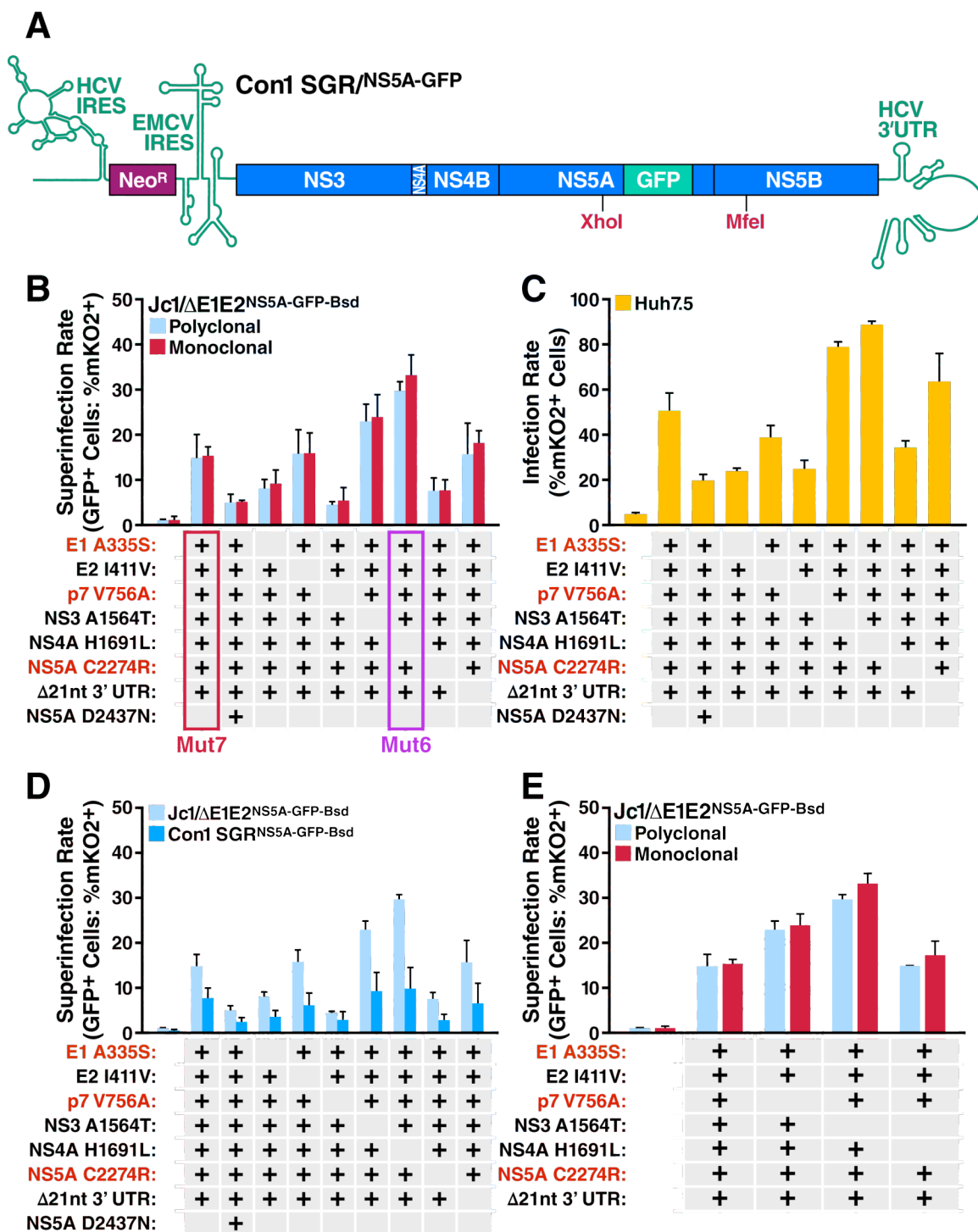


Figure 2.4: Contribution of identified mutations to the superinfectious phenotype.

(A) Schematic diagram of the genotype 1b Con1 SGR/<sup>NS5A-GFP</sup> replicon. Neo<sup>R</sup> indicates the neomycin resistance gene. (B) Recapitulation of the superinfectious phenotype with seven mutations. Mutations were introduced into the WT Jc1/<sup>NS5A-B-mKO2-Bsd</sup> construct, and viral supernatants were produced by transfection of these variants into Huh7.5 cells. Supernatants were normalized to the quantity of HCV core (determined by ELISA) and Jc1/ $\Delta$ E1E2<sup>NS5A-GFP</sup> replicon-containing cells were superinfected. The percent superinfection was assessed by flow cytometry 3 days later. To ensure that the superinfectious phenotype was not limited to a particular Jc1/ $\Delta$ E1E2<sup>NS5A-GFP</sup> replicon cell line, superinfections were performed in polyclonal and monoclonal replicon cells (replicon cell lines were isolated separately). Note that the NS5A D2437N mutation had a detrimental effect on superinfectivity and was thus excluded from the majority of variants analyzed. (C) Histogram of results from naive Huh7.5 cells infected with the given viral variants. Superinfectivity correlates with a higher degree of infectivity in naive cells. (D) Superinfection is reduced in a genotype 1b replicon cell line. Polyclonal Jc1/ $\Delta$ E1E2<sup>NS5A-GFP</sup> and Con1 SGR/<sup>NS5A-GFP</sup> replicon cells were superinfected with the given viral variants. (E) Both NS3 A1564T and NS4A H1691L increase superinfectivity alone but not when the mutations were combined.  $n=4$  independent viral preparations and infections; error bars indicate + SEM.



### **Adaptive mutations promote superinfectivity in a non-reporter Jc1 strain**

Is the increase in infectivity and superinfectivity afforded by the Mut7 and Mut6 mutations limited to the Jc1/<sup>NS5AB-mKO2-Bsd</sup> reporter strain of the virus? We introduced the Mut7 and Mut6 virus mutations (Figure 2.4B) into a non-reporter Jc1 strain to ensure this was not the case. Indeed, when analyzing viral infectivity in supernatants of transfected Huh7.5 cells, we observed a 1-log and 1.5-log increase in infectivity for the Mut7 and Mut6 virus, respectively, compared to WT Jc1 (Figure 2.5A).

Analysis of superinfection of replicon-containing cells is difficult in the absence of a reporter for the secondary virus, as the replicon causes the cells to immunostain positive for viral proteins and dsRNA. However, because the highly superinfectious virus excluded the primary replicon from cells (Figure 2.3C & E), we were able to use this exclusion as an indirect means of measuring superinfection efficiency in non-reporter Jc1 strains. We superinfected Jc1/ $\Delta$ E1E2<sup>NS5A-GFP-Bsd</sup> polyclonal replicon cells with Mut6, Mut7, and WT non-reporter Jc1, as well as with the superinfecting Jc1/<sup>NS5AB-mKO2-Bsd</sup> strain (Rounds 10, 11, & 13). The primary replicon (%GFP+ cells) was rapidly excluded when cells were superinfected with Mut7 or Mut6 Jc1, compared to WT Jc1 or uninfected cells (Figure 2.5B).

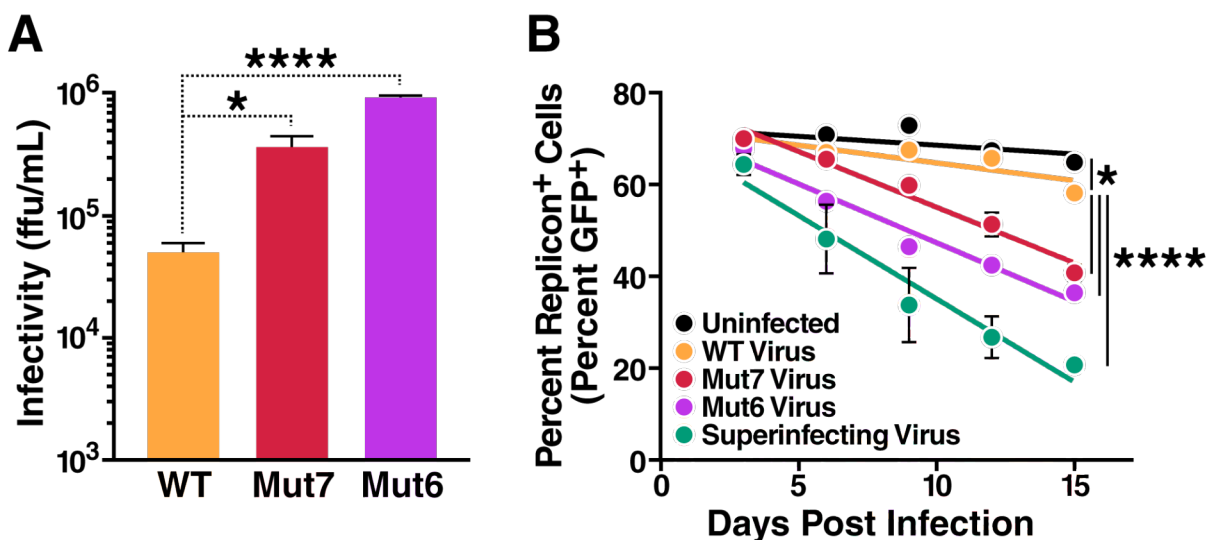


**Figure 2.5: The highly infectious and superinfectious phenotype of the Mut7 and Mut6 viruses is not limited to the Jc1/<sup>NS5AB-mKO2-Bsd</sup> reporter strain.**

(A) Infectivity of supernatants from Mut7 and Mut6 Jc1–transfected cultures is ~10-fold higher than WT Jc1–transfected cultures. Untagged Jc1 (WT, Mut7, or Mut6) viral supernatants produced by transfection of Huh7.5 cells were assessed for infectivity using the limiting dilution assay on naïve Huh7.5 cells. (\*:p<0.05, \*\*\*\*:p<0.0001, one-way ANOVA) (B) Exclusion of the primary replicon is enhanced in Mut7- and Mut6-superinfected cultures. Polyclonal Jc1/ΔE1E2<sup>NS5A-GFP</sup> replicon-containing cells were superinfected with untagged Jc1 (WT, Mut7, or Mut6) or superinfectious (Rounds 10, 11, & 13) viral supernatants. Exclusion of the primary replicon was assessed by flow cytometry. Note the greater loss of the primary replicon in Mut7 Jc1 and Mut6 Jc1-superinfected cultures compared to WT Jc1-superinfected or non-superinfected cultures. *n*=3 independent viral preparations and infections; error bars indicate ± SEM. (\*p<0.05, \*\*\*\*p<0.0001, analysis of covariance).

### **HCV strains with a poly-U/UC deletion and the NS5A C2274R mutation overcome the post-entry superinfection block**

We next focused our efforts on defining the specific mutations that could act at the post-entry step where superinfection exclusion typically occurs [52,53]. The E1, E2, and p7 mutations affect viral entry or assembly and are thus unlikely to play a role. The NS3 and NS4A mutations did not greatly increase superinfectivity, and are also unlikely candidates. In contrast, the NS5A C2274R mutation proved important for superinfection (Figure 2.4B-D), and increased the amount of viral protein in infected cells (Figure 2.6B-D). Although the poly-U/UC deletion appeared to be dispensable for superinfection, we observed that the median length of the poly-U/UC tract decreased as the superinfectious virus was passaged over replicon cells (Table 2.2). Furthermore, we found that overall HCV protein levels were increased in cells transfected with viral RNA carrying deletions in the poly-U/UC (Figure 2.6C), consistent with studies demonstrating that a shorter poly-U/UC increases HCV infectivity *in vitro* [61,62]. These results suggest that the deletion in the poly-U/UC region and the NS5A C2274R mutation are key to allowing the virus to overcome post-entry superinfection exclusion.

We analyzed the effects of the adaptive mutations on overcoming the post-entry superinfection block by “supertransfecting” Jc1/ $\Delta$ E1E2<sup>NS5A-GFP-Bsd</sup> polyclonal replicon cells with various mutant Jc1/<sup>NS5AB-mKO2-Bsd</sup> RNAs. Supertransfection (as opposed to superinfection) of replicon-containing cells focuses specifically on the post-entry block, as virion assembly and entry do not play a role. In addition to the 21-nt deletion of the poly-U/UC in the superinfection studies, viral genomes carrying a 36-

nt poly-U/UC deletion were also used (Figure 2.6A). Progressively shortening the poly-U/UC tract caused a corresponding increase in supertransfection (Figure 2.7A). By including the NS5A C2274R mutation in the context of the poly-U/UC deletions, a slight increase in supertransfection was observed. However, when the other Mut7 mutations were included (E1 A335S, E2 I411V, p7 V756A, NS3 A1564T, and NS4A H1691L), we detected no additional increase in supertransfection (Figure 2.7A). When these same viral RNAs were used to transfect naive Huh7.5 cells, we observed that a shorter poly-U/UC increased the transfection efficiency but not to the same extent, due to the high permissivity of naive cells (Figure 2.7B).

By superinfecting Jc1/ $\Delta$ E1E2<sup>NS5A-GFP-Bsd</sup> polyclonal replicon cells with these mutant strains, we again observed that a shorter poly-U/UC allowed the secondary virus to better overcome superinfection exclusion (Figure 2.7C). Furthermore, there appeared to be a synergistic effect of the shorter poly-U/UC and the NS5A C2274R mutation on superinfection efficiency. However, we did not observe an effect of the poly-U/UC deletion on superinfection in the context of the Mut7 mutations. This is likely to result from the highly infectious phenotype that results from the E1 and p7 mutations, which may allow for sufficiently high entry of the secondary virus to mask the effect of the poly-U/UC deletion.



(A) Sequence alignment of poly-U/UC sequences from mutant and WT viral variants. The sequence from the superinfecting virus reflects the 24-nt deletion found in all sequenced clones; the length of the poly-U tract varied according to each clone. Nucleotides are numbered according to the Jc1/<sup>NS5AB-mKO2-Bsd</sup> RNA. (B) Representative flow cytometry plot indicating an increase in the mean fluorescence intensity of mKO2 in Huh7.5 cells infected with WT or NS5A C2274R Jc1/<sup>NS5AB-mKO2-Bsd</sup>. (C) Western blots indicating an increase in HCV core and mKO2-Bsd in Huh7.5 cells transfected with HCV Jc1/<sup>NS5AB-mKO2-Bsd</sup> strains carrying the NS5A C2274R and  $\Delta$  3' UTR mutations. (D) Mean fluorescent intensity (MFI) of mKO2 transgene in naïve Huh7.5 cells infected with mutant and WT Jc1/<sup>NS5AB-mKO2-Bsd</sup> strains. Note that the MFI decreases in cells infected with viruses lacking the NS5A C2274R and p7 V756A mutations.  $n=4$  independent viral preparations and infections.

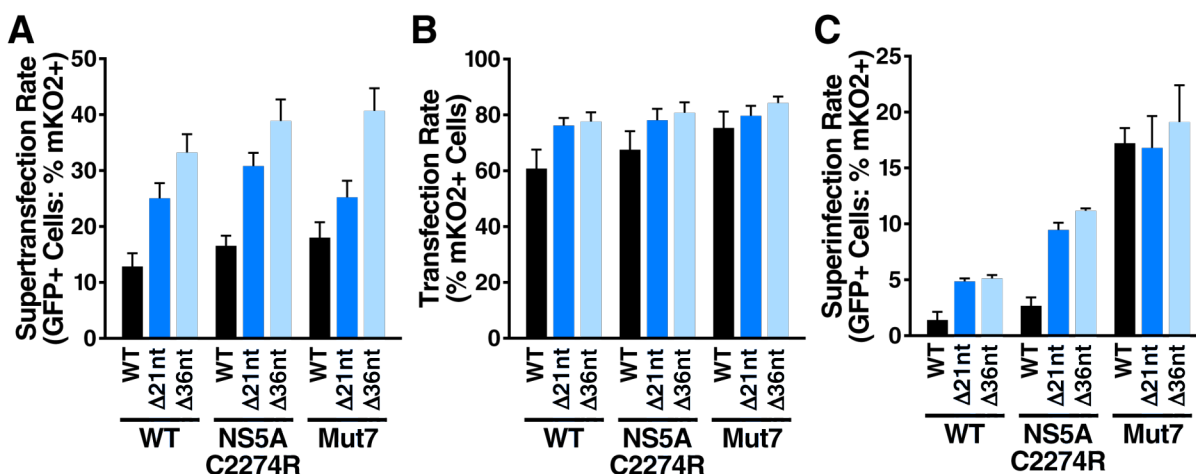


**Figure 2.7: NS5A C2274R and  $\Delta$  3' UTR mutations increase “supertransfection” in replicon-containing cells.**

(A) “Supertransfection” is greatly enhanced by poly-U/UC deletions and slightly enhanced by the NS5A C2274R mutation. Jc1/ $\Delta$ E1E2<sup>NS5A-GFP</sup> polyclonal replicon cells were transfected with WT and mutant Jc1/<sup>NS5AB-mKO2-Bsd</sup> transcripts. The “supertransfection” rate was assessed by flow cytometry as the percentage of replicon-positive cells (GFP+) that were also positive for the secondary Jc1/<sup>NS5AB-mKO2-Bsd</sup> virus (mKO2+) 2 days post-transfection.  $n=4$  independent transfections. (B) Transfection rates in naive cells are also enhanced by the poly-U/UC deletion and NS5A C2274R mutation. Naive Huh7.5 cells were transfected with WT and mutant Jc1/<sup>NS5AB-mKO2-Bsd</sup> transcripts and transfection rates (% mKO2+) were assessed by flow cytometry 2 days later.  $n=4$  independent transfections. (C) Superinfection rates are also enhanced by the poly-U/UC deletion and NS5A C2274R mutation. Jc1/ $\Delta$ E1E2<sup>NS5A-GFP</sup> polyclonal replicon cells were infected with WT and mutant Jc1/<sup>NS5AB-mKO2-Bsd</sup> viral supernatants (normalized to the amount of HCV core per

infection). Superinfection rates were assessed by flow cytometry 3 days later.  $n=3$  independent viral preparations and infections; error bars indicate + SEM.



### **Translation of superinfectious viral RNA is unaffected by poly-U/UC length or the NS5A C2274R mutation**

Results from prior studies have been inconsistent on whether superinfection exclusion is mediated in part by a block in translation of secondary viral RNA [52,53,63]. As the poly-U/UC deletion and the NS5A C2274R mutation appear to be key players in overcoming the post-entry superinfection block, we chose to assess the effect of these mutations on HCV IRES-mediated translation. RNAs encoding firefly luciferase (FLuc) driven by the HCV IRES were transfected into Jc1/ $\Delta$ E1E2<sup>NS5A-GFP-Bsd</sup> monoclonal replicon cells, as well as a replicon-cured variant of this cell line (cured by Ifn- $\alpha$  treatment). 5'-7-methyl-guanosine-capped and 3'-polyadenylated Renilla luciferase (RLuc) RNA was cotransfected as a transfection control, and luciferase activity was assessed 2 hours post-transfection. Deletions in the poly-U/UC tract of the 3' UTR did not appear to have any effect on translation, although including the 3' UTR did greatly enhance translation (Figure 2.8A). Furthermore, no difference was observed in replicon-containing and replicon-cured cells.

We assessed the effect of a shorter poly-U/UC and the NS5A C2274R mutation on HCV IRES-mediated translation in a more relevant context by introducing these mutations into Jc1/<sup>NS5AB-FLuc</sup>-GND constructs. The NS5B GND mutation ensures that viral RNA replication cannot occur [64]; therefore, FLuc luminescence will only reflect viral RNA translation. Viral RNA translation was not increased as a result of the mutations; if anything, the 21-nt deletion decreased translation (Figure 2.8B). Interestingly, viral RNA translation was ~two-fold greater in replicon cells than in

replicon-cured cells. We did not observe this effect with the minimal 5'UTR-FLuc-3'UTR constructs, suggesting that replicons enhance HCV IRES-mediated translation specifically in the context of the full-length viral sequence. Combined with this observation, the failure of the poly-U/UC deletion and NS5A C2274R mutations to enhance HCV IRES-mediated translation suggests that post-entry superinfection exclusion does not result from a block in secondary viral RNA translation.

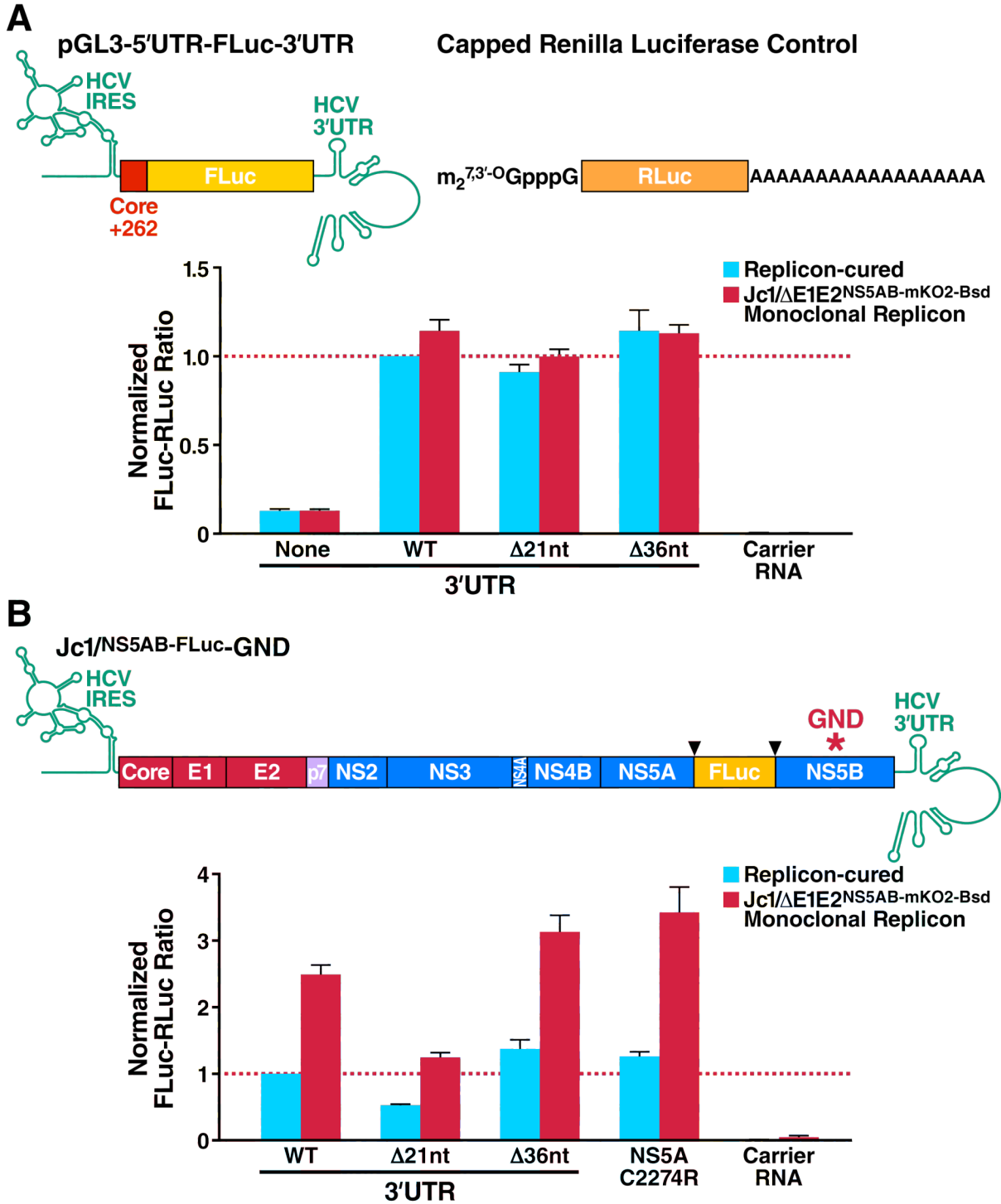


Figure 2.8: Viral RNA translation is not enhanced by the NS5A C2274R and  $\Delta$  3' UTR mutations.

(A) Deletions of the poly-U/UC tract do not enhance HCV IRES-mediated translation. Jc1/ $\Delta$ E1E2<sup>NS5A-GFP</sup> polyclonal replicon cells and Ifn- $\alpha$  replicon-cured cells were transfected with HCV IRES-dependent firefly luciferase (FLuc) transcripts containing WT and mutant HCV 3' UTRs, as well as a capped renilla luciferase (RLuc) transcript as a transfection control. Core+262 refers to a fusion of 262 nt of HC-J6 core sequence to FLuc to enhance HCV IRES-mediated translation. Luciferase activity was assessed 2 hours post-transfection, and the ratio of FLuc/RLuc activity was normalized to the WT 3'UTR construct in replicon-cured cells.  $n=3$  independent transfections. (B) Histogram of normalized FLuc/RLuc ratios showing that NS5A C2274R and  $\Delta$  3' UTR mutations do not enhance translation of replication-incompetent viral RNAs. Cells were transfected as in (A) with Jc1/<sup>NS5AB-FLuc</sup>-GND transcripts (polymerase defective, NS5B GDD $\rightarrow$ GND mutation) containing NS5A C2274R or  $\Delta$  3' UTR mutations. Arrowheads indicate NS5A/5B protease cleavage sites.  $n=3$  independent transfections of 2 replicates each; error bars indicate +SEM.

## DISCUSSION

In this study, we used highly infectious, Jc1/<sup>NS5AB</sup> fluorophore-tagged HCV genomes to select for a variant of HCV capable of high levels of superinfection. We find that the emergence of superinfectivity increases the fitness of the virus generally, and that superinfectious viruses can exclude the primary infection. The superinfectious phenotype of a virus also depends on the primary infection; the virus we isolated was far more capable of superinfecting genotype 2a compared to genotype 1a replicon-containing cells. We identified specific adaptive mutations that allow HCV to overcome the post-entry barrier to superinfection, namely a deletion in the poly-U/UC tract and a C2274R mutation in NS5A. Lastly, we demonstrate that these adaptive mutations do not alter translation of HCV RNA, and that superinfection exclusion generally is not caused by a block in the translation of the secondary viral RNA.

We demonstrate that Jc1/<sup>NS5AB</sup>-tagged genomes display infectious titers more closely resembling untagged Jc1 than the commonly used bicistronic and NS5A domain-III fusion-tagged Jc1 reporter genomes (Figure 2.1B) [26,53,65]. While this publication was in preparation, Jc1/<sup>NS5AB</sup> fluorophore-tagged genomes were described separately by Horwitz et al. [66]. In Horwitz et al., a Ypet tag was inserted between NS5A and NS5B bracketed by minimal NS3/4A cleavage sites (DTTVCC/SM); in contrast, we used longer cleavage sites (SEEDDTTVCC/SMSYS). We observed minor differences between our tagged Jc1/<sup>NS5AB</sup> genomes and, in contrast to their findings, observed incomplete cleavage between NS5A and the

fluorophore tag. Further, after 11 passages of infected cells (Figure 2.3C), we observed that only 4/18 (22%) of the sequenced viral genomes have deletions in the fluorophore tag (Table 2.2), while Horwitz et al. observed that ~50% of infected cells lose fluorophore-derived fluorescence after only 6 passages. However, our publications agree on the main finding that insertion of heterologous proteins between NS5A/5B in Jc1 genomes does not markedly affect infectious viral titers.

Interestingly, we observed that a fluorescent reporter from a bicistronic HCV strain (GFP-Jc1) is diffusible, while the reporter from Jc1/<sup>NS5AB-XFP</sup> HCV strains remains associated with the RC. This observation suggests that translation of HCV RNA and NS3/4A cleavage of the polyprotein occurs in separate subcellular compartments. Presumably, translation occurs while the nascent peptides are still exposed to the cytoplasm, allowing GFP to diffuse in the GFP-Jc1 strain. Cleavage of nonstructural proteins appears to occur inside the HCV RC, preventing the exit of fluorescent proteins in the Jc1/<sup>NS5A-XFP</sup> strains. Furthermore, the lack of reporter diffusion in Jc1/<sup>NS5AB-XFP</sup> strains suggests that the HCV RC is a tightly closed structure that prevents diffusion of soluble proteins, such as GFP or mKO2-Bsd. HCV RC is in a conformation that inhibits entry of proteins larger than 16 kDa, such as S7 nuclease or proteinase K [67]. Our data demonstrate that exit from the RC is likely to be prevented in a similar manner.

The Jc1/<sup>NS5AB-mKO2-Bsd</sup> viral genomes were highly infectious and produced bright orange fluorescence in infected cells, permitting simple analysis of the dynamics of HCV superinfection in replicon-containing hepatoma cells. These two characteristics allowed us, in the space of a few weeks, to select for a strain of HCV that could

superinfect genotype 2a replicon-containing cells. Notably, the superinfectious HCV strain had two key characteristics: it displayed higher infectivity overall, even in naive cells, and it excluded the primary replicon in the space of 9–15 days. Interestingly, the superinfectious phenotype was weaker in genotype 1a replicon-containing cells. Therefore, selection for superinfectivity may be limited to the primary strain of HCV already present in host cells.

The importance of a blockade to viral entry in the process of superinfection exclusion has been controversial, as initial studies found no defect in entry of HIV particles pseudotyped with an HCV envelope [53]. However, both increased and decreased expression of viral entry receptors can occur upon HCV infection, potentially enhancing or blockading HCV entry into infected cells [13,52,68,69,70]. Regardless of any effects on viral receptors, when a secondary replicon is “supertransfected” into cells already containing an HCV replicon, it replicates very poorly, clearly showing that post-entry superinfection exclusion exists [51,71]. This post-entry replication block may directly result from blocking replication of secondary viral RNA, or indirectly, by preventing translation of secondary viral RNA.

Initial analysis of the adaptive mutations acquired in the superinfectious strain suggested that the E1 A335S, p7 V756A, and NS5A C2274R mutations contributed significantly to the phenotype. However, mutations in E1, E2, or p7 were unlikely to allow the virus to overcome post-entry superinfection exclusion, as these proteins only affect viral entry or assembly. Indeed, by “supertransfecting” viral transcripts into replicon-containing cells, thus focusing specifically on the post-entry superinfection block, we found the NS5A C2274R mutation and poly-U/UC deletions

to be most crucial in overcoming the post-entry block. The importance of the E1 and p7 mutations in overcoming superinfection exclusion is likely a result of simply enhancing viral assembly and fusion, and increasing the number of secondary viral genomes in replicon-containing cells.

Interestingly, neither the NS5A C2274R mutation nor the poly-U/UC deletions affected viral RNA translation. Presumably, these mutations allow HCV to overcome the post-entry superinfection block by modulating HCV RNA replication. Further, we found that translation specifically of full-length HCV transcripts was enhanced in replicon-containing cells. This agrees with previous findings that HCV IRES-mediated translation is enhanced in replicon-containing cells [63], but disagrees with results indicating that translation of a secondary subgenomic viral RNA is decreased in replicon-containing cells [53]. However, Schaller et al. used a bicistronic construct in which translation of luciferase was driven by the HCV IRES and the viral polyprotein by EMCV IRES. In our study, the native HCV IRES drove translation of a full-length secondary viral RNA also encoding luciferase, and may be more physiologically relevant.

We demonstrate for the first time that HCV can be selected to overcome superinfection exclusion *in vitro* in a relatively short time span. In the setting of chronic infections in patients, which persist for decades, it is likely that HCV is similarly selected to gain this ability. Extremely high viral loads ( $10^5$ – $10^6$  IU/mL) are characteristic of chronic HCV infection [72], and HCV is a highly variable virus [73]. HCV almost certainly will evolve the ability to overcome superinfection exclusion *in vivo* if it can. Indeed, we find that superinfectious viruses are more infectious



generally, which suggests that superinfection exclusion acts to continually select for highly fit HCV variants in patients.

This higher overall infectivity of the superinfectious strain suggests that superinfection exclusion may be a double-edged sword for *in vivo* pathogenicity. On one hand, superinfection exclusion prevents two HCV strains from co-occupying the same cell, thus reducing recombination between viral strains. Indeed, natural recombination between HCV strains is generally understood to be a rare phenomenon [31,37,38]. Low levels of recombination tend to prevent transfer of drug resistance or immune evasion between viral strains, a beneficial outcome for patients. However, our results indicate that superinfecting HCV variants were more infectious overall, suggesting that superinfection exclusion may select for more fit HCV strains in an *in vivo* setting. Therefore, superinfection exclusion may act in a patient setting beneficially to reduce recombination, and detrimentally to select for highly infectious viral variants.

Of note, superinfectious viruses also rapidly excluded the primary replicon after superinfection. This phenomenon would act to further prevent co-occupancy of the same cell with multiple viral genomes and thus inter-strain recombination. The mechanism by which the superinfectious virus excludes the primary replicon is unclear. We recently described a mechanism of intracellular competition between HCV strains, whereby mitosis of host cells leads to a genetic bottleneck in HCV diversity [54]. The higher replicative capacity of the superinfectious strain may induce a bias in this intracellular competition in dividing cells, leading to eventual exclusion of the primary replicon.

The post-entry block to HCV superinfection has been postulated to result from sequestration of a limiting host factor(s) by the primary virus [52], as evidenced by a plateau in HCV RNA and protein levels shortly after infection. We found that the NS5A C2274R and poly-U/UC deletion are key players in allowing a secondary virus to overcome the post-entry superinfection block. In future studies, it will be interesting to determine whether the variants of these HCV proteins and RNA have a greater affinity for certain host proteins. Such host proteins would likely serve as rate-limiting factors in the HCV life cycle, and as such would be excellent targets for antiviral therapies.

## MATERIALS AND METHODS

**Cells and culture conditions.** Huh7.5 cells, a kind gift from C.M. Rice (Rockefeller University), [74] were maintained in Dulbecco's modified Eagle medium (DMEM), supplemented with 10% fetal bovine serum (FBS), 2 mM L-glutamine, 100 IU/mL penicillin, and 100  $\mu$ g/mL streptomycin (Mediatech). Cells were passaged every 3 days or when they became confluent. For isolation of replicon cell lines, cells were selected with blasticidin (10  $\mu$ g/mL, Invitrogen) or G418 sulfate (1 mg/mL, Axenia Biologics) 2–3 days post-transfection. Monoclonal replicon cell lines were obtained by limiting dilution of transfected cells. To obtain replicon-cured cell lines, the monoclonal Jc1/ $\Delta$ E1E2<sup>NS5A-GFP-Bsd</sup> replicon cell line was treated with 100 U/mL recombinant human interferon- $\alpha$  (Ifn- $\alpha$ , R&D Systems) for 2 weeks, followed by a recovery period of at least 9 days without Ifn- $\alpha$  treatment.

**Plasmid Construction.** To assemble NS5AB-reporter genomes, a linker with a multiple cloning site (*Bgl*III, *Eco*RI, *Xba*I, *Pac*I) flanked by NS5A/5B protease cleavage sites was introduced into the parental pBR322 Jc1 construct. Overlapping-PCR based gene synthesis was used to generate this linker, using the primers NS5ABmcs1-NS5ABmcs20 (Supplemental Table A.2). The linker and pBR322 Jc1 were digested with *Rsr*II and *Bsr*GI and ligated to generate pBR322 Jc1/<sup>NS5AB-MCS</sup>. Firefly luciferase (FLuc), GFP, mKO2, GFP-Bsd and mKO2-Bsd were amplified using the NS5AB\_*Bgl*III\_Fw and NS5AB\_*Eco*RI\_Rev primers given in Supplemental Table A.2. The resulting PCR products were digested with *Eco*RI and *Bgl*III and

ligated into pBR322 Jc1/<sup>NS5AB-MCS</sup> to generate pBR322 Jc1/<sup>NS5AB-FLuc</sup>, pBR322 Jc1/<sup>NS5AB-GFP</sup>, pBR322 Jc1/<sup>NS5AB-mKO2</sup>, pBR322 Jc1/<sup>NS5AB-GFP-Bsd</sup>, and pBR322 Jc1/<sup>NS5AB-mKO2-Bsd</sup>, respectively. To generate the dually-tagged replicon construct, pBR322 Jc1/ $\Delta$ E1E2<sup>NS5A-GFP</sup> [54] was digested with *RsrII* and *SanDI* and the resulting NS5A-GFP fragment was cloned into pBR322 Jc1/<sup>NS5AB-mKO2</sup> to generate pBR322 Jc1/<sup>NS5A-GFP;NS5AB-mKO2-Bsd</sup>. An envelope-deleted variant of this plasmid was created by digesting pBR322 Jc1/ $\Delta$ E1E2<sup>NS5A-GFP</sup> with *KpnI* and the resulting fragment was ligated into pBR322 Jc1/<sup>NS5A-GFP;NS5AB-mKO2-Bsd</sup> to generate pBR322 Jc1/ $\Delta$ E1E2<sup>NS5A-GFP;NS5AB-mKO2-Bsd</sup>.

The assembly of the viral constructs EGFP-Jc1, pBR322 Jc1/<sup>NS5A-GFP-Bsd</sup>, and the pBR322 Jc1/ $\Delta$ E1E2<sup>NS5A-GFP-Bsd</sup> replicon construct was described previously [54,75]. To generate the fluorochrome-tagged Con1 subgenomic replicon, three-piece overlap PCR was carried out. The upstream piece was generated using the primers Con1\_1253\_XhoI\_Fw & Con1\_1365\_GFP overlap Rev New, the middle piece using the primers GFP\_Fw & GFP\_Rev\_-stop, and the downstream piece using the primers Con1\_1366\_GFP\_overlap\_Fw & Con1\_1530\_MfeI\_Rev. The 3 products were mixed and amplified using the flanking primers Con1\_1253\_XhoI\_Fw & Con1\_1530\_MfeI\_Rev. The resulting DNA fragment was digested with *XhoI* & *MfeI* and cloned into pUC Con1.

To generate the mutant variants of pBR322 Jc1/<sup>NS5AB-mKO2-Bsd</sup>, overlapping PCR was carried out using the mutagenesis primers given in Supplemental Table A.3. The upstream flanking primer and the reverse mutagenesis primer were used to generate the upstream product, and the forward mutagenesis primer and the

downstream flanking primer were used to generate the downstream product. Overlap PCR was then carried out using the flanking primers on the upstream and downstream products, and the restriction enzymes given in Supplemental Table A.3 were used to clone the resulting mutants into pBR322 Jc1/<sup>NS5AB-mKO2-Bsd</sup>. To generate untagged mutant variants of Jc1, the *RsrII-BsrGI* fragment from pBR322 Jc1 was ligated into *RsrII-BsrGI*-digested pBR322 Jc1/<sup>NS5AB-mKO2-Bsd</sup> mutant variants.

The HIV-1 based transfer plasmid for HCVpp was generated by amplifying the mCherry sequence with primers GFP\_Fw\_NheI and GFP\_Rev\_stop\_PmeI. The resulting fragment was digested with *NheI* & *PmeI* and ligated into pSicoR MCS [76], to generate the transfer plasmid pSicoR mCherry. To construct HC-J6 HCV envelope plasmids, a fragment corresponding to amino acids 171-750 of the Jc1 sequence was amplified from wild-type and mutant Jc1 viruses using the primers E1E2\_171\_Fw\_NheI and E1E2\_750\_Rev\_PmeI. The resulting fragments were digested with *NheI* & *PmeI* and ligated into pcDNA3.1(+) (Invitrogen), to generate the following plasmids: pcDNA3.1 E1E2 (WT HC-J6 envelope), pcDNA3.1 E1mE2 (E1 A335S), pcDNA3.1 E1E2m (E2 I411V), and pcDNA3.1 E1mE2m (E1 A335S E2 I411V).

To assemble the polymerase-defective Jc1 firefly luciferase constructs for translational analysis, the NS5B GND mutation was transferred from pBR322 JFH1-GND to pBR322 Jc1/<sup>NS5AB-FLuc</sup> by digestion with *HindIII* & *AscI* and ligation. From the resulting Jc1/<sup>NS5AB-FLuc</sup>-GND, a section of DNA comprising NS5AB-FLuc and NS5B-GND was transferred into mutant variants of pBR322 Jc1/<sup>NS5AB-mKO2-Bsd</sup> by digestion with *BglII* & *EcoRV* and ligation.

To generate the firefly luciferase reporters containing the Jc1 5' and 3' UTRs, a PCR product comprising the T7 promoter-5'UTR (+261 nt of the 5' HCV core sequence) was amplified with the primers T7\_5'UTR\_Fw\_BglIII and Core\_+262\_Rev\_HindIII. The resulting PCR product was cloned into pGL3 (Promega) by *BglIII* & *HindIII* digestion to generate 5'UTR-pGL3. To generate the variants with the wildtype,  $\Delta$ 21nt, and  $\Delta$ 36nt 3'UTR, PCR was carried out using the primers 3'UTR\_Fw\_XbaI and T7\_Terminator\_Rev\_Sall. To generate the variant with no HCV 3'UTR, PCR was performed using the primers HDV Ribo\_Fw\_XbaI and T7\_Terminator\_Rev\_Sall. The resulting PCR products were cloned into 5'UTR-pGL3 by *XbaI* & *Sall* digestion to generate pGL3-5'UTR-FLuc-WT3'UTR-HDVRibo-T7term, pGL3-5'UTR-Fluc- $\Delta$ 21nt3'UTR-HDVRibo-T7term, pGL3-5'UTR-Fluc- $\Delta$ 36nt3'UTR-HDVRibo-T7term, and pGL3-5'UTR-Fluc-HDVRibo-T7term, respectively. The Renilla luciferase template for capped RNA synthesis was amplified using pRL\_Fw\_T7 and pRL\_Rev\_polyA; the resulting PCR product was purified using the QIAquick PCR purification kit (Qiagen) prior to T7 transcription.

**Western blotting.** Western blotting was carried out using standard techniques. The antibodies used were anti-mKO2 (rabbit polyclonal, MBL International), anti-HCV core (C750, Abcam), anti-GFP (rabbit monoclonal, Life Technologies), anti-calreticulin (rabbit polyclonal, Enzo Life Sciences), anti-hnRNP C1/C2 (4F4, Abcam), anti-CD81 (JS81, BD Pharmingen), anti-Hsp90 (4F10, Santa Cruz Biotech).

**RNA synthesis and transfection.** *In vitro* transcription of viral RNA and electroporation was carried out as described [26,77], with minor modifications. Viral RNA or firefly luciferase construct RNA was transcribed using a Megascript T7 Kit (Ambion), and capped Renilla luciferase RNA was transcribed using the mMessage T7 Kit (Ambion). All transcripts were purified by lithium chloride precipitation. For production of virus or supertransfection experiments,  $7.5 \times 10^6$  Huh7.5 or Jc1/ $\Delta$ E1E2<sup>NS5A-GFP-Bsd</sup> replicon cells were electroporated with 10  $\mu$ g of viral RNA. In experiments using luciferase constructs to assess viral translation,  $5.63 \times 10^6$  Huh7.5 cells were transfected with 5  $\mu$ g of the firefly luciferase reporter or 10  $\mu$ g of the various Jc1/<sup>NS5AB-FLuc</sup>-GND RNAs, mixed with 1  $\mu$ g of capped Renilla luciferase RNA. In some cases, poly-A carrier RNA (Qiagen) was used as a transfection control.

**Virus production, titration, and infections.** For virus production, 1–5 days after initial transfection, supernatants were collected from cultures. During serial passage of the superinfecting virus over Jc1/ $\Delta$ E1E2<sup>NS5A-GFP-Bsd</sup> replicon cells, viral supernatants were collected from 3–12 days post-infection. The viral supernatants were clarified by filtration at 0.2  $\mu$ m (Steriflip, Millipore) and stored at -80°C. HCV

virions in the supernatants were titrated by HCV core antigen ELISA, reverse transcriptase-PCR (RT-PCR), or assessment of viral focus-forming units (FFU).

The HCV core antigen ELISA (CellBiolabs) was carried out according to the manufacturer's protocol with a 1:2 dilution of viral supernatant in Dulbecco's phosphate-buffered saline without  $\text{Ca}^{2+}$  or  $\text{Mg}^{2+}$  (DPBS, Mediatech). For RT-PCR analysis, viral RNA was purified from supernatants with the ZR-96 Viral RNA purification kit (Zymo Research). Reverse-transcription and subsequent real-time PCR was performed in one step with the Quantitect probe RT-PCR system (Qiagen). Real-time PCR was performed on a 7900HT fast real-time PCR system (Applied Biosystems), according to the manufacturer's protocol. A probe/primer set corresponding to the HCV core region was used [54].

Viral FFU were assessed by infecting naive Huh7.5 cells with various dilutions of viral supernatants, followed by detection of infected cells by flow cytometry 3 days later, as described [78]. HCV-infected cells were identified by the presence of the virally derived fluorescent reporter or immunostaining for dsRNA. Viral FFU calculations were based on counts of 1–10% fluorescent protein-positive or dsRNA-positive cells. Flow cytometry-based counts of viral FFU were in close agreement to the standard limiting dilution method [27] of assessing FFU titers (data not shown).

After normalizing to HCV core amounts or FFU/mL, naive or replicon cell lines were infected with clarified supernatants overnight. The exception was during serial passage of the superinfecting virus over Jc1/ $\Delta\text{E1E2}^{\text{NS5A-GFP-Bsd}}$  replicon cells; in this case, the virus was not normalized before infection. Infected cells were passaged



approximately every 3 days. When infecting replicon cell lines, antibiotics (G418 or blasticidin) were removed at the time of infection for the duration of the culture.

**Epifluorescence microscopy.** Viral or replicon RNA-transfected Huh7.5 cells were plated on #1 thickness 12-mm circular cover glasses (Fisher Scientific) ( $3.75 \times 10^4$  cells) or on Labtek 2 well coverslip chambers (Nunc) ( $150 \times 10^3$  cells).

Two days later, the cells were immediately imaged by epifluorescence microscopy for live-cell analysis, or fixed in 4% paraformaldehyde and permeabilized in 90% methanol/10% DPBS for 1 hour at  $-20^\circ\text{C}$ . Cells were stained with anti-dsRNA antibody (J2, English and Scientific Consulting), followed by staining with an anti-mouse IgG Alexa 633 antibody (Invitrogen). The cells were imaged at 630x magnification on an Axio Observer Z1 microscope (Zeiss). Axiovision software (Zeiss) was used to analyze colocalization using the Pearson coefficient.

**Ioxidanol gradient separations.** Separations of membranous fractions by gradient separations were performed as described [79], with minor modifications.  $\text{Jc1}/\Delta\text{E1E2}^{\text{NS5A-GFP};\text{NS5AB-mKO2-Bsd}}$  replicon-containing or naive Huh7.5 cells were collected from 140-mm culture dishes by treatment with Versene. The collected cells were washed twice in DPBS and resuspended in 2 mL of DPBS with 0.25 M sucrose, 1 mM PMSF, and protease inhibitor cocktail set III (Calbiochem). The cells were lysed by 80 strokes in a Dounce homogenizer (Wheaton). Nuclei were removed by centrifugation at  $2400 \times g$  for 10 minutes at  $4^\circ\text{C}$ , and protein content in the resulting supernatant was measured by the bicinchoninic acid assay (Bio-rad). A

total of 5 mg of protein in 2 mL was overlaid on a discontinuous iodixanol gradient (Sigma-Aldrich) of 1.3 mL each of 4, 8, 12, 20, 30, and 35% iodixanol in DPBS/0.25M sucrose. Gradients were centrifuged at 140,000xg for 2 hours at 4°C in an SW28 rotor. Eleven fractions of 890  $\mu$ L each were collected from top to bottom and subjected to western blot analysis and bicinchoninic acid assay for protein content.

**Magnetic bead transfection and cell isolation.** A mixture of a total of  $7.5 \times 10^6$  Jc1/ $\Delta$ E1E2<sup>NS5A-GFP-Bsd</sup> polyclonal replicon cells and 7.5-H2B-EFBP2 cells [54] were transfected with 10  $\mu$ g of Jc1/<sup>NS5AB-mKO2-Bsd</sup> RNA. Three days later, the cells were transfected with 10 pg of iron/cell of FeOLabel-Texas Red paramagnetic beads in serum-free medium, according to the manufacturer's protocol (Bulldog Bio). After transfection, FeOLabel-positive cells were isolated by magnetic separation on an LS magnetic column (Miltenyi). The FeOLabel-positive cells were immediately mixed with  $3.75 \times 10^6$  infection-naive Jc1/ $\Delta$ E1E2<sup>NS5A-GFP-Bsd</sup> polyclonal replicon cells and  $3.75 \times 10^6$  7.5-H2B-EFBP2 cells. Three days later, the FeOLabel-negative cells were isolated by negative selection of the entire mixture of cells on an LS magnetic column.

**Sequencing of viral RNA.** Supernatants were collected from infected cells and clarified by filtration at 0.2  $\mu$ m. The supernatants were concentrated by ultrafiltration in 100-KDa MWCO Amicon-15 columns (Millipore). RNA was isolated from 200  $\mu$ L of the concentrated supernatant by Trizol extraction (Invitrogen), followed by LiCl

precipitation (Ambion) to further purify the RNA. cDNA was prepared by random hexamer-mediated reverse transcription with the Superscript III first-strand synthesis kit (Invitrogen). PCR was carried out on eight overlapping regions of the Jc1<sup>NS5AB-mKO2-Bsd</sup> genome with the primers in Supplemental Table A.1. The resulting PCR products were cloned into pCR4 Topo (Invitrogen), and the resulting clones were sequenced. Alignment and sequence analysis were performed with the Sequencher 4.9 program (Gene Codes).

**Flow cytometry.** Cells to be analyzed by flow cytometry were trypsinized and treated for at least 1 h in 4% paraformaldehyde. For analysis of dsRNA, the cells were permeabilized in 90% methanol/10% DPBS for 1 h at -20°C. Cells were stained with the J2 mouse anti-dsRNA antibody, followed by staining with a polyclonal anti-mouse Ig allophycocyanin antibody (BD Biosciences). The cells were analyzed for fluorescence on an LSRII flow cytometer equipped with a high-throughput microplate reader (BD Biosciences).

**Luciferase assays.** After electroporation, cells were plated at  $235 \times 10^3$  cells/well on a 12-well plate. At 2, 4, 8, and 24 h post-electroporation, the cells were washed with DPBS and stored at -80°C. The cells were lysed in 200  $\mu$ L of Passive Lysis Buffer, and 50  $\mu$ L of lysate was used for the analysis of firefly and Renilla luciferase, according to the manufacturer's protocol (Dual Luciferase Assay, Promega).

**Statistical Analysis.** Statistical analysis was carried out using Prism 5 software (Graphpad). For analysis of the exclusion of the primary replicon following infection with untagged Jc1, linear regression and analysis of covariance was used to determine whether the slopes of the exclusion curves were significantly different. For all other tests, one-way ANOVA with Bonferroni multiple-comparison correction was used.

## **ACKNOWLEDGMENTS**

We thank Ralf Bartenschlager (University of Heidelberg) for the Jc1 construct, Charles Rice (Rockefeller University) for Huh7.5 cells, Takaji Wakita (National Institute of Infectious Disease, Japan) for the JFH1 construct, and Matthew Spindler for the pSicoR construct. We are grateful to Jane Gordon, Tara Rambaldo, and Sarah Elmes from the UCSF Laboratory for Cell Analysis, as well as Marielle Cavrois and the Gladstone Flow Cytometry Core for assistance with flow cytometric assays. We thank John Carroll for help in preparation of the figures, and members of the Greene laboratory for helpful discussion and support. This work was supported by the Gladstone Institutes and funds from the US Public Health Service (T32: A1060537-05 (UCSF Program in Microbial Pathogenesis and Host Defense)).

## **CHAPTER 3**

# **RAPID INTRACELLULAR COMPETITION BETWEEN HCV GENOMES AS A RESULT OF MITOSIS**

**ABSTRACT**

Cells infected with hepatitis C virus (HCV) become refractory to further infection by HCV [52,53]. This process, termed superinfection exclusion, does not involve down-regulation of surface viral receptors but instead occurs inside the cell at the level of RNA replication. The originally infecting virus may occupy replication niches or sequester host factors necessary for viral growth, preventing effective growth of viruses that enter the cell later. However, there appears to be an additional level of intracellular competition between viral genomes that occurs at, or shortly following mitosis. In the setting of cellular division, when two viral replicons of equivalent fitness are present within a cell, they have an equal opportunity to exclude the other. In a population of dividing cells, the competition between viral genomes proceeds apace, randomly clearing one or the other genome from cells in the span of 9-12 days. These findings demonstrate a new mechanism of intracellular competition between HCV strains, which may act to further limit HCV's genetic diversity and ability to recombine *in vivo*.

## INTRODUCTION

Hepatitis C virus (HCV) is a positive-stranded, enveloped ssRNA virus in the *Flavivirus* family. Currently, HCV infects more than 180 million people worldwide, and the associated morbidity and mortality are second only to HIV among emerging infections [80]. HCV is primarily transmitted parenterally, but vertical and sexual transmission may also occur. After acute infection, approximately 25% of patients spontaneously clear the virus. The remainder are chronically infected and may go on to develop hepatic steatosis, cirrhosis, and hepatocellular carcinoma [81].

Complete *in vitro* replication of an HCV molecular clone was first demonstrated in 2005, using the genotype 2a virus JFH-1 [25,26,27]. This clone, isolated from a Japanese male patient with fulminant hepatitis [28], replicated robustly in Huh7 cells and produced infectious virions in the absence of cell culture adaptive mutations. The availability of this infectious molecular clone provided a powerful experimental model with many advantages over the previously described HCV replicons [29]. More recently, other groups have constructed highly infectious intergenotypic chimeras of JFH-1 and other HCV strains by substituting the region from core to a portion of NS2 [56,82,83]. The genotype 2a/2a chimera Jc1 is especially infectious [56].

HCV blocks infection by other incoming HCV virions through a process known as superinfection exclusion [52,53]. This process appears to occur after the virus enters the cell, which is different from the superinfection exclusion mechanism found in many other viral systems where downregulation of cell surface viral receptors is



involved. The intracellular superinfection block during HCV infection might result from competition between the primary and secondary viruses involving sequestration of key host factor(s) needed for viral replication or through occupancy of replicative niches on the ER membrane.

Superinfection exclusion has clear implications for treating HCV infection. If HCV could successfully superinfect cells, the evolution of drug and/or vaccine resistance, especially in a virus that is already hypervariant, would be greatly enhanced. Superinfection exclusion during HCV replication likely reduces the prevalence of viral recombination which left unchecked, could result in an even greater degree of immune escape variants and drug-resistant strains within this already variable virus.

In this study, we have explored whether mechanisms beyond classical superinfection exclusion contribute to limiting the possibility of HCV recombination. We now define an additional mechanism that limits the degree of HCV coinfection. We specifically show that cells replicating two or more HCV viral genomes convert into cells replicating only one viral genome due to genetic bottlenecks occurring during, or shortly after, mitosis. Furthermore, this process is biased toward replicons that have accumulated higher levels of viral RNA in host cells. We postulate that this bottleneck involves disruption of the viral replication niches in mitotic cells.

## **RESULTS**

### **Replication competence of the replicons used in the study.**

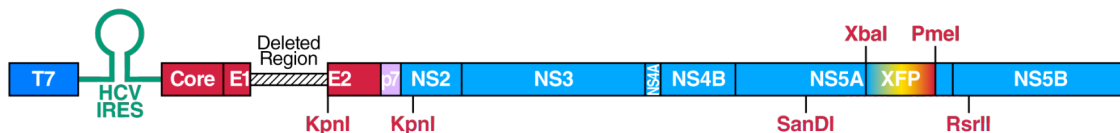
As we were interested in analyzing the replication of multiple HCV strains, we created fluorescently tagged monocistronic Jc1 replicon constructs similar to those

described by Schaller et al [53]. By fusing fluorescent reporters to the viral NS5A protein, we could measure the replication potential of multiple replicon strains in one cell (Figure 3.1A). By additionally adding a blasticidin resistance gene (BSD) in the context of NS5A domain III, we were able to select specifically for replicon-containing cells. To determine the relative fitness of the viral replicons, highly permissive Huh7.5 cells were singly transfected with 10  $\mu$ g of each replicon. The efficiency of establishment of replication in host cells was measured by flow cytometry as well as viral replicon RNA accumulation by quantitative RT-PCR (Figure 3.1B & C). As demonstrated by both percentage of replicon-positive cells as well as RNA accumulation, the peak of replication was 2 days after transfection.

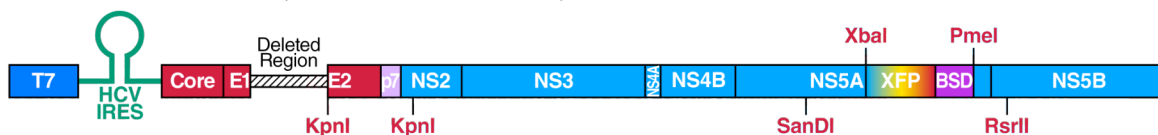
In agreement with prior studies [53], we did not observe differences in fitness of different Jc1/ $\Delta$ E1E2<sup>NS5A-XFP</sup> constructs (hereafter referred to as Jc1/ $\Delta$ <sup>XFP</sup> for simplicity). The Jc1/ $\Delta$ E1E2<sup>NS5A-XFP-BSD</sup> replicons, however, did appear to differ in fitness, although differences in RNA accumulation were statistically greater than differences in transfection efficiency (Figure 3.1C). It is known that GFP fusion to domain III of NS5A negatively affects RNA replication efficiency of replicons [84]; different inserted protein sequences (e.g., fluorescent proteins) may differentially affect the overall fitness. The addition of the BSD sequence reduced the replication efficiency of the Jc1/ $\Delta$ <sup>XFP-BSD</sup> replicons overall, potentially unmasking changes that different fluorescent proteins exert on replicon fitness. The natively high replication efficiency of JFH-1-based replicons may have masked any subtle differences in replication of the Jc1/ $\Delta$ <sup>XFP</sup> strains.

A

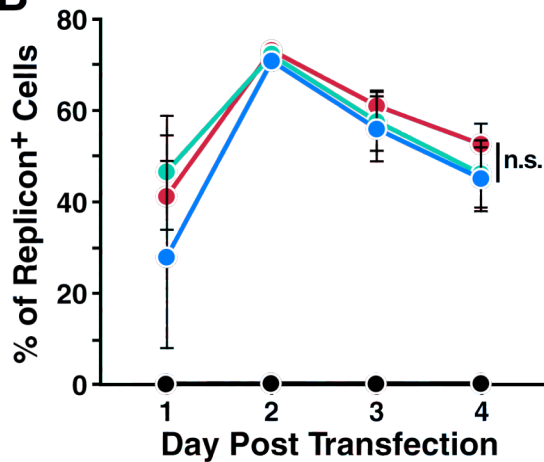
Jc1/ $\Delta$ E1E2<sup>NS5A-GFP</sup>, Jc1/ $\Delta$ E1E2<sup>NS5A-mCherry</sup>, Jc1/ $\Delta$ E1E2<sup>NS5A-EBFP2</sup>



Jc1/ $\Delta$ E1E2<sup>NS5A-mKO2-Bsd</sup>, Jc1/ $\Delta$ E1E2<sup>NS5A-GFP-Bsd</sup>, Jc1/ $\Delta$ E1E2<sup>NS5A-mCherry-Bsd</sup>



B



C

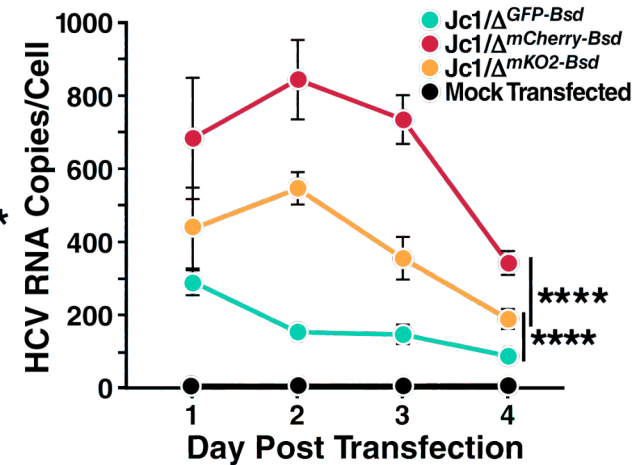
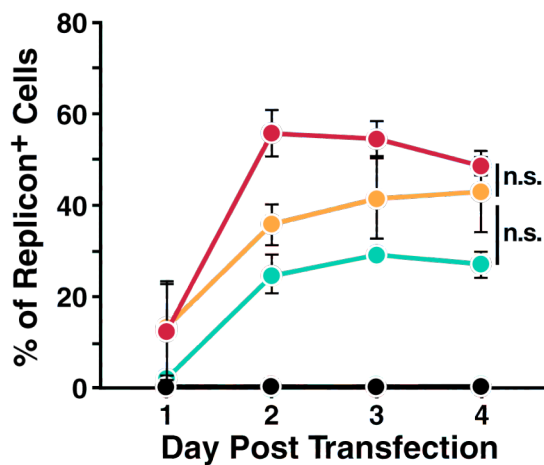
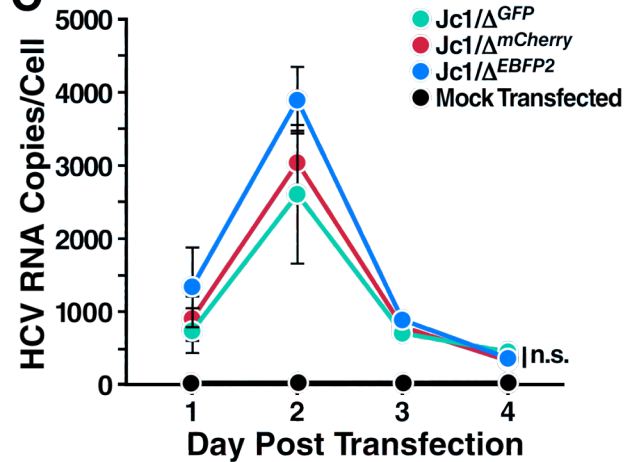


Figure 3.1: Genomic HCV constructs employed in this study and relative efficiencies of each.

(A) Schematic diagram of constructs used; XFP represents the fluorophore tag inserted into NS5A, and BSD represents the blasticidin resistance gene. (B,C) Comparison of replicon fitness by transfection efficiency and viral RNA accumulation in host cells. Huh7.5 cells were mock-transfected or transfected with 10  $\mu$ g of Jc1/ $\Delta$ <sup>GFP</sup>, Jc1/ $\Delta$ <sup>EBFP2</sup>, Jc1/ $\Delta$ <sup>mCherry</sup>, Jc1/ $\Delta$ <sup>GFP-BSD</sup>, Jc1/ $\Delta$ <sup>mKO2-BSD</sup>, and Jc1/ $\Delta$ <sup>mCherry-BSD</sup> replicon RNAs. (B) Transfection efficiency of each replicon strain. Flow cytometric analysis was carried out at the given time points to determine the percentage of replicon-positive cells. (C) RNA accumulation in host cells transfected with each replicon strain. RNA was extracted from transfected cells at the indicated time points and subjected to quantitative RT-PCR analysis using a core-specific HCV probe. A GAPDH probe was used for normalization of RNA samples, using mock-transfected cells as a calibrator. Error bars indicate  $\pm$  SEM. Differences in transfection efficiencies or RNA accumulation were assessed by obtaining the integrated area under the curve (AUC) for each independent experiment, followed by one-way ANOVA with Bonferroni multiple comparison correction to assess statistically significant differences (\*:  $p < 0.05$ , \*\*\*\*:  $p < 0.0001$ , ns: non-significant).

**More than one genomic strain is unstable in HCV replicon-containing cells.**

Superinfection exclusion has been demonstrated to occur at a post-entry step in the viral life cycle [52,53]. Prior studies have also demonstrated a degree of compartmentalization of viral replication complexes [51,85]. We therefore hypothesized that intracellular competition for either limiting host proviral factors or replicative niches could occur even in cells productively replicating two strains of HCV. Intracellular competition would then lead to the progressive loss, or decay, of viral genomes until only one strain remained in a particular cell.

To address this possibility, studies were performed to test whether host cells could stably replicate two HCV genomic strains using the equally fit Jc1/ $\Delta$ <sup>XFP</sup> replicons. These replicons lack the E1E2 proteins, preventing the confounding effects of spreading infection following the initial transfection. Huh7.5 cells were transfected simultaneously with Jc1/ $\Delta$ E1E2<sup>NS5A-GFP</sup> and Jc1/ $\Delta$ E1E2<sup>NS5A-mCherry</sup>. Dual-replicon (GFP+/mCherry+) cells were isolated by fluorescence-activated cell sorting (FACS) 2 days later. These cells were then monitored at various time points post-sorting by flow cytometry to determine the stability of the dual-replicon state. We found that dual-replicon cells were progressively lost over time with near complete disappearance within 9 days (Figure 3.2A). The replicon-negative cell population expanded in these cultures likely because HCV infection is associated with both apoptosis [86,87] and cell-cycle abnormalities [88,89]. However, when only the replicon-positive cells were evaluated (Figure 3.2B), the loss of dual-replicon cells and a concomitant rise in single-replicon cells was readily apparent. Neither the Jc1/ $\Delta$ <sup>GFP</sup> nor the Jc1/ $\Delta$ <sup>mCherry</sup> genome seemed to have an advantage in this decay

process, as there was no significant difference in the proportion of single-replicon-containing cells of each type (Supplemental Table B.1). However, in these experiments we could not rule out the possibility that single-replicon cells might exhibit a selective growth advantage over dual-replicon cells (less cell death, faster growth rate) culminating in more single-replicon cells after 7-9 days. To demonstrate the sample sizes of the analyzed cells, the absolute cell counts of all experiments analyzing the decay phenomena are provided in Supplemental Figure B.1.

We hypothesized that triple-replicon cells would decay in an ordered manner transitioning through a dual-replicon state and on to a single-replicon state reflecting the sequential loss of viral genomes. Conversely, if single-replicon cells simply displayed an increased growth advantage, such single-replicon cells would increase more quickly than dual-replicon cells. To distinguish between these possibilities, cells were transfected with Jc1/ $\Delta$ <sup>GFP</sup>, Jc1/ $\Delta$ <sup>mCherry</sup>, and Jc1/ $\Delta$ <sup>EBFP2</sup>, and triple-replicon (GFP+/mCherry+/EBFP2+) cells were isolated by FACS 2 days later. At various times afterward, the cells were analyzed for the presence of GFP/mCherry/EBFP2 fluorescence. We observed an ordered progression of viral genome decay from triple- to dual- to single-replicon cells (Figure 3.2). Specifically, dual-replicon cells increased until day 5 when single-replicon cells became predominant (Supplemental Figure B.2).

Both dual- and single-replicon cells display a consistent exponential decay when compared to replicon-negative cells (Supplemental Figure B.2). As isolated triple-replicon cells always contain a small proportion of contaminating dual- and single-replicon cells, we cannot completely rule out the null hypothesis that the increase in

the number of dual- and single-replicon cells is a result of a selective growth advantage of these small numbers of contaminating cells. We have used the exponential decay rates of isolated dual- and single-replicon cells to model the expected numbers of dual- and single-replicon cells over time in isolated triple-replicon cell cultures. Interestingly, there are far more dual- and single-replicon cells over time in isolated triple-replicon cultures than would be expected due to simple expansion of contaminating cells (Supplemental Figure B.2). This fact further reinforces the conclusion that multiple-replicon cells sequentially eliminate viral genomes over time.

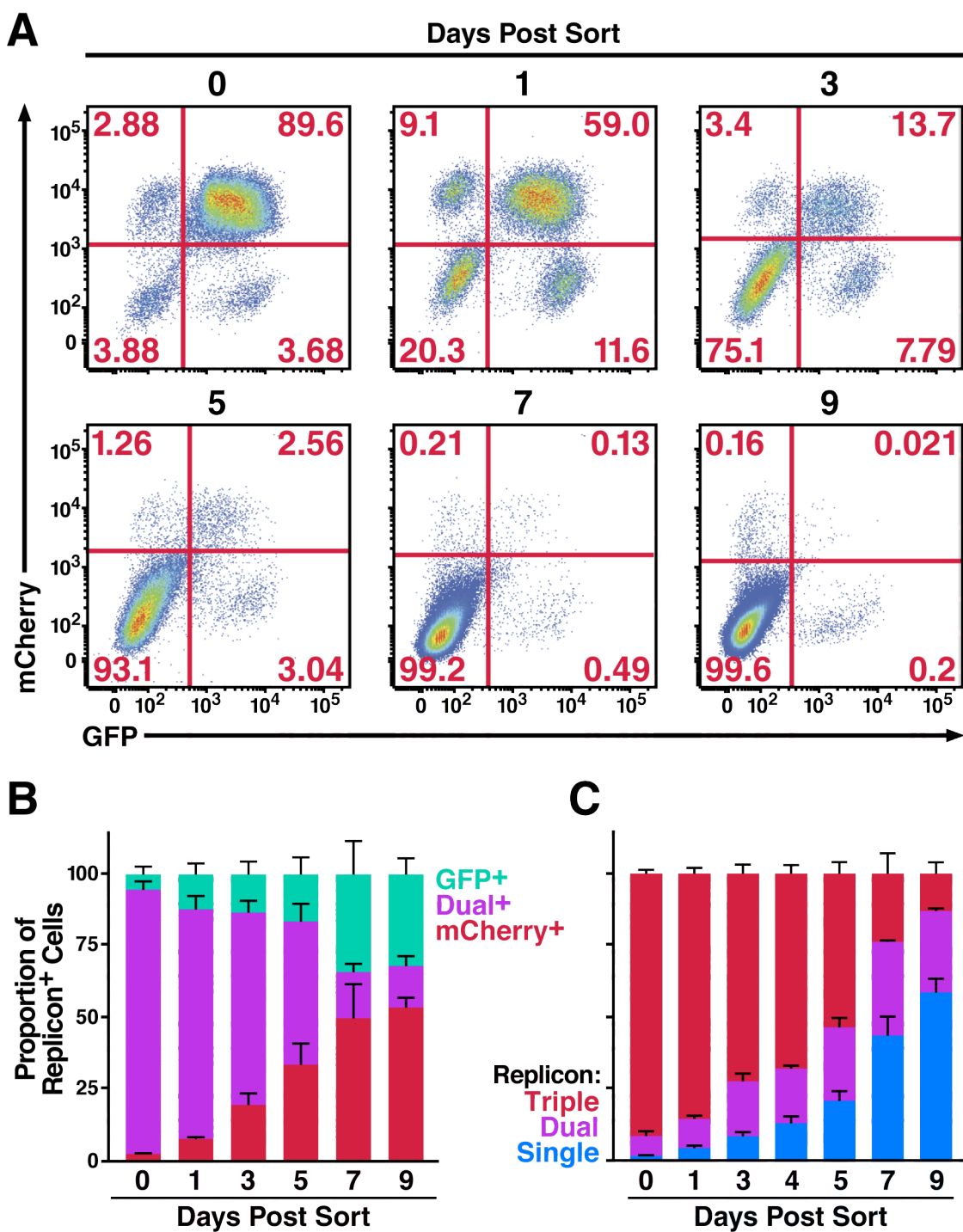


Figure 3.2: Decay of cells multiply transfected with congenic Jc1 replicon strains.



(A) The dual-replicon state is unstable. Huh7.5 cells were transfected with Jc1/ $\Delta^{GFP}$  and Jc1/ $\Delta^{mCherry}$  RNA, followed 48 hours later by FACS isolation of dual-replicon (mCherry+/GFP+) cells. Cells were then analyzed by flow cytometry for mCherry/GFP expression on days 0, 1, 3, 5, 7 and 9 post-sorting (data are representative of 5 independent experiments). (B) Flow cytometric analysis of replicon decay occurring within dual-replicon cells. The total number of replicon-positive cells was set to 100%. Jc1/ $\Delta^{GFP}$ -only replicon-containing cells (green), Jc1/ $\Delta^{mCherry}$ -only replicon-containing cells (red), and dual-replicon cells (orange). Error bars indicate + SEM ( $n=5$ ). (C) Triple-replicon cells decay through a dual-replicon state to single-replicon cells. The total number of replicon-positive cells was set to 100%; blue, single-replicon cells (GFP+ only, mCherry+ only, or EBFP2+ only), green, dual-replicon cells (GFP+/mCherry+ only, mCherry+/EBFP2+ only, or GFP+/EBFP2+ only), red, triple-replicon cells (GFP+/mCherry+/EBFP2+). Error bars indicate +SEM ( $n=4$ ).

**Dual-replicon cells do not exhibit higher rates of cell death.**

To further test a potential selective survival advantage for cells containing fewer HCV replicons, we measured the apoptosis rate in single- and dual-replicon cells. Huh7.5 cells were transfected with Jc1/ $\Delta^{GFP}$  and Jc1/ $\Delta^{EBFP2}$ , then separated by FACS into dual-replicon (GFP+/EBFP2+), single-replicon (GFP+/EBFP2- or GFP-/EBFP2+), and replicon-negative (GFP-/EBFP2-) populations (Supplemental Figure B.3). Beginning 48 hours post-isolation, cells were stained with 7-AAD and Annexin-V APC. We analyzed these cells by flow cytometry for early apoptotic cells in the standard manner, using staurosporine as positive control (Figure 3.3). The 7-AAD-:Annexin-V+ cells represent apoptotic cells, and 7-AAD+ cells represent dead cells. With adherent cells, dead cells are often excluded from the analysis [90], since they could potentially have died due to membrane rupture during trypsinization. However, we observed similar patterns in all apoptosis assays when dead cells were either included or excluded (data not shown).

The apoptosis rates of dual-replicon and single-replicon cells were similar at all time points analyzed ( $p > 0.05$ ) (Figure 3.3, Supplemental Table B.2). However, at each time point from 3–7 days post-isolation, the apoptosis rate was significantly greater in each of the replicon-positive populations compared to the replicon-negative population ( $p < 0.05$ ). The initially high apoptosis rate of replicon-negative cells likely reflects the stresses of electroporation followed by FACS isolation. These findings highlight a cytopathic effect of HCV within these cells but further show that apoptosis rates do not differ between dual- and single-replicon cells.

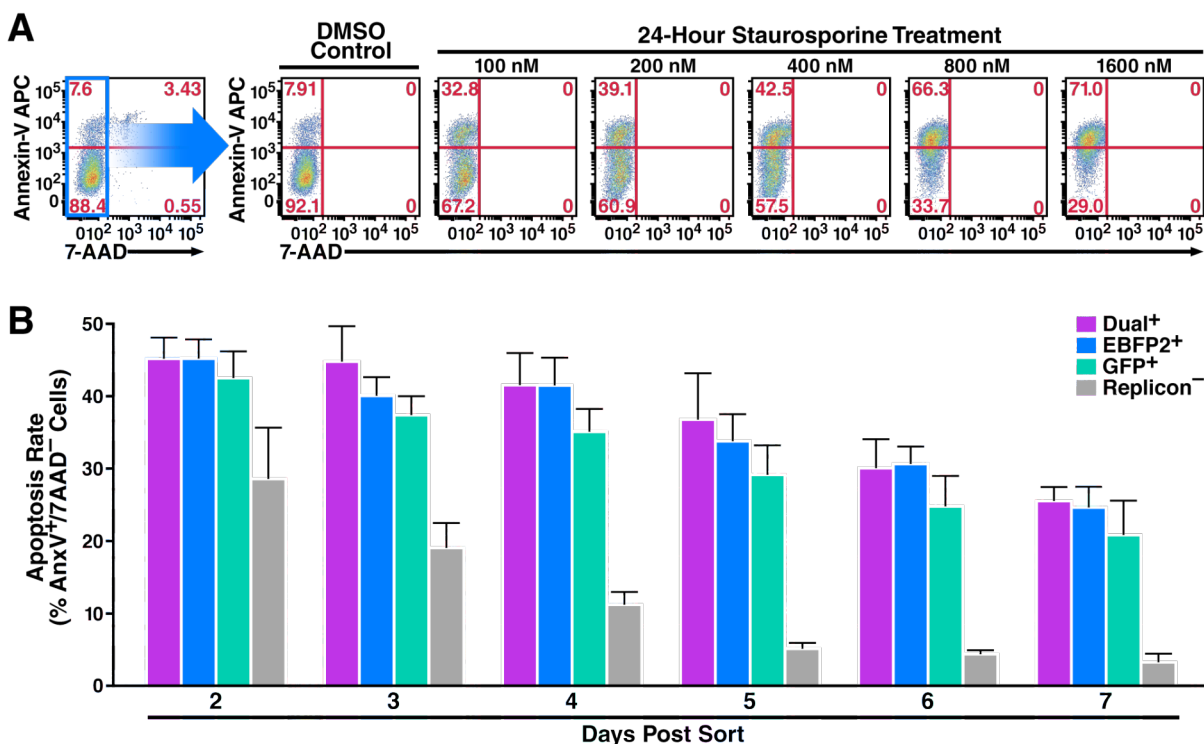


**Figure 3.3: The apoptosis rate in  $Jc1/\Delta^{XFP}$  dual- or single-replicon-containing cells is similar.**

(A) Demonstration of the gating strategy used to analyze apoptotic cells. Huh7.5 cells were treated for 24 hours with various concentrations of staurosporine to induce apoptosis, or DMSO vehicle control. The cells were then stained with Annexin-V APC and 7-AAD. Apoptotic cells are defined as 7-AAD<sup>-</sup>:AnnexinV<sup>+</sup> cells.

(B) No difference in apoptosis rates in dual- or single-replicon cells. Huh7.5 cells were transfected with  $Jc1/\Delta^{GFP}$  and  $Jc1/\Delta^{EBFP2}$  RNA, followed 48 hours later by FACS isolation of  $Jc1/\Delta^{GFP}$ -only replicon-containing cells,  $Jc1/\Delta^{EBFP2}$ -only replicon-containing cells, replicon-negative cells, and dual-replicon cells. Cells were stained with Annexin-V APC and 7-AAD and analyzed at the given time points post-isolation by flow cytometry. Cells were washed with medium 24 hours post-isolation and

every 24 hours thereafter, so the apoptosis rate reflects the preceding 24 hours.  
Error bars indicate +SEM.

**Isolated dual- and single-replicon cells exhibit no difference in proliferation as assessed by CFSE dilution.**

Single-replicon cells might have a selective advantage over dual-replicon cells by dividing more quickly. To test this possibility, we examined Huh7.5 cells transfected with Jc1/ $\Delta^{\text{mCherry}}$  and Jc1/ $\Delta^{\text{EBFP2}}$  for carboxyfluorescein diacetate succidimidyl ester (CFSE) dilution [87]. As CFSE is equally partitioned between daughter cells following division, the dilution of CFSE fluorescence loss is an excellent marker for cellular proliferation. One day after transfection, we treated cells with 10  $\mu\text{M}$  CFSE and 24 hours later dual-replicon (mCherry+/EBFP2+), single-replicon (mCherry-/EBFP2+ or mCherry+/EBFP2-), and replicon negative cells (mCherry-/EBFP2-) by were isolated by FACS. When analyzing CFSE dilution in replicon-positive cell samples, the replicon-negative cells were gated out to simplify the analyses (Figure 3.4A).

In agreement with previous studies [86,88,89,91], we did observe a significant proliferative defect in replicon-positive compared to replicon-negative cells (Figure 3.4B). However, no significant difference in the CFSE dilution rate was observed with any of the replicon-positive samples (assessed by extra-sum-of-squares F test,  $p > 0.05$ ). If there a proliferative advantage for single-replicon over dual-replicon cells existed, the slope of the CFSE dilution curves for dual- and single-replicon cells would have been significantly different. We conclude that Jc1/ $\Delta^{\text{XFP}}$  dual-replicon cells exhibit no apparent differences in either proliferation or apoptosis rates compared to single replicon cells. Therefore, the decay of dual-replicon cells is not an artifact

caused by a selective growth or survival advantage of single-replicon cells that happen to be contaminating the dual-replicon population.

**Mitosis is a key event promoting the decay of dual-replicon cells.**

During mitosis, the endoplasmic reticulum (ER) membrane is disrupted [92,93], which may cause the viral replication niches to break down. These events could produce a genetic bottleneck that would be responsible for the observed decay of dual-replicon cells. CFSE dilution analysis can be used to determine whether mitosis is indeed a key part of the decay of dual-replicon cells; if so, division of dual-replicon cells will result in both CFSE dilution and decay into single-replicon cells. To test this possibility, cells were transfected with Jc1/ $\Delta^{\text{mCherry}}$  and Jc1/ $\Delta^{\text{EBFP2}}$  and treated with CFSE as in the previous experiment (Figure 3.4C). However, dual- and single-replicon cells were not isolated from each other by flow-based sorting as in the prior experiment. In that experiment, using pure populations of single-replicon cells, decay of dual-replicon cells did not occur; thus, the CFSE dilution curves only reflected the division of the single-replicon cells (Figure 3.4B). In this experiment, the decay of dual-replicon cells contributed to the overall population of single-replicon cells. Thus, in this experiment the CFSE dilution rate of single-replicon cells would be expected to additionally reflect the division and attendant decay of dual-replicon cells. Hence, if mitosis is a key part of this decay, this should manifest as a difference in the slope of the CFSE dilution curve in dual- and single-replicon cells. In contrast to the similar rates of CFSE dilution of isolated, pure populations of single- and dual-replicon cells (Figure 3.4B), there is indeed a significant difference in CFSE dilution rates of dual- and single-replicon cells in mixed cultures ( $p < 0.0001$ , Figure 3.4C).

If mitosis indeed forms the transition point in the decay from dual- to single-replicon cells, we should be able to slow the decay process by slowing cellular division rates. To test this possibility, the same CFSE dilution experiment was performed with cells treated with 1% DMSO for 15 days before transfection. This treatment is known to slow and ultimately arrest the growth of hepatoma cells [94]. After 15 days, the confluent cells were indeed growth-arrested as assessed by serial cell counts (data not shown). These cells were then transfected with the replicon RNAs. When the transfected cells were re-plated in the continued presence of 1% DMSO, they began to divide again, albeit more slowly. We observed that the DMSO-induced cell cycle retardation was sufficient to cause dual- and single- replicon cells to dilute CFSE at similar rates (Figure 3.4E). Concomitantly, the DMSO treatment also slowed (or halted) the conversion of dual-replicon into single-replicon cells (Figure 3.4D & F), indicating that mitosis may play an important role in the decay process.

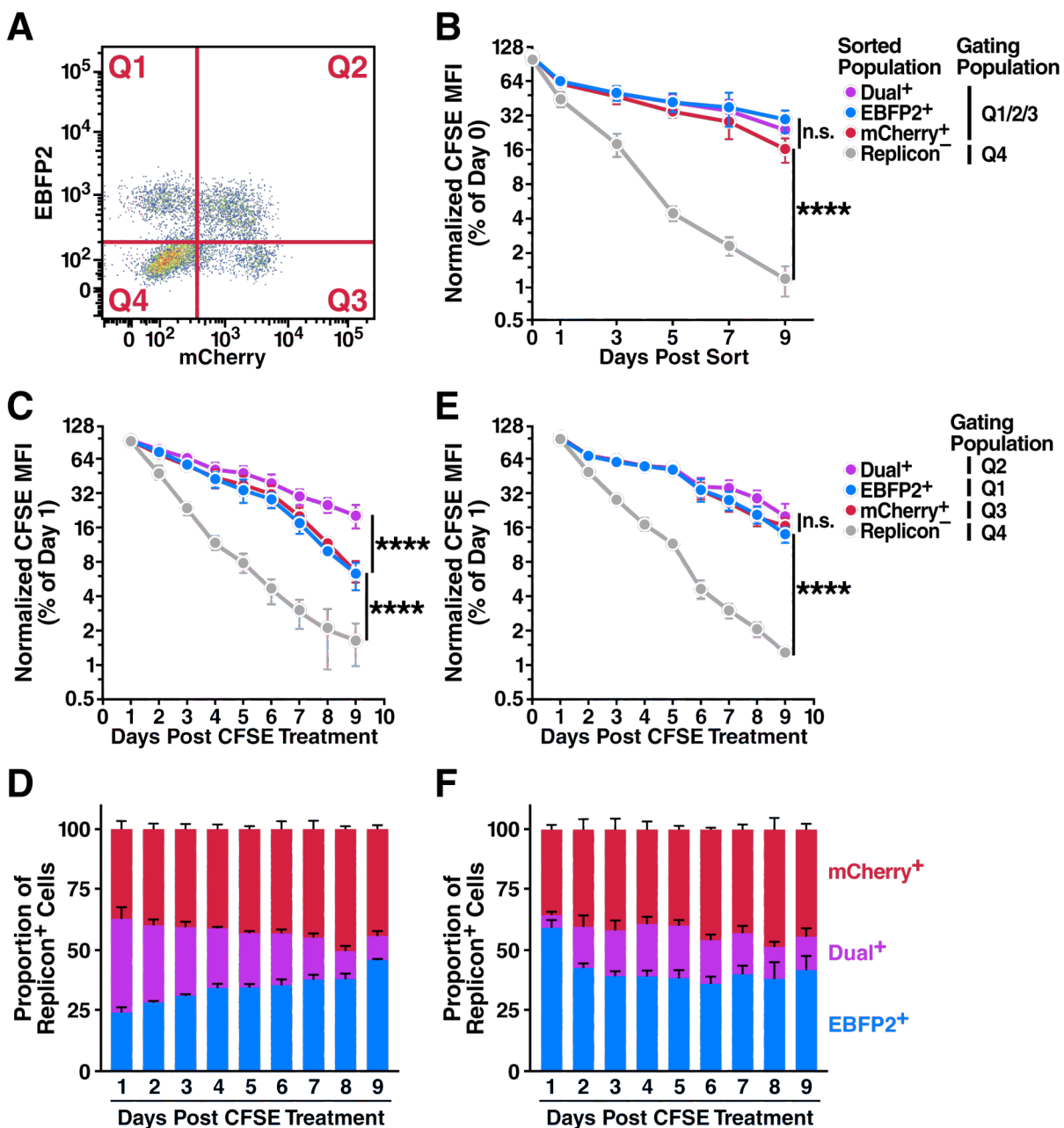


**Figure 3.4: Progression through the cell cycle is important in the dual- to single-replicon decay process.**

Huh7.5 cells were transfected with Jc1/ $\Delta^{EBFP2}$  and Jc1/ $\Delta^{mCherry}$  RNA and treated with 5 or 10  $\mu$ M CFSE 24 hours later. (A) Representative flow cytometry plot demonstrating gating quadrants. (B) No difference in proliferation of isolated dual-



and single-replicon cells assessed by CFSE dilution. 2 days after transfection, dual-replicon, single-replicon, and replicon-negative cells were isolated by FACS. Cells were analyzed for CFSE/EBFP2/mCherry by flow cytometry; the gating quadrants represent the cells used in the analysis. Values were normalized to the CFSE mean fluorescence intensity (MFI) at day 0 post-sort ( $n=4$ ). (C) In mixed-replicon cultures, dual-replicon cells dilute CFSE more slowly than single-replicon cells. Cells were not isolated by cell sorting; instead, each population was separated by the given quadrant gates ( $n=3$ ). (D) Decay of dual-replicon cells in mixed cultures. The chart indicates the proportion of single- and dual-replicon cells in the samples in (C). (E) No significant difference in CFSE dilution of dual- or single-replicon cells in mixed-replicon DMSO-treated cultures. Huh7.5 cells were treated for 15 days with 1% DMSO to induce a differentiated, growth-arrested phenotype before transfection and were otherwise treated as in (C). ( $n=3$ ) (F) DMSO treatment of cells slows the dual-replicon decay process. The chart indicates the proportion of single- and dual-replicon cells in the samples in (E). Error bars indicate SEM (\*\*\*\*:  $p<0.001$ , ns: non-significant by extra sum of squares F-test using semilog regression).

### **Dual- and single-replicon cells are equally competent for proliferation.**

To conclusively assure that dual-replicon cells are not defective in proliferation relative to single-replicon cells, we examined the cell-cycle profiles by DNA content analysis of Huh7.5 cells transfected with Jc1/ $\Delta$ <sup>GFP</sup> and Jc1/ $\Delta$ <sup>mCherry</sup> RNA. We compared the proportions of dual- and single-replicon cells in each phase of the cell cycle, and found that there was no significant cell cycle arrest specific to dual-replicon cells (data not shown).

Since cell-cycle profiles represent a relatively insensitive method for measuring proliferation competence, we elected to use a modified version of the Fucci system [95] to isolate dual- and single-replicon-containing pre-mitotic and mitotic (S/G<sub>2</sub>/M phase) cells or cells in the G<sub>1</sub> phase. We then assessed the ability of these cells to progress into the next phase(s) of the cell cycle. The hCdt1 (human Cdt1) and hGem (human Geminin) proteins are expressed during different phases of the cell cycle. Cdt1 is ubiquitinated by the SCF<sup>Skp2</sup> complex during S and G<sub>2</sub> phase while Gem is ubiquitinated by the APC/C E3 ligase complex during late M and G<sub>1</sub> phase. Both are rapidly degraded by the proteasome [96]. Probes containing the region of hCdt1 and hGem necessary for ubiquitination/degradation fused to a fluorophore are selectively present during G<sub>1</sub> and S/G<sub>2</sub>/M phases, respectively.

In our hands, a GFP-hGem (Figure 3.5A) or an EBFP2-hGem probe was sufficient to distinguish between S/G<sub>2</sub>/M and G<sub>1</sub> phase cells in stable Huh7.5 cell lines transduced with lentiviral constructs encoding these probes. Therefore, we used the hGem probe alone to reduce fluorophore overlap. 7.5-GFP-hGem cells were transfected with Jc1/ $\Delta$ <sup>EBFP2</sup> and Jc1/ $\Delta$ <sup>mCherry</sup> RNA, and 2 days later, the

following populations were isolated by FACS: G<sub>1</sub> phase (GFP-) single-replicon cells (EBFP2+/mCherry-), G<sub>1</sub> phase (GFP-) dual-replicon cells (EBFP2+/mCherry+), G<sub>2</sub>/S/M phase (GFP+) single-replicon cells (EBFP2+/mCherry+), and G<sub>2</sub>/S/M phase (GFP+) dual-replicon cells (EBFP2+/mCherry+).

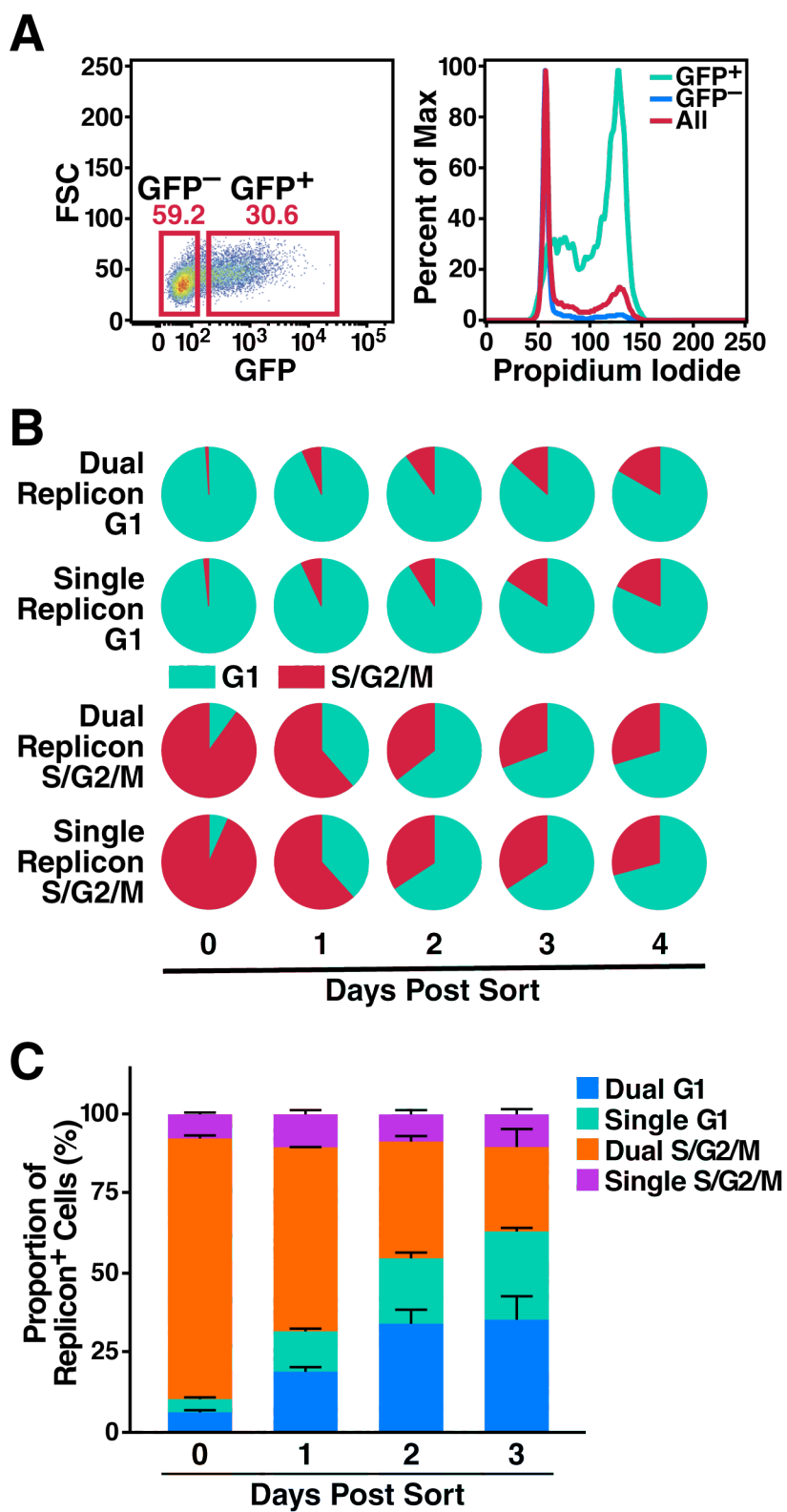
Beginning at 24 hours post-isolation, we used flow cytometry to assess whether cells had progressed through the G<sub>1</sub>-S transition (gain of GFP fluorescence) or through the M-G<sub>1</sub> transition (loss of GFP fluorescence). Of note, we observed that dual- and single-replicon cells progressed through the cell cycle at equivalent rates (Figure 3.5B), based on the fact that a delay in cell cycle progression in dual-replicon cells should cause them either to lose (M→G<sub>1</sub>) or gain (G<sub>1</sub>→S) GFP fluorescence more slowly than single-replicon cells. These findings further indicate that dual- and single-replicon cells proliferate at quite similar rates.

### **Dual-replicon cell transition through mitosis is associated with enrichment in single-replicon cells.**

Slowing the cell cycle in replicon-transfected cells by DMSO treatment also slowed the decay of dual-replicon cells (Figure 3.4). Accordingly, we investigated the possibility that the decay from dual- to single-replicon cells is linked to mitosis. 7.5-GFP-hGem cells were transfected with Jc1/ $\Delta^{EBFP2}$  and Jc1/ $\Delta^{mCherry}$  RNA. Two days later, we isolated dual-replicon S/G<sub>2</sub>/M phase cells by FACS (EBFP2+/mCherry+, dual-replicon; GFP+, S/G<sub>2</sub>/M phase). We next analyzed the cells beginning at day 1 post-isolation for the transition into G<sub>1</sub> phase (loss of GFP fluorescence) and the decay from dual-replicon cells into single-replicon cells. Completion of mitosis in dual-replicon cells (the transition from S/G<sub>2</sub>/M to G<sub>1</sub> phase) was associated with a

marked increase in the proportion of single-replicon cells, relative to replicon-positive cells remaining in S/G<sub>2</sub>/M phase that had not completed cell division (Figure 3.5C). At day 2 post-sort when the proportions of post- and pre-division cells were similar (54.8% versus 45.2%), there were significantly more post-division single-replicon cells compared to pre-division single-replicon cells ( $p < 0.01$ ). However, there was no difference in the proportion of post- versus pre-division dual-replicon cells at this time point ( $p > 0.6$ ).

These findings indicate that, following mitosis, dual-replicon cells tend to decay into a single-replicon state, although the persistence of post-mitotic dual-replicon cells implies that decay does not necessarily occur in conjunction with every mitotic division. Nevertheless, these findings underscore the importance of mitosis in the viral genome decay process. We hypothesize that this decay results from a bottleneck in HCV genome diversity occurring during or shortly after mitosis. Of note, this bottleneck acts without regard to viral fitness, as we observed this decay phenomenon in congenic Jc1 viral strains differing only by their fluorophore tag.



(A) Validation of the fluorescent hGem probe for cells in S/G<sub>2</sub>/M phase of the cell cycle. 7.5-GFP-hGem cells were stained with propidium iodide (PI) and analyzed for GFP and PI by flow cytometry. As shown, the GFP<sup>+</sup> cells are highly enriched in the S/G<sub>2</sub>/M phases of the cell cycle, while the GFP<sup>-</sup> cells are enriched for the G<sub>1</sub> phase of the cell cycle. (B) Dual-replicon cells are equally competent as single-replicon cells for cell-cycle progression. 7.5-GFP-hGem cells were transfected with Jc1/ $\Delta$ <sup>GFP</sup> and Jc1/ $\Delta$ <sup>mCherry</sup> RNA. Dual-replicon (EBFP2+/mCherry+) and single-replicon (mCherry+ only) cells were isolated in G<sub>1</sub> (GFP-) and S/G<sub>2</sub>/M (GFP+) phases of the cell cycle by FACS. No difference was observed by student's t-test in the cell cycle phase of single- and dual-replicon cells at any time point ( $p > 0.2$ ,  $n = 3$ ). (C) As dual-replicon cells progress through mitosis, single-replicon cells are enriched. 7.5-GFP-hGem cells were transfected with Jc1/ $\Delta$ <sup>EBFP2</sup> & Jc1/ $\Delta$ <sup>mCherry</sup>. Dual-replicon (EBFP2+/mCherry+) S/G<sub>2</sub>/M phase (GFP+) cells were isolated by FACS and analyzed by flow cytometry for the dual- to single-replicon transition, as well as cell-cycle progression. Error bars indicate +SEM. ( $n = 3$ ).

**Mitosis is associated with a loss of fluorescence from one of the NS5A fluorophore-tagged genomes in dual-replicon cells.**

To further demonstrate that decay from the dual- to single-replicon state occurs during, or shortly after, mitosis, 7.5-H2B-EBFP2 cells were transfected with Jc1/ $\Delta^{GFP}$  & Jc1/ $\Delta^{mCherry}$  or Jc1/ $\Delta^{GFP-BSD}$  & Jc1/ $\Delta^{mKO2-BSD}$  RNA and, 2 days later, imaged via time-lapse microscopy for ~40 hours. Dual-replicon cells entering mitosis were identified by GFP/mCherry or GFP/mKO2 fluorescence and chromatin condensation of the H2B-EBFP2 tag. The relative fluorescence of the GFP/mCherry or GFP/mKO2 tags markedly shifts after mitosis (Figure 3.6). Although we never observed complete loss of fluorescence of one of the NS5A tags, a marked shift in fluorescence favoring one of the two replicons was observed in nearly every post mitotic daughter cell that was successfully imaged for more than 24 hours following division. Near-complete loss of fluorescence of one of the NS5A tags was observed only when one of the two replicons already had an advantage. We hypothesize that one mitotic bottleneck may randomly lead to a bias in the number of genomes of one of the replicons; an additional round of mitosis and thus another bottleneck may be necessary to fully purge the other replicon.

Interestingly, in 9 of 12 observations displaying a shift in fluorescence, one replicon became dominant in both daughter cells. This tendency to favor the same genome in both daughter cells suggests that the genetic bottleneck does not typically partition the genomes between daughter cells. In one case, a shift in replicon fluorescence was observed in a dual-replicon cell that initiated mitosis but failed to undergo cytokinesis, resulting in a multinucleate or multilobed nucleated

cell. Thus, cytokinesis and partitioning of viral RNA to the daughter cells does not appear to be necessary for the genetic bottleneck; instead, the structural changes that occur in the host cell during mitosis may be the cause of the genetic bottleneck. In summary, mitosis of dual-replicon cells appears to restrict HCV genome recombination by promoting the elimination of one of the two viral genomes. This elimination depends on compartmentalization of the HCV genomes.



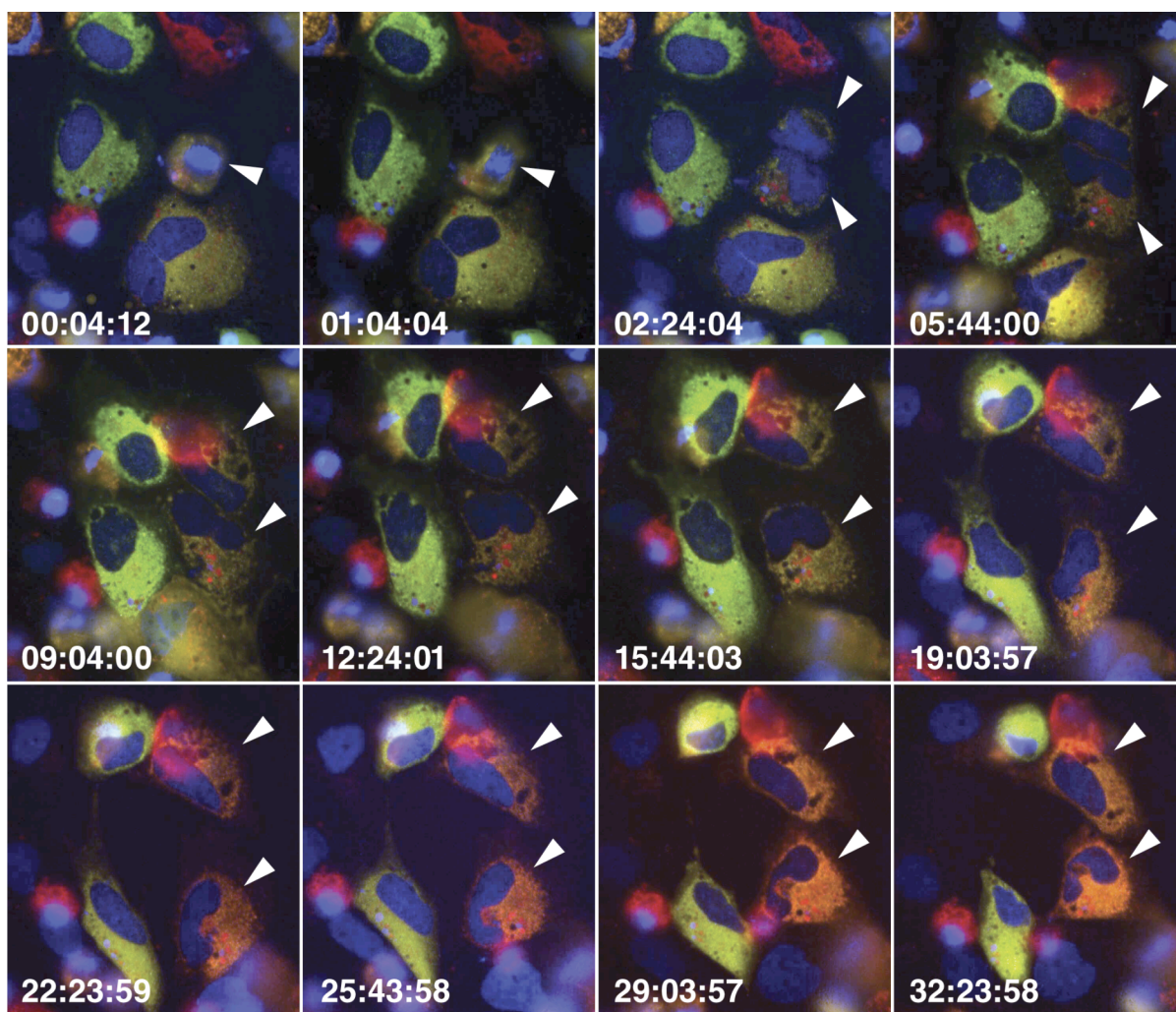


**Figure 3.6: Loss of fluorophore-NS5A epifluorescence in dual-replicon cells after mitosis.**

7.5-H2B-EBFP2 (blue) cells were transfected with Jc1/ $\Delta^{\text{GFP}}$  (green) and Jc1/ $\Delta^{\text{mCherry}}$  (red) RNA and imaged by time-lapse epifluorescence microscopy, taking images every 20 min. Arrowheads indicate parental and daughter cells. Times are indicated as hours:minutes:seconds. Note the drastic shift in fluorescence favoring the Jc1/ $\Delta^{\text{mCherry}}$  replicon in both daughter cells.

### **Decay of dual-replicon cells is biased toward the more-fit replicon.**

The previous analysis of the decay phenomenon in dual-replicon cells was performed only using replicons that were essentially equally replication-competent. Although unexpected, the fitness differences of the Jc1/ $\Delta$ <sup>XFP-BSD</sup> replicons permitted determination of whether the decay of dual-replicon cells is biased toward the replicon that accumulates higher levels of viral RNA. We predicted that the replicon with higher RNA levels would be more likely to survive the bottleneck. Huh7.5 cells were transfected with Jc1/ $\Delta$ <sup>GFP-BSD</sup> & Jc1/ $\Delta$ <sup>mKO2-BSD</sup> or Jc1/ $\Delta$ <sup>mCherry-BSD</sup> & Jc1/ $\Delta$ <sup>mKO2-BSD</sup>, then separated by FACS into dual-replicon, single-replicon, and replicon-negative populations (Supplemental Figure B.4 & Supplemental Figure B.5). After isolation, blasticidin selection was used to prevent the confounding outgrowth of replicon-negative cells. Beginning 48 hours post-isolation, cells were stained with 7-AAD and Annexin-V APC, and analyzed by flow cytometry for GFP/mKO2/mCherry/7-AAD/Annexin-V APC fluorescence.

Replicons that accumulate higher levels of RNA have an advantage in the decay process (Figure 3.1, Figure 3.7A, B, D, & E). The replicons, in order of increasing RNA accumulation are Jc1/ $\Delta$ <sup>GFP-BSD</sup> < Jc1/ $\Delta$ <sup>mKO2-BSD</sup> < Jc1/ $\Delta$ <sup>mCherry-BSD</sup>. In the decay process, the same order is observed: Jc1/ $\Delta$ <sup>mKO2-BSD</sup> has the advantage over Jc1/ $\Delta$ <sup>GFP-BSD</sup>, and Jc1/ $\Delta$ <sup>mCherry-BSD</sup> has the advantage over Jc1/ $\Delta$ <sup>mKO2-BSD</sup>. While the advantage of Jc1/ $\Delta$ <sup>mKO2-BSD</sup> over Jc1/ $\Delta$ <sup>GFP-BSD</sup> was quite marked, the advantage of Jc1/ $\Delta$ <sup>mCherry-BSD</sup> over Jc1/ $\Delta$ <sup>mKO2-BSD</sup> was not as pronounced (Supplemental Table B.3 & Supplemental Table B.4). This may reflect the smaller difference in Jc1/ $\Delta$ <sup>mCherry-BSD</sup> and Jc1/ $\Delta$ <sup>mKO2-BSD</sup> RNA levels (Figure 3.1C). Further, the decay process can

apparently be slowed when the overall load of viral RNA is higher, as more dual-replicon cells are observed by day 11 when Jc1/ $\Delta^{\text{mCherry-BSD}}$  & Jc1/ $\Delta^{\text{mKO2-BSD}}$  are used, compared to Jc1/ $\Delta^{\text{GFP-BSD}}$  & Jc1/ $\Delta^{\text{mKO2-BSD}}$ .

Consistent replication of each replicon over the time course is demonstrated by the fact that isolated single-replicon populations remained >75% HCV-positive over the period of study (Supplemental Figure B.4 & Supplemental Figure B.5). To assure that the blasticidin selection pressure was not too high for the less fit replicons, live cell counts of isolated single- and dual-replicon cultures are shown in Supplemental Figure B.6. Indeed, the less fit replicon-containing cells actually survived/proliferated to a higher level.

Importantly, in both comparisons made between alternately-fit replicons, the bias in decay of dual-replicon cells was toward the replicon that induced *higher* apoptosis rates (Figure 3.7C & F) and *lower* proliferation rates in host cells (Supplemental Figure B.6). Again, when comparing the Jc1/ $\Delta^{\text{mCherry-BSD}}$  and Jc1/ $\Delta^{\text{mKO2-BSD}}$  replicons, the differences in apoptosis rates and proliferation were not significant (Supplemental Table B.5 & Supplemental Table B.6). Apart from demonstrating that the level of RNA of each replicon is important in determining which replicon is lost following mitosis, these results conclusively demonstrate that contaminating single-replicon cells play no role in the observed decay. Otherwise, the replicon inducing more apoptosis and less proliferation in host cells would be expected to be at a disadvantage. In conclusion, the decay process is biased in cases where one replicon has the advantage over the other replicon in terms of a greater number of

viral RNAs per cell. Additionally, the kinetics of decay are faster when the overall numbers of viral RNA per cell are lower.

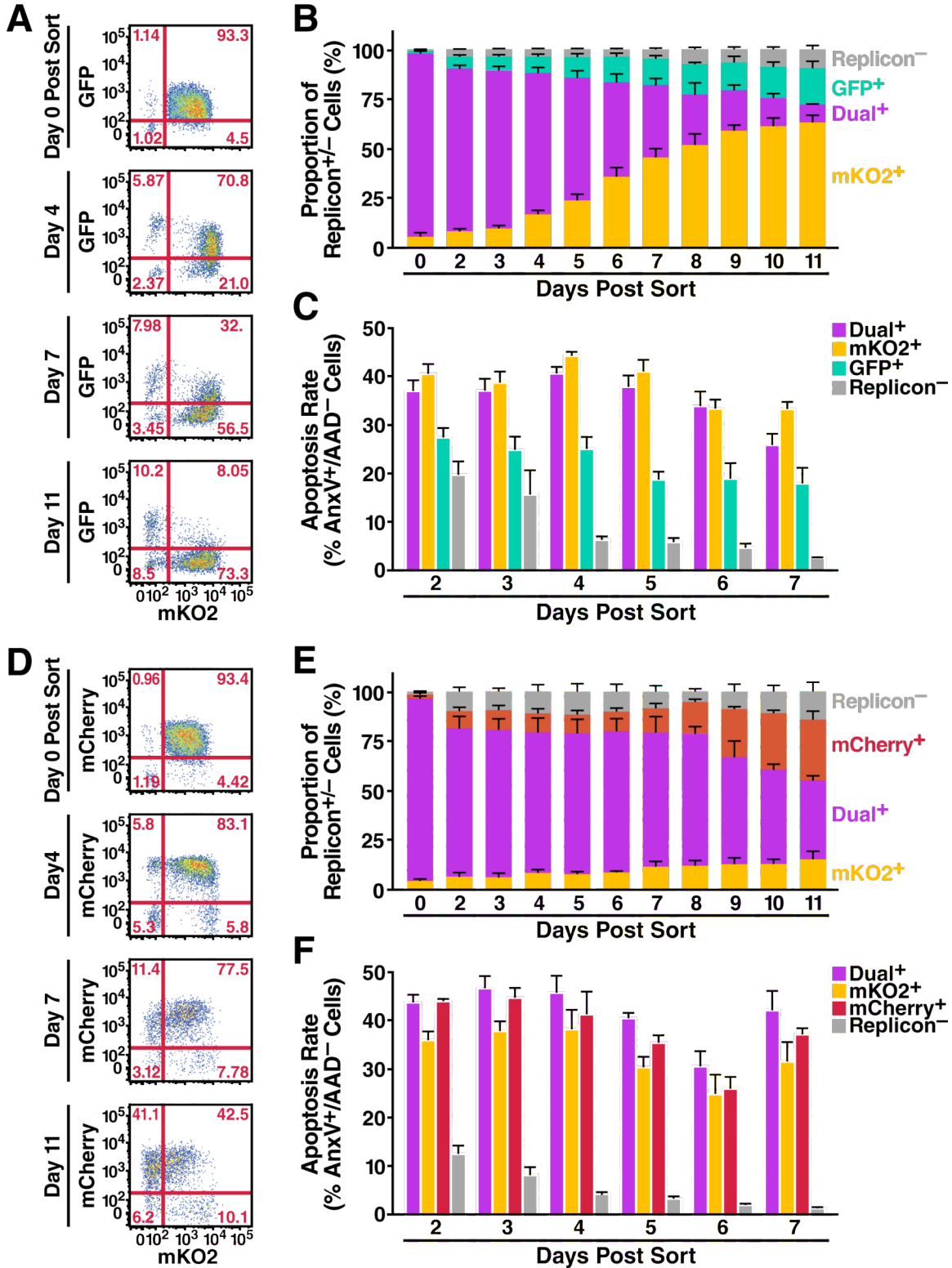


Figure 3.7: Bias in decay of Jc1/ $\Delta$ <sup>XFP-BSD</sup> dual-replicon-containing cells.

Huh7.5 cells were transfected with the following RNAs: (A,B,C) Jc1/ $\Delta$ <sup>GFP-BSD</sup> & Jc1/ $\Delta$ <sup>mKO2-BSD</sup> ( $n=5$  independent experiments); (D,E,F) Jc1/ $\Delta$ <sup>mCherry-BSD</sup> & Jc1/ $\Delta$ <sup>mKO2-BSD</sup> ( $n=3$  independent experiments). 48 hours later, the following populations were isolated by FACS: single-replicon-containing cells, dual-replicon cells, and replicon-negative cells. Replicon-containing cells were kept under selection with 10  $\mu$ g/mL blasticidin after FACS isolation, with media changed for all cells every 24 hours. Cells were collected and stained with 7-AAD and Annexin-V APC at the given time points. (A,D) Representative flow cytometry plots demonstrating the decay of each dual-replicon population. (B,E) Graphic representation of decay of dual-replicon cells. (C,F) Apoptosis rates in each isolated population of cells. Apoptosis rates were assessed as in Figure 3.3. Note that, in each case, the bias in the decay of the dual-replicon cells is toward the replicon with higher RNA levels (Figure 3.1). Error bars indicate +SEM.

### **Transition of dual-replicon cells leads to explicit loss of viral genomes.**

The decay of dual-replicon into single-replicon cells was previously measured by loss of fluorescence conferred by an NS5A-fluorophore fusion. We elected to further study this transition using an independent method since cryptic replication can occur below the limits of fluorescent detection. First, dual-replicon cells were isolated and allowed to transition into single-replicon cells, followed by isolation of the two single-replicon populations using flow cytometry. The relative level of each viral genome was then measured by quantitative RT-PCR. As replicon-negative cells quickly dominate in cultures of Jc1/ $\Delta^{\text{XFP}}$ -transfected cells, we used the Jc1/ $\Delta^{\text{GFP-BSD}}$  and Jc1/ $\Delta^{\text{mKO2-BSD}}$  replicons, where blasticidin selection can minimize the numbers of replicon-negative cells. For these cultures, the selection pressure was less stringent as new blasticidin-containing media was added every 3 days, compared to every day in the earlier experiments. This allowed us to maximize the number of cells obtained at the end of the culture. However, this was not sufficient to keep replicon-negative cells from continuing to proliferate, and apparently erased the advantage of the Jc1/ $\Delta^{\text{mKO2-BSD}}$  over the Jc1/ $\Delta^{\text{GFP-BSD}}$  replicon in the decay process (Figure 3.8A).

Following separation of the indicated populations in Sorts 1&2 (Figure 3.8A), RNA was isolated from cells, reverse-transcribed, and subjected to quantitative PCR using the following: mKO2/GFP probes specific for each viral genome, and a GAPDH probe to normalize for RNA quantities. Negative and positive control RNAs were isolated from untransfected Huh7.5 cells as well as Jc1/ $\Delta^{\text{mKO2-BSD}}$  & Jc1/ $\Delta^{\text{GFP-BSD}}$  stable replicon cell lines (expanded for >45 days post-transfection under blasticidin selection; data not shown). As shown in Figure 3.8B, following decay of

dual-replicon cells into single-replicon populations, Jc1/ $\Delta^{GFP-BSD}$  RNAs were >100-fold more abundant in GFP+ cells compared to mKO2+ cells, and vice versa for Jc1/ $\Delta^{mKO2-BSD}$  RNA in mKO2+ versus GFP+ cells. Indeed, the level of Jc1/ $\Delta^{GFP-BSD}$  RNA in mKO2+ cells and the level of Jc1/ $\Delta^{mKO2-BSD}$  RNA in GFP+ cells approximated that found in the “replicon-negative” population, and thus likely represents the level of contaminating cells in the culture following FACS isolation. The attempt was made in Sort 2 to reisolate dual-replicon cells following the decay period; due to the small numbers of these cells, we only successfully reisolated dual-replicon cells once for RNA analysis. In this case, the levels of Jc1/ $\Delta^{mKO2-BSD}$  & Jc1/ $\Delta^{GFP-BSD}$  RNA were comparable to the levels in the Sort 2 isolation of mKO2+ and GFP+ cells, respectively. These studies indicate that the decay of dual-replicon into single-replicon cells is associated with at least a 100-fold reduction in the RNA of one of the two replicon genomes. Hence, the decay phenomenon results in an explicit loss of replicon RNA.



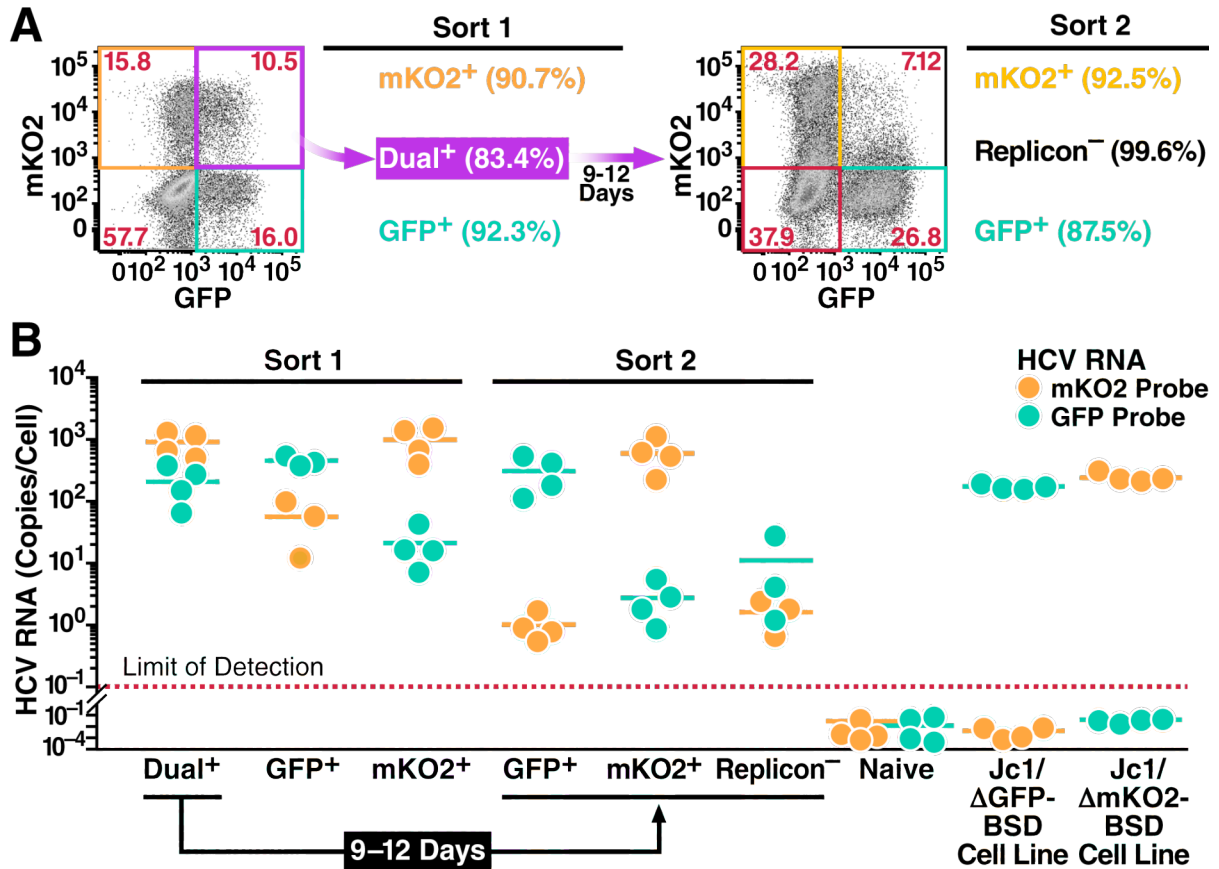


**Figure 3.8: Explicit loss of viral RNA during the decay process.**

Huh7.5 cells were transfected with Jc1/ $\Delta$ <sup>GFP-BSD</sup> and Jc1/ $\Delta$ <sup>mKO2-BSD</sup> RNA. 48 hours later, the following populations were isolated by FACS (Sort 1): Jc1/ $\Delta$ <sup>GFP-BSD</sup>-only replicon-containing cells; Jc1/ $\Delta$ <sup>mKO2-BSD</sup>-only replicon-containing cells; and dual-replicon cells. The dual-replicon cells were further cultured for 9-12 days to allow decay to occur, and replicon-negative and single-replicon cells were isolated as before (Sort 2). (A) Flow cytometric analysis of cells used for Sorts 1 & 2. Gates shown represent those used for isolation of each population. (B) Loss of viral RNA of one species during the decay process. RNA was extracted from each isolated population as well as naïve Huh7.5, stable Jc1/ $\Delta$ <sup>GFP-BSD</sup>, and stable Jc1/ $\Delta$ <sup>mKO2-BSD</sup> replicon-containing cell lines. Quantitative RT-PCR was used to determine the level

of Jc1/ $\Delta^{GFP-BSD}$  and Jc1/ $\Delta^{mKO2-BSD}$  RNA (mKO2/GFP probes). A GAPDH probe was used for normalization of the RNA samples, using the stable Jc1/ $\Delta^{GFP-BSD}$  & Jc1/ $\Delta^{mKO2-BSD}$  cell lines as calibrators. Each data point is shown, with lines indicating the mean ( $n=4$  independent experiments).

## DISCUSSION

In this study, we identify a new mechanism for intracellular competition between different HCV strains. We demonstrate that cells replicating two or more congenic HCV replicons decay over time into a single-replicon state, and that this process is propelled by cellular mitosis. Importantly, the decay of isolated dual-replicon cells to a single-replicon state is not explained by a selective proliferation of a few contaminating single-replicon cells. Although HCV infection can induce cytotoxic effects and cell-cycle abnormalities, these effects were not more prominent in dual-replicon versus single-replicon cells. The decay of dual-replicon cells seems instead to be due to a genetic bottleneck limiting the diversity of HCV strains. On a population level, when congenic, equally fit dual-replicon cells decay into a single-replicon state, neither strain dominates, indicating that this is generally a random phenomenon. However, we observe a clear bias in the dual-replicon decay when using replicons that accumulate different amounts of viral RNA, indicating that this process is influenced by viral fitness. Of note, when examining isolated dual-replicon cells during mitosis, the decay phenomenon tends to favor the same strain in both daughter cells, indicating that the reduction in genetic diversity is similar in both daughters. This decay phenomenon likely explains previous findings that competition can occur between HCV replicons, where the presence of one replicon reduces the replication levels of another replicon [51].

As the genetic bottleneck appears to occur every time the host cell divides, this represents a sequential bottleneck for HCV diversity in a population of dividing host

cells. Sequential bottlenecks are well known in population genetics to lead to the loss of even beneficial mutations [97,98]. A population of two equally fit HCV replicon strains (e.g., Jc1/ $\Delta^{\text{GFP}}$  and Jc1/ $\Delta^{\text{mCherry}}$ ) within one cell can be considered to be a haploid asexual population with a neutral difference at one locus. In this type of population, genetic drift will eventually lead to fixation of Jc1/ $\Delta^{\text{GFP}}$  or Jc1/ $\Delta^{\text{mCherry}}$  in a host cell, even in the absence of a bottleneck. The average number of generations ( $\bar{t}(p)$ ) required for fixation is given by the equation  $\bar{t}(p) = -\frac{1}{p}\{2N_e(1-p)\ln(1-p)\}$  [99,100]. A new generation occurs each time the host cell divides ( $\sim 1.3$  days in naïve Huh7.5 cells) and the frequency of one replicon “allele” initially is  $p=0.5$  since both have equal amounts of RNA. The “effective breeding population size”  $N_e$  represents the number of viral RNAs that populate the new generation of daughter cells. In the absence of a bottleneck,  $N_e$  will be  $\sim 1000$  viral RNAs (Figure 3.1), meaning that fixation will occur in about 5 years! However, according to our data we can very conservatively estimate average fixation at  $\sim 9$  days, meaning half the dual-replicon cells remain. This gives  $N_e \approx 5$ , or the population bottleneck that survives mitosis at approximately five viral RNAs.

Of note, the probability that a neutral allele goes to fixation is simply the initial prevalence  $p$ . For equally fit replicons, where  $p=0.5$ , this suggests equal numbers of single-replicon cells resulting from decay. However, for replicons that accumulate different amounts of RNA, the RNA levels can be used to calculate the expected numbers of single replicon cells. The peak viral RNA accumulations 2 days after transfection for Jc1/ $\Delta^{\text{GFP-BSD}}$ , Jc1/ $\Delta^{\text{mKO2-BSD}}$ , and Jc1/ $\Delta^{\text{mCherry-BSD}}$  are 155, 549, and 845 copies/cell, respectively. This gives  $p=0.220$  for Jc1/ $\Delta^{\text{GFP-BSD}}$  in Jc1/ $\Delta^{\text{GFP-BSD}}$  &

Jc1/ $\Delta^{\text{mKO2-BSD}}$  dual-replicon cells (155/(155+549)), meaning that 22.0% of the single-replicon cells resulting from the decay should be Jc1/ $\Delta^{\text{GFP-BSD}}$ -positive. The actual measured proportion is 22.5% at day 11 (Figure 3.7). In the case of Jc1/ $\Delta^{\text{mKO2-BSD}}$  in Jc1/ $\Delta^{\text{mKO2-BSD}}$  & Jc1/ $\Delta^{\text{mCherry-BSD}}$  dual-replicon cells,  $p=0.394$ . The actual measured proportion of Jc1/ $\Delta^{\text{mKO2-BSD}}$  single-replicon cells at day 11 is in close agreement at 38.7%.

An important caveat to the hypothesis that a genetic bottleneck can occur during the HCV life cycle is that genomes of different viral strains must be compartmentalized separately. HCV RNA replication occurs in specialized replication complexes (RCs) termed the “membranous web,” which are thought to be formed by invaginations of the ER membrane [14,15,101]. If viral genomes from multiple strains were fully mixed in the RCs, it would be difficult to understand how any process could specifically lead to loss of the genomes of one strain. However, of the RC components NS3, NS4B, NS5A, and NS5B, only the highly diffusible NS5A protein is capable of high levels of transcomplementation between defective replicons [51,85], similar to the related pestivirus bovine diarrhea virus [102]. However, a lack of transcomplementation with specific NS5A mutants has demonstrated that even NS5A has some activity that is only exerted *in cis* [103]. These studies thus demonstrate that viral genomes must be sequestered separately; otherwise, functional RC components could replicate defective genomes *in trans*. A more recent study using NS4B-defective replicons demonstrated low levels of transcomplementation; however, the authors postulate that this occurs only when two viral RNAs are incorporated into a newly formed RC [104].

The mechanism underlying this viral winnowing during mitosis is unclear. We suspect that structural changes within the ER or cytoskeletal network occurring during mitosis disrupt the niches normally occupied by HCV RCs. Major structural changes occur in the ER during mitosis, including the stripping of ribosomes and, controversially, either a loss of ER cisternae [93] or ER tubules [92]. Interestingly, HCV nonstructural proteins preferentially localize to ER cisternae near mitochondria [105], and HCV RCs preferentially reside within cholesterol-rich lipid rafts [106,107,108,109]. Since HCV RNA replication occurs on specialized regions of the ER membrane, many of the RCs in a productively infected cell may be disrupted during the major ER structural changes associated with mitosis. Alternatively, the rearrangement of the cytoskeletal network during mitosis [110] might be involved in the genetic bottleneck. The actin and microtubule networks are both necessary for HCV RNA replication [111], NS3 and NS5A specifically associate with tubulin and actin, and depolymerization of either leads to loss of the normal punctate pattern of RC localization [112]. The loss of normal connections between HCV RCs or the ER with the cytoskeletal network during mitosis may indeed be responsible for this mitotic effect. It will be interesting in the future to examine the ultrastructure of HCV RCs by electron microscopy, to determine if there is a visible disruption during mitosis.

Superinfection exclusion in HCV infection has been characterized as host cells productively infected with one HCV strain becoming refractory to further HCV infection within 48 hours after infection [52,53]. Superinfection exclusion was originally postulated to occur at the level of RNA replication or translation, and not at

the level of viral entry, since HIV particles pseudotyped with an HCV envelope showed no defect in viral fusion with HCV-infected cells [53]. However, other work has called into question whether viral entry does play a role in superinfection exclusion. Some studies have found that viral receptors (Claudin-1, NPC1L1, CD81) are downregulated upon infection [13,52,70]. However, another study reported upregulation of Claudin-1 [69], and another found mixed effects (Occludin, LDL-R downregulation; Claudin-1 upregulation) [68]. Regardless of the effects HCV infection has on viral receptor expression, a post-entry block to further viral RNA replication has been well demonstrated in cells replicating HCV RNA [51,52,53,71]. This post-entry block is thought to involve sequestration of one or more limiting host factor(s) or occupancy of replication sites, although the nature of these factor(s) or replicative niches remains to be characterized.

The genetic bottleneck in HCV genomic diversity we observe may have some additional mechanistic parallels to the previously described post-entry superinfection block. The genetic bottleneck occurring during mitosis may similarly result in one strain dominating because it is able to appropriate key host factors or fill replication sites emptied during the process of cell division. Importantly, both the genetic bottleneck and superinfection exclusion act even when viral strains are equally fit. Superinfection exclusion occurs between congenic equally fit strains of HCV, and the genetic bottleneck causes decay of cells dually infected with congenic equally fit strains of HCV. In the case of the genetic bottleneck, however, coinfection with alternately fit strains will demonstrate a bias over time toward the strain that accumulates higher levels of viral RNA. Importantly, the genetic bottleneck will act to

eliminate one or more viral strains even if multiple infections occur within the 48-hour window when superinfection is permissible.

The existence of multiple tiers of intracellular competition between HCV strains has important implications for HCV biology. Each of these competition mechanisms serves to limit the time in which a cell is productively co-infected. Limiting productive co-infection reduces the chances of recombination between HCV strains and the transfer of drug resistance or adaptive mutations between viral strains. Indeed, intra- and intergenotypic recombinant strains of HCV are rare even among patients with multiple infections [31,37,38], although a few examples have been detected [41,42,43,44,113]. Interestingly, it has been suggested that coinfection with multiple strains of HCV leads to exacerbation of chronic HCV disease correlates [36]. Multiple levels of competition may help to explain the recent finding that, when HCV-infected patients are transplanted with HCV-infected liver grafts, one strain (either donor or recipient) exhibits a dominance within as little as 1 day post-transplantation [114]. Naturally, in a patient setting, differences in viral fitness come into play, instituting an additional level of competition between HCV strains. The relative dearth of natural recombinants of HCV strains may be a result of the interplay of the various levels of competition between strains in multitypic infections.

The *in vivo* relevance of a mitotic genetic bottleneck is as yet unclear, as most hepatocytes are not actively cycling. We further demonstrate (Figure 3.4, Supplemental Figure B.6) that cellular division is retarded in host cells replicating HCV genomes, in line with previous findings [86,88]. Cell cycle arrest and decreased proliferation would act to slow the decay of multiply-infected cells by this genetic



bottleneck *in vivo*. Notably, one study found that HCV-infected cells *in vitro* are arrested specifically at the G<sub>2</sub>/M boundary [91], suggesting that HCV may have evolved a means of avoiding this bottleneck. On the other hand, some studies have indicated that HCV genome replication is enhanced in proliferating cells [115,116], and hepatocyte proliferation increases in chronic HCV infection [117,118]. Additionally, the pathway leading from chronic HCV infection to fibrosis, cirrhosis, and hepatocellular carcinoma is intimately linked with an increase in hepatocyte proliferation and turnover [119,120]. A number of studies have suggested that this increase in hepatocyte proliferation is linked to the increased inflammation present in chronic HCV infection [121,122,123,124], raising the possibility that this bottleneck may have a greater role *in vivo* during the latter stages of HCV infection. Interestingly, interferon- $\alpha$  (IFN- $\alpha$ ), part of the present standard of care for chronic HCV treatment, has been demonstrated to induce G<sub>0</sub>/G<sub>1</sub>-phase cell cycle arrest [125,126]. In the context of the mitosis-associated bottleneck, IFN- $\alpha$  treatment would potentially act to retain a higher level of HCV diversity or facilitate viral recombination in treated patients.

A singular strength of HCV is its genomic diversity, leading to the emergence immune escape variants and drug resistant strains. Our results, aside from their potential role in the natural biology of HCV infection suggest that targeting the stability of the HCV replication complex or mimicking the state of the cell in mitosis, aside from any antiviral effects, may act to nonspecifically reduce the quasispecies diversity of HCV. Hopefully, future studies will demonstrate to what extent these multiple levels of competition act on viral quasispecies diversity and recombination in

patients. Understanding this process and learning how to exploit it may have important implications for future drug and vaccine development [31].

## MATERIALS AND METHODS

**Cells and culture conditions.** Huh7.5 cells, a kind gift from C.M. Rice (The Rockefeller University), [74] were maintained in Dulbecco's modified Eagle medium (DMEM), supplemented with 10% fetal bovine serum (FBS), 2 mM L-glutamine, 100 IU/mL penicillin, and 100  $\mu$ g/mL streptomycin (Mediatech). Cells were passaged when they became confluent. In all cases when replicon-positive cells were grown using the Jc1/ $\Delta$ E1E2<sup>NS5A-XFP-BSD</sup> replicons, blasticidin (Invitrogen) selection was begun 2 days post-transfection at 10  $\mu$ g/mL. Continuous selection over a period of 45 days following transfection was used to obtain Jc1/ $\Delta$ E1E2<sup>NS5A-GFP-BSD</sup> and Jc1/ $\Delta$ E1E2<sup>NS5A-mKO2-BSD</sup> replicon cell lines (data not shown).

**Plasmid construction.** NS5A-fluorophore fusion Jc1 genomes were generated by introducing a linker containing an XbaI and PmeI site into amino acid position 383 of NS5A as described [53]. Briefly, a region 5' of the linker site was amplified (primers S6660 and Alinker\_XbaIPmeI\_NS5Aaa383) and a region 3' of the linker was amplified (primers Slinker\_XbaIPmeI\_NS5Aaa383 and A7759). Overlap PCR with primers S6660 and A7759 was used to fuse the 5' and 3' sequences, and the resulting sequence was cloned into pCR4 Topo by TA cloning. The sequence was verified, and a SanDI-RsrII fragment was excised and ligated into the Jc1 parental plasmid [56] to create the Jc1<sup>NS5A-linker</sup> plasmid carrying the linker in NS5A.

Fluorophore-tagged genomes were constructed by amplifying GFP, mCherry, or EBFP2 (with primers GFP\_Fw\_XbaI\_NS5A and GFP\_Rev\_PmeI\_NS5A), digesting

with XbaI and PmeI, and ligating into Jc1<sup>NS5A-linker</sup> to create plasmids: Jc1<sup>NS5A-GFP</sup>, Jc1<sup>NS5A-mCherry</sup>, and Jc1<sup>NS5A-EBFP2</sup>. Envelope-deleted versions of these reporter constructs were constructed by deleting a portion of the E1&E2 genes, from amino acids 313–567 in the Jc1 polyprotein. Briefly, the region from amino acids 568–865 was amplified, introducing a KpnI site before amino acid 568 (primers Jc1\_567\_KpnI\_Fw and Jc1\_865\_KpnI\_Rev). The resulting fragment was cut with KpnI and ligated into the Jc1<sup>NS5A-GFP</sup>, Jc1<sup>NS5A-mCherry</sup>, and Jc1<sup>NS5A-EBFP2</sup> reporter plasmids, where the KpnI fragment encompassing amino acids 313–865 had been digested out. The resulting plasmids were named: Jc1/ΔE1E2<sup>NS5A-GFP</sup>, Jc1/ΔE1E2<sup>NS5A-mCherry</sup>, and Jc1/ΔE1E2<sup>NS5A-EBFP2</sup>.

Fluorophore- and resistance gene-tagged genomes were constructed as follows. Monomeric Kusabira Orange 2 (mKO2) [95] was synthesized *in vitro* by assembly PCR-based gene synthesis. The primers used as template (mKO2 1 – mKO2 30) were designed using the DNAsworks program [127]. GFP and mCherry were amplified using primers GFP\_Fw\_XbaI\_NS5A & GFP\_Rev\_Gly\_Linkers, and mKO2 was amplified using primers mKO2\_Fw\_XbaI\_NS5A & mKO2\_Rev\_Gly\_Linkers, respectively. The blasticidin resistance gene (BSD) was amplified using primers BSD\_Fw\_Gly\_Linkers and BSD\_Rev\_PmeI\_NS5A, and overlap PCR was carried out to fuse GFP, mCherry and mKO2 to the BSD gene. The resulting products were digested with XbaI and PmeI, and ligated into Jc1/ΔE1E2<sup>NS5A-GFP</sup>, replacing the GFP fluorophore, to create the constructs Jc1/ΔE1E2<sup>NS5A-GFP-BSD</sup> and Jc1/ΔE1E2<sup>NS5A-mKO2-BSD</sup>.

The Fucci cell-cycle system [95] was reconstructed by fusing the coding sequence of EBFP2 or GFP to the sequence encoding the N-terminal 110 amino acids of human Geminin (hGem) protein. EBFP2 or GFP was amplified using primers GFP\_Fw\_XbaI\_Kozak and GFP\_Rev\_Gly\_Linkers (encoding a GGGGK linker), and human Geminin was amplified from HeLa cDNA and reverse transcribed from the control HeLa RNA in the SuperscriptIII kit (Invitrogen), using primers hGem\_Fw\_Gly\_Linkers and hGem\_Rev\_EcoRI. Overlap PCR was used to fuse hGem and EBFP2 or GFP sequences. The resulting fragments were cut with XbaI and EcoRI and ligated into the lentiviral expression plasmid pSicoR MCS [76]. Histone H2B-EBFP2, used to locate mitotic cells by chromatin condensation, was similarly constructed by fusing the H2B sequence (amplified using primers H2B\_Fw\_NheI\_Kozak and H2B\_Rev\_Gly\_Linkers) to the EBFP2 sequence (amplified using primers GFP\_Fw\_Gly\_Linkers and GFP\_Rev\_+stop\_PmeI) by overlap PCR. The resulting fragment was digested with NheI and PmeI and ligated into pSicoR MCS. All primer sequences are provided in Supplemental Table B.7.

**RNA synthesis and transfection** *In vitro* transcription of viral RNA and electroporation were carried out as previously described [26,77], with minor modifications. Viral RNA was transcribed using a Megascript T7 Kit (Ambion), and purified by LiCl precipitation.  $7.5 \times 10^6$  Huh7.5 cells were electroporated with 10  $\mu$ g of viral RNA when transfecting a single strain of HCV or 5  $\mu$ g each when multiple strains were used.

**Production of Huh7.5 cell lines by lentiviral transduction.** Lentiviral particles were produced using an HIV-1-based vesicular stomatitis virus (VSV)-G pseudotyped lentiviral system, as described [128]. The transfer plasmids pSicoR H2B-EBFP2 or pSicoR hGem-GFP were cotransfected into 293T cells along with the HIV-1-based packaging construct pCMV $\Delta$ R8.91 and the VSV-G envelope vector pMD.G. Supernatants were collected 48 hours post-transfection and concentrated by ultracentrifugation for 2 hours at 53,000x *g* in a SW28 rotor.  $2.7 \times 10^5$  Huh7.5 cells were spinoculated with 700  $\mu$ L of concentrated viral supernatant at 1000x *g* for 2 hours at room temperature and expanded in culture. Cells were sorted by flow cytometry for EBFP2 or GFP fluorescence to assure full transduction of the resulting 7.5-H2B-EBFP2 and 7.5-GFP-hGem cell lines.

**Flow cytometry.** In experiments where single-, dual- or triple-replicon-containing cells were isolated by sorting, the indicated cell lines were transfected with 5  $\mu$ g each of the HCV RNAs. The exception was the triply-transfected cells used in the modeling analysis (Supplemental Figure B.2), where 3.33  $\mu$ g each of the HCV RNAs were used for consistent comparison with dually-transfected cells. Two days after electroporation, cells were sorted using a FACSAria III fluorescence-activated cell sorter (Becton Dickinson), plated on 24-well plates at  $1 \times 10^5$  (Jc1/ $\Delta$ E1E2<sup>NS5A-XFP</sup> replicons) or  $5 \times 10^4$  (Jc1/ $\Delta$ E1E2<sup>NS5A-XFP-BSD</sup> replicons) cells/well, and analyzed on a LSRII flow cytometer (Becton Dickinson) at various times afterward. In experiments to analyze the loss of dual/triple-replicon cells, the cells were washed with medium

every 2 days to remove dead/apoptotic cells and then fixed in 4% paraformaldehyde (Sigma) before flow cytometric analysis.

In apoptotic cell analysis, the cells were washed every 24 hours so that the measured apoptosis rate would reflect only the preceding 24 hours. Cells were trypsinized and combined with cells from the medium, washed once in Annexin-V binding buffer (10 mM HEPES, 140 mM NaCl, 2.5 mM CaCl<sub>2</sub>), and stained with 7-aminoactinomycin-D (7-AAD; 2.5 ng/μL, eBioscience) and Annexin-V APC (1:20 dilution, BD Biosciences) in Annexin-V binding buffer. Cells were immediately analyzed on an LSRII. To generate a positive apoptotic control, naïve Huh7.5 cells were treated for 24 hours with 100-1600 nM staurosporine (Sigma-Aldrich).

For cell-cycle analysis, the cells were fixed in ice-cold 70% EtOH for 30 min, washed twice in phosphate-citrate buffer (200 mM Na<sub>2</sub>HPO<sub>4</sub>, 4 mM citric acid), treated with 100 μg/mL RNase A (Qiagen) for 30 min, and stained with 50 μg/mL propidium iodide (PI) (Invitrogen). Cells were immediately analyzed on an LSRII.

To analyze the loss of viral RNA in the decay of dual-replicon cultures, Huh7.5 cells were transfected with 5 μg each of Jc1/ΔE1E2<sup>NS5A-GFP-BSD</sup> and Jc1/ΔE1E2<sup>NS5A-mKO2-BSD</sup> RNA. Two days post-transfection, dual- and single-replicon cells were isolated by FACS (Sort 1). The dual-replicon cells were cultured in the presence of 10 μg/mL blasticidin (Invitrogen) for 9-12 days following Sort 1 to allow decay to occur (media changed every third day), and single-replicon and replicon-negative cells were isolated by FACS (Sort 2).

**CFSE dilution and growth arrest studies.** For carboxyfluorescein diacetate-succinimidyl ester (CFSE) dilution analyses, cells were electroporated with 5  $\mu\text{g}$  of Jc1/ $\Delta\text{E1E2}^{\text{NS5A-mCherry}}$  and Jc1/ $\Delta\text{E1E2}^{\text{NS5A-EBFP2}}$  RNA and plated at  $37.5 \times 10^3$  cells/well in 24-well plates, or at  $7.5 \times 10^6$  cells in 140-mm plates. One day later cells were treated with 5 or 10  $\mu\text{M}$  CFSE (Invitrogen) for 30 min, washed twice with medium, and analyzed for fluorophore expression and CFSE median fluorescence intensity on an LSRII at various times after the CFSE treatment. To generate growth-arrested Huh7.5 cells, cells were grown for 15 days on 140-mm plates coated with 50  $\mu\text{g}/\text{mL}$  rat tail collagen type I (Becton Dickinson) in the presence of 1% (vol-vol) DMSO (Sigma-Aldrich), as described [94]. Following transfection of growth-arrested cells, cells were replated on collagen-coated culture vessels in the presence of 1% DMSO.

**RNA isolation and quantitative PCR analysis.** Total RNA was extracted from each population with Trizol (Invitrogen). Reverse-transcription and subsequent real-time PCR was performed in two steps using the Superscript III first strand cDNA synthesis system (Invitrogen) followed by the Quantitect probe PCR system, or in one step using the Quantitect probe RT-PCR system (Qiagen). Real-time PCR was performed on a 7900HT fast real-time PCR system (Applied Biosystems), according to the manufacturer's protocol. The probes and primers were purchased from Applied Biosystems, and are given in Supplemental Table B.8. The GFP probe/primer set was as described previously [129].



**Live-cell epifluorescence microscopy.** Huh7.5 or 7.5-H2B-EBFP2 cells were electroporated with Jc1/ $\Delta$ E1E2<sup>NS5A-GFP</sup>, Jc1/ $\Delta$ E1E2<sup>NS5A-mCherry</sup>, or Jc1/ $\Delta$ E1E2<sup>NS5A-EBFP2</sup> RNA. The cells were plated at  $5 \times 10^4$  cells/well in LabTek 8-well coverslip chambers (Nunc) and incubated for 2 days in a 37°C incubator. For time-lapse microscopy, cells were imaged on the UCSF Nikon Imaging Center Eclipse TI-E epifluorescence microscope (Nikon) at 37°C, 5% CO<sub>2</sub>. Images were colorized for clarity and ease of viewing using Photoshop (Adobe) in the publication figures. Supplemental videos were assembled using ImageJ software (National Institutes of Health).

**Statistical analysis.** Statistical analysis was carried out using Prism 5 software (Graphpad). For CFSE dilution curve analysis, semilog regression and the extra-sum of squares F test was used to determine whether the slopes of the dilution curves were significantly different. For data that was not amenable to regression analysis (analysis of transfection efficiency, RNA accumulation, and cell proliferation by cell count over time) the integrated area under the curve (AUC) was obtained, followed by one-way ANOVA with Bonferroni multiple comparison correction to ascertain statistical differences in AUC. Regression curves and AUC data are not shown. The comparison of cell cycle progression in dual- and single-replicon-containing cells was assessed by a Student's t-test, as only one comparison was being made. For all other tests, one- or two-way ANOVA with Bonferroni multiple comparison corrections were used, as appropriate.

## **ACKNOWLEDGMENTS**

We thank Ralf Bartenschlager (University of Heidelberg) for the Jc1 construct, Charles Rice (Rockefeller University) for Huh7.5 cells, Takaji Wakita (National Institute of Infectious Disease, Japan) for the JFH1 construct, and Matthew Spindler for the pSicoR construct. We thank Kurt Thorn and the Nikon Imaging Center at UCSF for assistance with microscopic analysis. We are grateful to Jane Gordon, Tara Rambaldo, and Sarah Elmes from the UCSF Laboratory for Cell Analysis, as well as Marielle Cavrois and the Gladstone Flow Cytometry Core for assistance with flow cytometric assays. We thank Jill Dunham for critical reading of the manuscript, John Carroll for help in preparation of the figures, and members of the Greene laboratory for helpful discussion and support. This work was supported by the Gladstone Institutes and funds from the US Public Health Service (T32: A1060537-05 (UCSF Program in Microbial Pathogenesis and Host Defense)).

**CHAPTER 4**  
**CONCLUSIONS**

## Summary

The goal of this thesis work was to further characterize viral competition in HCV infection, with a focus on improving our understanding of the basic biology underpinning the HCV life cycle and why natural HCV recombinants are so rare. Toward this end, we concentrated on further understanding the superinfection exclusion phenomenon and interrogating any potentially means of competition in HCV infection.

In Chapter 2, we attempted to isolate a strain of HCV that was capable of overcoming the superinfection exclusion process. We were successful in doing so, demonstrating that HCV could indeed evolve the ability to overcome this superinfection block. Interestingly, we observed that the superinfectious HCV strain was more infectious even in naïve cells, and excluded HCV genomes already present in host cells from replicating. We identified key mutations in the viral NS5A protein and the 3' UTR that allow HCV to evade the post-entry barrier to superinfection. Finally, we demonstrated that these mutations do not alter the translation of HCV RNA, and that superinfection exclusion itself is not mediated by a block in the translation of the secondary viral RNA.

In Chapter 3, we identified a novel mechanism of competition between HCV genomes. We demonstrate that, even in host cells where two or more viral genomes are productively replicating, inter-viral competition occurs. Over the space of 9–12 days, a population of dually infected, dividing host cells will resolve into singly infected cells. This competition happens at, or shortly following, mitosis of the host cell and likely results from disruption of HCV replication complexes (RCs) during cell

division. Notably, this competition appears to be stochastic, resulting from a random genetic bottleneck that occurs during mitosis.

### **Significance**

Throughout the course of this work, our findings have consistently shown that viral competition in HCV infection is a dynamic, multi-tiered process. Previous studies have established that HCV has less than 48 hours after a primary infection to establish a secondary infection in a host cell. Outside that window, superinfection exclusion begins to operate, and the chances of recombination between viral strains are greatly reduced. We show in Chapter 3 that this state is inherently unstable even when multiple infections occur within this 48-hour window, and that dually infected cells rapidly decay into singly infected cells as a result of mitosis. In Chapter 2, we demonstrate that HCV can develop the ability to overcome superinfection exclusion; however, the viral genome already present in the host cell is rapidly excluded by the superinfectious strain. All of these processes tend to limit the time that multiple HCV genomes co-occupy a host cell. Recombination in HCV occurs far less than in other plus-stranded RNA viruses, even in model *in vitro* systems [130], and our work demonstrates that this may be a result of multiple levels of viral competition.

Beyond demonstrating why recombination is so rare in HCV biology, our work uncovered key aspects of the basic biology of the HCV life cycle. In Chapter 2, we found that mutations in NS5A and the 3' UTR were sufficient to allow HCV to overcome the post-entry superinfection block. It is likely that superinfection exclusion occurs when a primary virus sequesters a host factor or factors necessary for the successful replication of a secondary virus. As these host factors would serve as

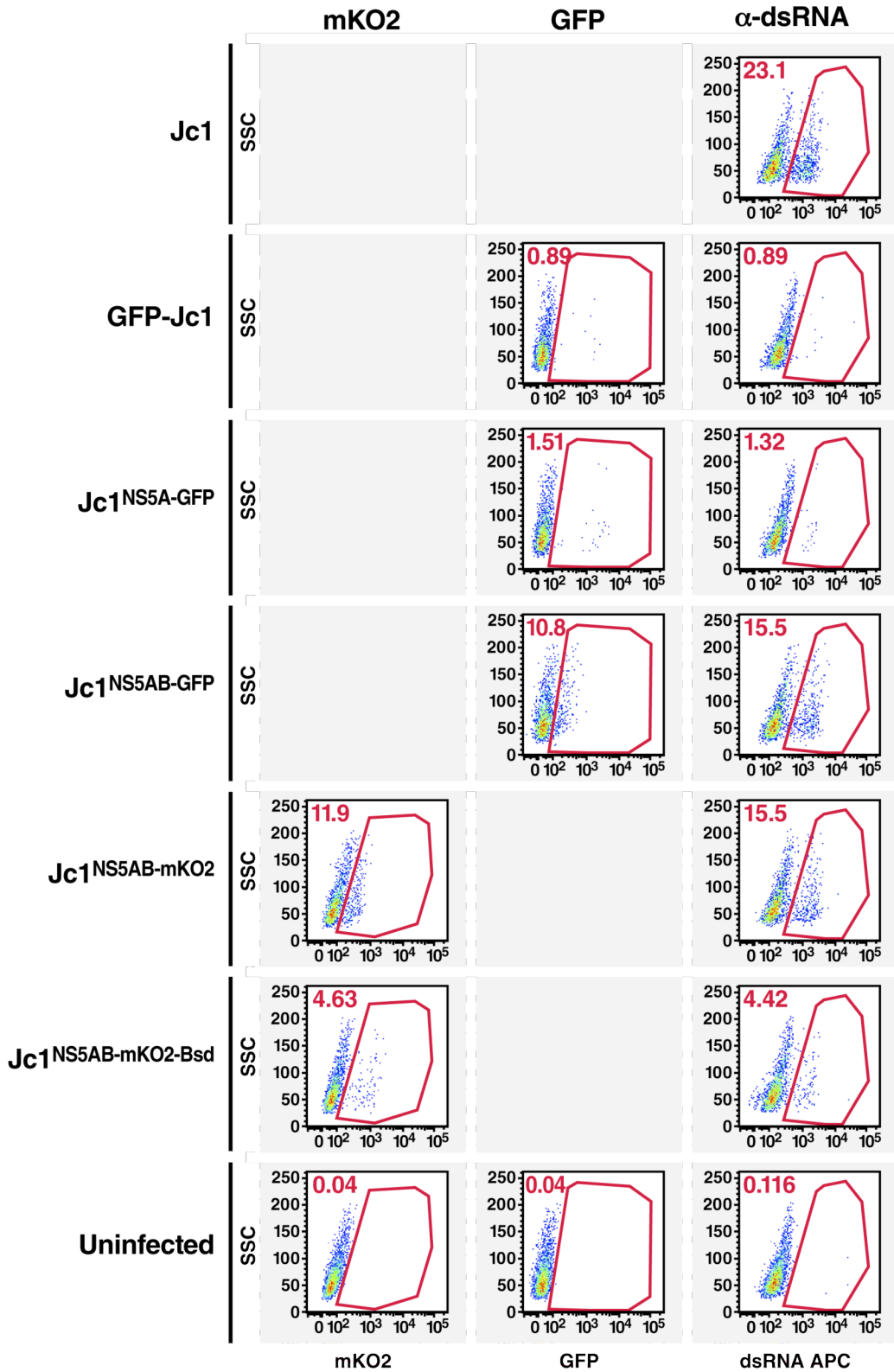
rate-limiting components of the HCV life cycle, they would be highly attractive as candidates for novel drug therapies. Further work to elucidate the interaction partners of the mutant NS5A and 3' UTR could identify these rate-limiting factors.

We further showed that mitosis of host cells leads to a genetic bottleneck that apparently reduces the number of HCV genomes 30–200 fold. This bottleneck is likely a result of host cell structural changes during mitosis and attendant disruption of the HCV RC. The replication of HCV genomes could therefore be reduced using drug therapies that mimic the structural changes found in mitosis or disrupt the RC. These therapies would have the added benefit of reducing the diversity of HCV, due to the genetic bottleneck.

Our demonstration that viral competition plays a large role in HCV biology helps to solve the puzzle of why recombination is so rare in HCV infections. A clear understanding of the degree to which recombination can occur is critical in an age of directly acting antiviral drugs, to understand how drug resistance may be transferred between strains. Beyond this aspect of HCV treatment and epidemiology, we hope that our work in gaining a greater understanding of the HCV life cycle may lead one day to the creation of new drugs that help millions of patients around the world.

## REFERENCES AND SUPPLEMENTAL MATERIAL

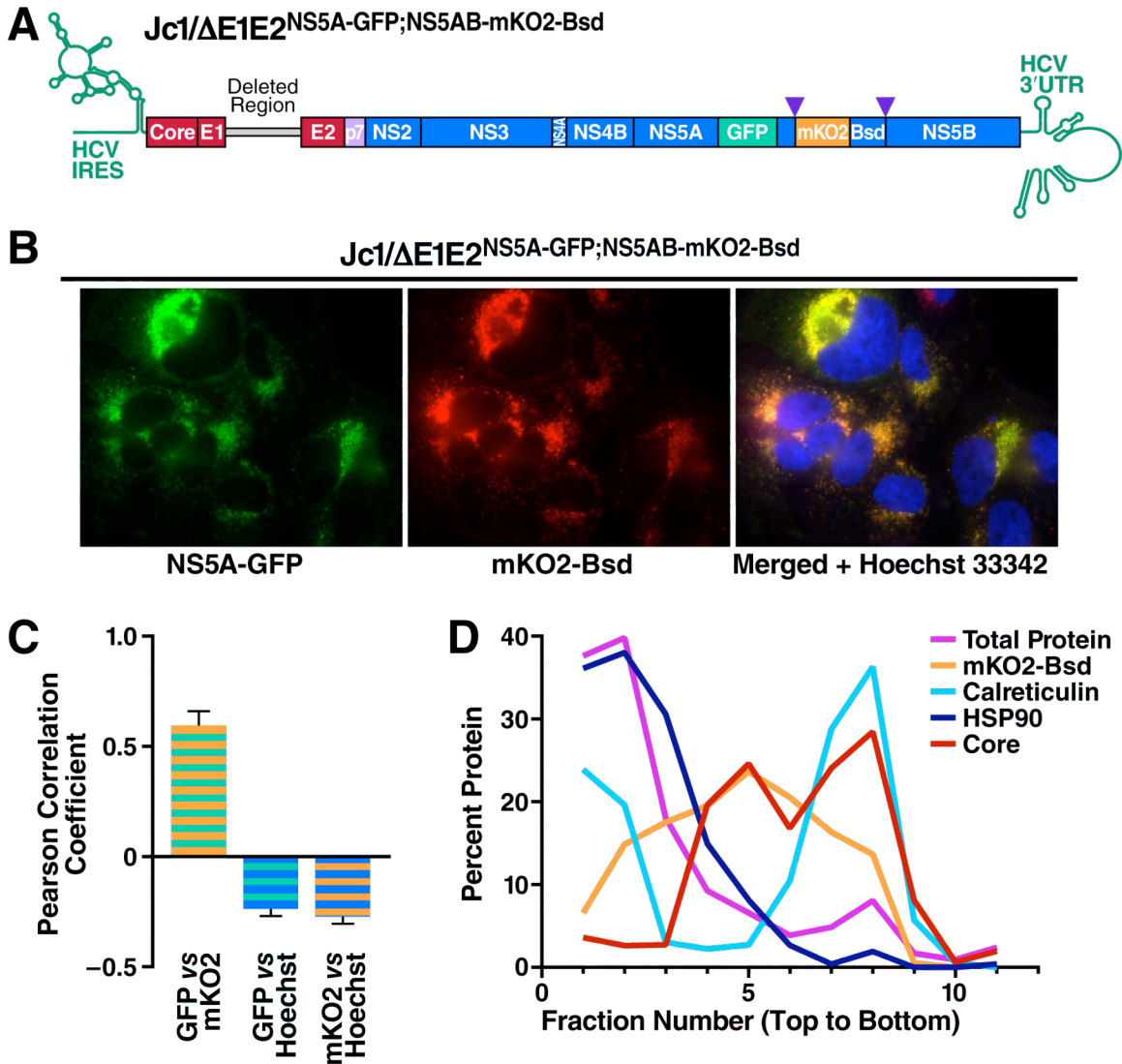
## Appendix A. Supplemental Material to Chapter 2.





**Supplemental Figure A.1: Representative flow cytometry plots indicating infection rates of viral supernatants.**

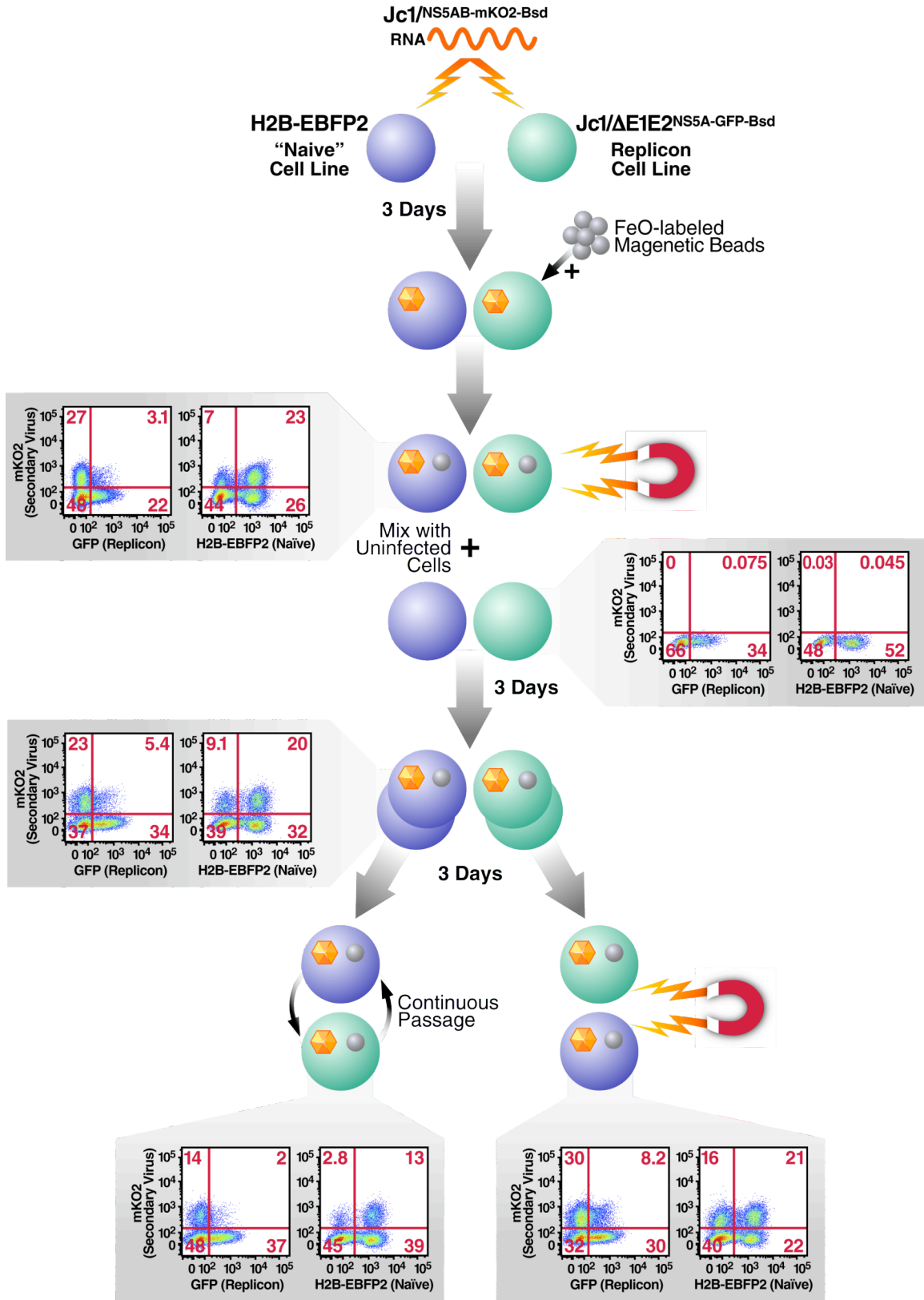
Huh7.5 cells were transfected with the indicated viral transcripts, and viral supernatants were collected 2 days later. Naïve Huh7.5 cells were infected with undiluted viral supernatants, and the cells were analyzed by flow cytometry 3 days later for GFP and mKO2 autofluorescence from the reporter viral genomes, as well as dsRNA staining for general HCV infection.



**Supplemental Figure A.2: Subcellular localization of the mKO2-Bsd transgene in Jc1/ΔE1E2<sup>NS5A-GFP;NS5AB-mKO2-Bsd</sup> replicon-containing cells.**

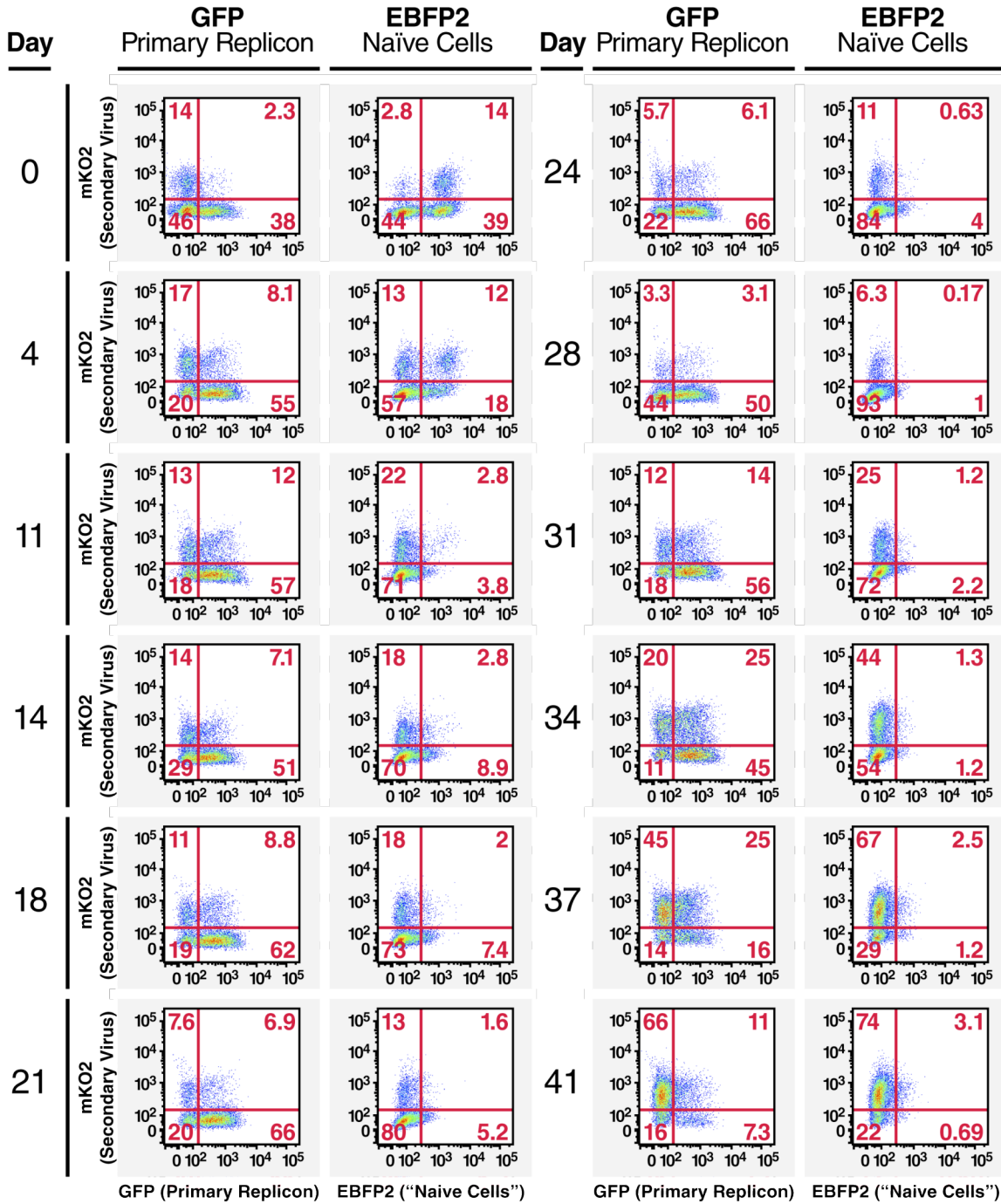
(A) Schematic diagram of the Jc1/ΔE1E2<sup>NS5A-GFP;NS5AB-mKO2-Bsd</sup> replicon construct. (B) Epifluorescence microscopy of live Huh7.5 cells transfected with Jc1/ΔE1E2<sup>NS5A-GFP;NS5AB-mKO2-Bsd</sup> RNA. (C) Quantification of colocalization between NS5A-GFP and mKO2-BSD in Jc1/ΔE1E2<sup>NS5A-GFP;NS5AB-mKO2-Bsd</sup> replicon-containing cells. Eighteen

microscopic fields containing 166 cells were analyzed for the Pearson colocalization coefficients of NS5A-GFP, mKO2-Bsd, and Hoescht 33342. A Pearson coefficient of +1 indicates perfect colocalization, 0 indicates random distribution, and -1 indicates perfect exclusion of two fluorophores relative to each other. The high positive Pearson coefficient for NS5A-GFP versus mKO2-Bsd indicates significant colocalization. Error bars indicate +SEM. (D) Profile of protein localization in iodixanol fractionation of Jc1/ $\Delta$ E1E2<sup>NS5A-GFP;NS5AB-mKO2-Bsd</sup> replicon-containing cell lysates (from Figure 2.2). Protein amounts reflect the amount of protein in each fraction as a percentage of the total protein in all fractions; the mKO2-Bsd profile represents the fully cleaved ~36 kDa fragment.



**Supplemental Figure A.3: Flow cytometry plots of cells used in the FeOLabel magnetic bead isolation protocol.**

GFP indicates the Jc1/ $\Delta$ E1E2<sup>NS5A-GFP</sup> replicon-positive cells, EBFP2 indicates the “HCV-naïve” 7.5-H2B-EBFP2 cells, and mKO2 indicates the secondary Jc1/<sup>NS5AB-mKO2-Bsd</sup> virus. Note the higher Jc1/<sup>NS5AB-mKO2-Bsd</sup> infection rates in the FeOLabel-positive magnetically selected cells; these cells were initially transfected with Jc1/<sup>NS5AB-mKO2-Bsd</sup>. Spread of the Jc1/<sup>NS5AB-mKO2-Bsd</sup> virus into the FeOLabel-negative cells occurred over the 3 day coculture period; hence, the Jc1/<sup>NS5AB-mKO2-Bsd</sup> infection rate is lower in these cells. Flow cytometry plots refer to the experimental scheme shown in Figure 2.3B.



**Supplemental Figure A.4: Flow cytometry plots from superinfected cells during continuous cell passage.**

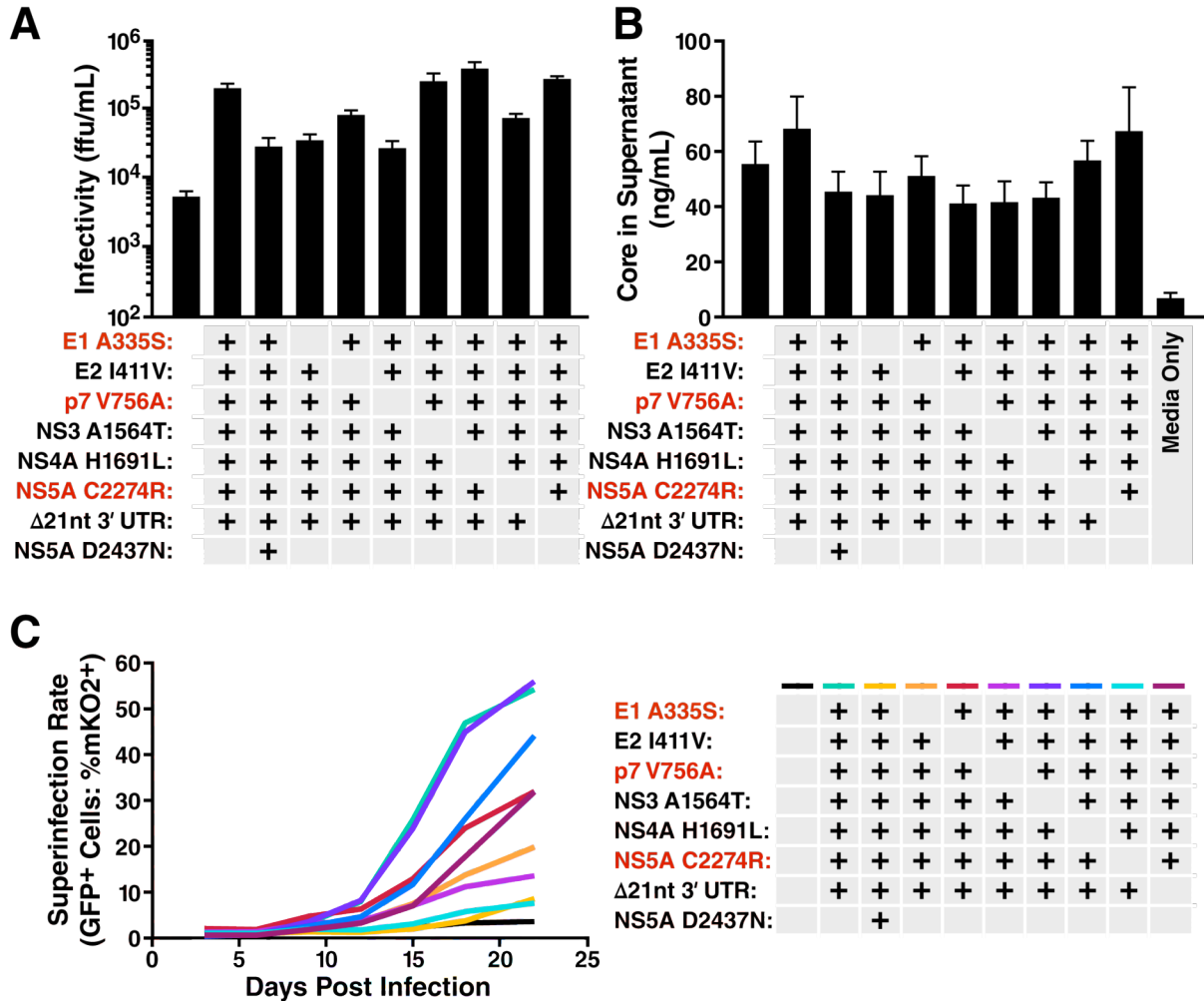
These plots show FeOLabel cell cultures following magnetic isolation (from Figure 2.3B & C). The rapid disappearance of the 7.5-H2B-EBFP2 cells through day 11

post-isolation is likely a result of their higher susceptibility to infection and death induced by Jc1/<sup>NS5AB-mKO2-Bsd</sup> infection. Note that superinfection (GFP+mKO2+ cells) dramatically increases from day 31–41 post-isolation; the high levels of superinfection correlate with an exclusion of the primary Jc1/ $\Delta$ E1E2<sup>NS5A-GFP</sup> replicon at days 37–41 post-isolation.

| Round 1 Amplification Primers  |                  |                           |  |
|--------------------------------|------------------|---------------------------|--|
| Amplicon                       | Primer Name      | Primer Sequence           | Template                                 |
| 1                              | Jc1 Amplicon 1F  | TCCCGGGAGAGCCATAGTGGT     | Viral supernatant<br>cDNA for sequencing |
|                                | Jc1 Amplicon 5R  | GCCGCATTTGAGGTAAGTGGTA    |  |
| 2                              | Jc1 Amplicon 6F  | TTCAACGCCAGCACGGACCTGT    |  |
|                                | Jc1 Amplicon 8R  | CGCCACCTGAACATACCTACC     |  |
| 3                              | Jc1 Amplicon 9F  | AGGGCCGCTTTGACACA         |  |
|                                | Jc1 Amplicon 10R | GCCGTAGCCAGCACAGTTAGTCTGA |  |
| 4                              | Jc1 Amplicon 11F | CGATGAATGCCACGCTGTGGATGCT |  |
|                                | Jc1 Amplicon 12R | AGTGTGACAATCCTGCGAGGTATT  |  |
| 5                              | Jc1 Amplicon 13F | AGCAGGCCAGGACATACAAC      |  |
|                                | Jc1 Amplicon 14R | GGCTCGAGAAAGTCCAGAACGG    |  |
| 6                              | Jc1 Amplicon 15F | TGACGTGGACATGGTCGATGCCAAC |  |
|                                | Jc1 Amplicon 15R | CCGCTAGCTTGATGTCCTTTAAGAC |  |
| 7                              | Jc1 Amplicon 16F | TCACAGAGGGCTAAAAAGGTAACT  |  |
|                                | Jc1 Amplicon 16R | TCCCCTGGCTTCTGAGATGACTAC  |  |
| 8                              | Jc1 Amplicon 17F | CCATGTTCAACAGCAAGGTCAAAC  |  |
|                                | Jc1 Amplicon 18R | GGACCTTTCACAGCTAGCCGTGACT |  |
| Round 9 Amplification Primers* |                  |                           |  |
| Amplicon                       | Primer Name      | Primer Sequence           | Template                                 |
| 1                              | Jc1 Amplicon 0F  | ACCTGCCCTAATAGGGGCGA      | Viral supernatant<br>cDNA for sequencing |
|                                | Jc1 Amplicon 5R  | GCCGCATTTGAGGTAAGTGGTA    |  |
| 2                              | Jc1 Amplicon 6F  | TTCAACGCCAGCACGGACCTGT    |  |
|                                | Jc1 Amplicon 8R  | CGCCACCTGAACATACCTACC     |  |
| 3                              | Jc1 Amplicon 9F  | AGGGCCGCTTTGACACA         |  |
|                                | Jc1 Amplicon 10R | GCCGTAGCCAGCACAGTTAGTCTGA |  |
| 4                              | Jc1 Amplicon 11F | CGATGAATGCCACGCTGTGGATGCT |  |
|                                | Jc1 Amplicon 12R | AGTGTGACAATCCTGCGAGGTATT  |  |
| 5                              | Jc1 Amplicon 13F | AGCAGGCCAGGACATACAAC      |  |
|                                | Jc1 Amplicon 14R | GGCTCGAGAAAGTCCAGAACGG    |  |
| 6                              | Jc1 Amplicon 15F | TGACGTGGACATGGTCGATGCCAAC |  |
|                                | Jc1 Amplicon 15R | CCGCTAGCTTGATGTCCTTTAAGAC |  |
| 7                              | Jc1 Amplicon 16F | TCACAGAGGGCTAAAAAGGTAACT  |  |
|                                | Jc1 Amplicon 16R | TCCCCTGGCTTCTGAGATGACTAC  |  |
| 8                              | Jc1 Amplicon 17F | CCATGTTCAACAGCAAGGTCAAAC  |  |
|                                | Jc1 Amplicon 19R | ACATGATCTGCAGAGACCAGTTA   |  |

**Supplemental Table A.1: Primers used to amplify fragments of the superinfectious virus in Rounds 1 & 9.**





**Supplemental Figure A.5: Viral accumulation, infectivity, and viral spread of mutant and WT Jc1/<sup>NS5AB-mKO2-Bsd</sup> strains.**

(A) Viral accumulation in supernatants of transfected cells. Huh7.5 cells were transfected with WT and mutant Jc1/<sup>NS5AB-mKO2-Bsd</sup> transcripts, and supernatants were collected 2–5 days later. HCV core protein levels in the supernatants were assessed by HCV core ELISA.  $n \geq 4$  independent virus preparations; error bars indicate +SEM. (B) Viral titers of the supernatants in (A) as assessed by limiting dilution assay.  $n \geq 4$  independent virus preparations; error bars indicate + SEM. (C) Superinfection spread in replicon cells. Jc1/ $\Delta$ E1E2<sup>NS5A-GFP</sup> replicon-containing cells

were superinfected at an MOI of 0.1, and cultures were continuously passaged for 22 days-post infection. The superinfection rate (GFP+ cells: %mKO2+) was analyzed at various time points by flow cytometry. Note that the superinfectious phenotype is still present even when viral input is normalized by infectious titer rather than HCV core; a long period of viral spread, however, is required to observe this phenotype.

| Primer Name                   | Primer Sequence  | Template  |
|-------------------------------|--|---|
| NS5ABmcs1                     | TCCGGCGGTCCGACGTCC                                       | Overlapping PCR-based gene synthesis  |
| NS5ABmcs2                     | TCTCTGAGGGGGCCGGCTCACCAGGGGACGTCGGACCGCC                 |   |
| NS5ABmcs3                     | CCGGCCCCCTCAGAGACAGGTTCCGCCCTCTATGCCCC                   |   |
| NS5ABmcs4                     | ATCTCCAGGCTCCCCCTCGAGGGGGGCGATAGAGGAGCG                  |   |
| NS5ABmcs5                     | AGGGGAGCCTGGAGATCCGGACCTGGAGTCTGATCAGGT                  |   |
| NS5ABmcsnew6                  | GACCTGGAGTCTGATCAGGTAGAGCTCAACCTCCACCCC                  |   |
| NS5ABmcsnew7                  | GCTTCAACCTCCACCCCAAGTGGGGGAGTGGCTCCCGGT                  |   |
| NS5ABmcsnew8                  | GGGAGTGGCTCCCGGTTCCGGCTCCGGGCTTGGTCTACT                  |   |
| NS5ABmcs9                     | CTCGGGGCTTGGTCTACTTGTCTCCGAGGAGGACATACC                  |   |
| NS5ABmcsnew10a                | CTCCGAGGAGGACGATACCACCGTGTGCTGCTCCATGTCATACTCCGC         |   |
| NS5ABmcsnew11                 | GCTCCATGTCATACTCCGCAGCAGCAAGATCTTTAGAAATTTCTTA           |   |
| NS5ABmcsnew12                 | CTGCTGCTTTCGAATCTAGATTAATTAAGAATTTAAAGATCTTGCTGCT        |   |
| NS5ABmcsnew13                 | ATTAATCTAGATTCGAAAGCAGCAGCCAGCGAAGAGGACGACA              |   |
| NS5ABmcsnew14                 | CTCATGGAGCAACACACCGTGGTGTCTCTCTCGTGG                     |   |
| NS5ABmcs15                    | ACGACACCACGGTGTGTGCTCCATGAGCTACAGTGGAC                   |   |
| NS5ABmcs16                    | CAAGGGGTGATCAATGCTCCGGTCCAGCTGTAGCTCATGG                 |   |
| NS5ABmcs17                    | GGAGCATTGATCACCCCTTGTAGCCCGAAGAAGAAAAGC                  |   |
| NS5ABmcs18                    | TGCTGAGGGGGTGTAGGGGAGCTTTTCTTCTCGGGGCT                   |   |
| NS5ABmcs19                    | CCATCAACCCCTCAGCACTCCCTGCTCAGGTATCACAA                   |   |
| NS5ABmcs20                    | TGAGGTTGTACAGTACACCTTGTGTGATACCTGAGCAGGGA                |   |
| GFP NS5AB BqIII Fw            | GTTTCTTAGATCTATGGTGAGCAAGGGCGAGGAG                       | pIRES2-EGFP   |
| GFP NS5AB EcoRI Rev           | GTTTCTGAATTCCTTGTACAGCTCCATCCATGCCG                      | pBR322 Jc1/AE1E2-NS5A-mKO2-BSD  |
| mKO2 NS5AB BqIII Fw           | GTTTCTTAGATCTATGGTCTTGTGATCAAGCCCGAAA                    |   |
| mKO2 NS5AB EcoRI Rev          | GTTTCTGAATTCGCTGTAGTGGGCCACGGCGTCT                       | pBR322 Jc1/AE1E2-NS5A-mKO2-BSD,<br>pBR322 Jc1/AE1E2-NS5A-GFP-BSD  |
| BSD NS5AB EcoRI Rev           | GTTTCTGAATTCGCCCTCCACACATAACCAGAG                        | pGL3  |
| Luc NS5AB BqIII Fw            | GTTTCTTAGATCTATGGAAGCAGCCAAAACATAAAGAAAG                 |   |
| Luc NS5AB EcoRI Rev           | GTTTCTGAATTCACCGGCGATCTTTCCGCCCTT                        | pUC Con1  |
| Con1 1253 XhoI Fw             | GTTTCTCAGGAAATTCCTCGAGCGGATG                             |   |
| Con1 1365 GFP overlap Rev New | CTCCTCGCCCTTGCTCACCATGGGGGGCATGGAGGAGTAC                 |   |
| Con1 1366 GFP overlap Fw      | CGGCATGGACGAGCTGTACAAGCTTGGAGGGGGAGCCGGGG                | pIRES2-EGFP   |
| Con1 1530 MfeI Rev            | GTTTCTGGTGTCAATGGTGTCTCAGTGTCT                           |   |
| GFP Fw                        | ATGGTGAGCAAGGGCGAGGAG                                    | pMCherry  |
| GFP Rev -stop                 | CTTGTACAGCTCGTCCATGCCG                                   |   |
| GFP Fw NheI                   | GTTTCTGCTAGCTCCATGGTGAGCAAGGGCGAGGAG                     |   |
| GFP Rev stop PmeI             | GTTTCTGTTAAACCCCTTACTTGTACAGCTCGTCCATGCC                 | pBR322 Jc1, pBR322 Jc1/NS5AB-mKO2-Bsd A335S, pBR322 Jc1/NS5AB-mKO2-Bsd I411V, pBR322 Jc1/NS5AB-mKO2-Bsd A335S I411V |
| E1E2 171 Fw NheI              | GTTTCTGCTAGCGCCACCATGGGTTGCTCCTTTTCTATCTTCTTGCT          |   |
| E1E2 750 Rev PmeI             | GTTTCTGTTAAACTTATGCTTCGGCTGGCCCAACA                      | pBR322 Jc1  |
| T7 5' UTR Fw BqIII            | GTTTCTAGATCTTGCAGGTAATACGACTCACTATAG                     |   |
| Core +262 Rev HindIII         | GTTTCTAAGCTTTCCCGTATAGGGGCCAGGG                          | pBR322 Jc1, pBR322 Jc1/NS5AB-mKO2-Bsd Δ21 nt 3'UTR, pBR322 Jc1/NS5AB-mKO2-Bsd Δ36 nt 3'UTR                          |
| 3' UTR Fw XbaI                | GTTTCTTCTAGAAGCGGCACACACTAGGTACACT                       |   |
| T7 Terminator Rev SalI        | GTTTCTGTCGACCAAAAACCCCTCAAGACCCGTTTA                     | pBR322 Jc1  |
| HDV Ribo Fw XbaI              | GTTTCTTCTAGAGGCCGCGATGGTCCACGC                           |   |
| pRL Fw T7                     | GCTCTAATACGACTCACTATAGGGACTTAATACGACTCACTATAGGCTAG       | pRL-Null  |
| pRL Rev polyA                 | TTTTTTTTTTTTTTTTTTTTTTTTTTTTTTTTCACCTGCATTCAGTTGTGGTTTGT |   |

**Supplemental Table A.2: Primer sequences and templates used in plasmid and T7 template construction.**

| Mutation      | Upstream Flanking Primer (Forward) | Reverse Mutagenesis Primer  | Forward Mutagenesis Primer   | Downstream Flanking Primer (Reverse)         | Upstream Restriction Site | Downstream Restriction Site |
|---------------|------------------------------------|---|--|--|---------------------------|-----------------------------|
| E1 A335S      | GCTCTGCTCTGCCCTCTACGTG             | CACGCATCGCGTACGACAAGAT<br>CATGGTAGC   | GCTACCATGATCTTGTGCTACG<br>CGATGCGTG  | GCCGCGCACCTGCATGGGTG                         | <i>KpnI</i>               | <i>KpnI</i>                 |
| E2 I411V      | GCTCTGCTCTGCCCTCTACGTG             | CGAGCTGGACTTTCTGCCTGGG<br>GCCCA   | TGGGCCCCAGGCAGAAAGTCCA<br>GCTCG  | GCCGCGCACCTGCATGGGTG                         | <i>KpnI</i>               | <i>KpnI</i>                 |
| p7 V756A      | GCTCTGCTCTGCCCTCTACGTG             | GCAGCGTGAAGATGGCCAGCT<br>TCTCTAGTG  | CACTAGAGAAGCTGGCCATCTT<br>GCACGCTGC  | GCCGCGCACCTGCATGGGTG                         | <i>KpnI</i>               | <i>KpnI</i>                 |
| NS3 A1564T    | TGCTGAGGGGACTTGGTAG                | GAGGCCGGTGAAGACTGCTCC<br>CAAAATTCAGAT   | ATCTTGAATTTGGGAGACAGT<br>TTTCACCGGCCTC   | GTTTCGCGGCCGCATGTGGGG<br>CGGATCTGTTAGCA      | <i>AvrII</i>              | <i>SanDI</i>                |
| NS4A H1691L   | TGCTGAGGGGACTTGGTAG                | CGCTGGTTGACGAGCAAGCGGC<br>CGA   | TCGGCCGCTTGTCTGTCACCA<br>GCG   | GTTTCGCGGCCGCATGTGGGG<br>CGGATCTGTTAGCA      | <i>AvrII</i>              | <i>SanDI</i>                |
| NS5A C2274R   | TCT                                | CCTGGGGAGCATGCGTCCGAT<br>GGTATTG  | CAATACCATCGGAGCGCATGCT<br>CCCCAGG  | GACGCTGCCGTCATGTTAGTAC<br>CTCATCTTCATTTCCGGC | <i>SanDI</i>              | <i>BglII</i>                |
| NS5A D2437N   | TCT                                | GCACACGGTGGTATTGCTCTCC<br>TCGAGC  | GCTCCGAGGAGACAATACCAC<br>CGTGTGC   | GACGCTGCCGTCATGTTAGTAC<br>CTCATCTTCATTTCCGGC | <i>SanDI</i>              | <i>BglII</i>                |
| 3' UTR A21 nt | GAGAGGTTACACGGGCTTGAC              | AAGATGGAGCCACCAAGAAAGA<br>AAGTAGAATAAAAAAAAAAAAAA<br>AGAAAAAAAAAAAAAAAAAAAAA<br>AAAAAAAAAAAAAAAAAAAAA<br>AG | CTTTTTTTTTTTTTTTTTTTTT<br>TTTTTTTTTTTTTTTTTTTT<br>CTTTTTTTTTTTTTTATTCTAC<br>TTTTCTTCTTGGTGGCTCCATC<br>TT | ATTAACCCCTACTAAAGGGA                         | <i>AscI</i>               | <i>MluI</i>                 |
| 3' UTR A36 nt | GAGAGGTTACACGGGCTTGAC              | TGGAGCCACCAAGAAAGAAAGT<br>AGAATAAAAAAAAAAAAAAAAAA<br>AAAAAAAAAAAAAAAAAAAAA<br>AAAAAAGGAACAG                 | CTGTTCTTTTTTTTTTTTTTT<br>TTTTTTTTTTTTTTTTTTTT<br>TTTTTTTTTATTCTACTTTCTT<br>TCTTGGTGGCTCCA                | ATTAACCCCTACTAAAGGGA                         | <i>AscI</i>               | <i>MluI</i>                 |

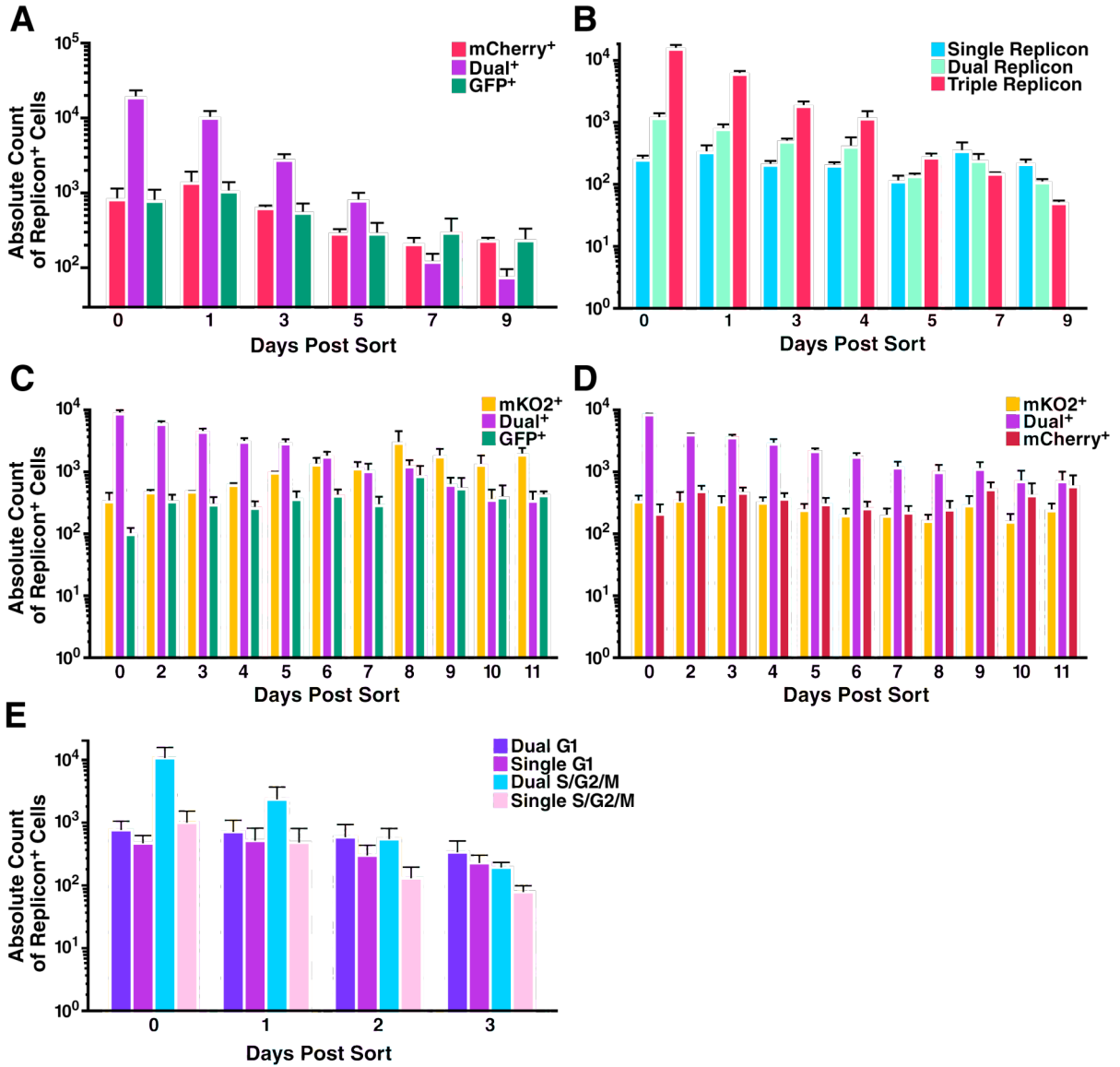
**Supplemental Table A.3: Primer sequences and restriction sites used in site-directed mutagenesis of pBR322 Jc1/<sup>NS5A</sup>mKO2-Bsd plasmid DNA.**

**Appendix B. Supplemental Material to Chapter 3.**

| Transfection: Jc1/ $\Delta$ GFP & Jc1/ $\Delta$ mCherry |           |                |                    |                    |                    |                   |
|---|-----------|----------------|--------------------|--------------------|--------------------|-------------------|
| Days  | Post-Sort | Dual+ vs. GFP+ | Dual+ vs. mCherry+ | Dual+ vs. mCherry+ | Dual+ vs. mCherry+ | mCherry+ vs. GFP+ |
|   | <b>0</b>  | p<0.0001       | p<0.0001           | p<0.0001           | p<0.0001           | ns                |
|   | <b>1</b>  | p<0.0001       | p<0.0001           | p<0.0001           | p<0.0001           | ns                |
|   | <b>3</b>  | p<0.0001       | p<0.0001           | p<0.0001           | p<0.0001           | ns                |
|   | <b>5</b>  | p<0.001        | ns                 | ns                 | ns                 | ns                |
|   | <b>7</b>  | ns             | p<0.05             | p<0.05             | p<0.05             | ns                |
|   | <b>9</b>  | ns             | p<0.01             | p<0.01             | p<0.01             | ns                |

**Supplemental Table B.1. Statistical significance of the differences in the proportions of replicon-positive cells in dual-replicon decay experiments<sup>a</sup>.**

<sup>a</sup> Two-way ANOVA with Bonferroni multiple comparison correction was used to analyze the difference in proportions of each replicon-positive cell population (ns: non-significant).



**Supplemental Figure B.1. Absolute cell counts of replicon-positive cells in dual-replicon decay experiments.**

The absolute cell counts of each replicon-positive population were obtained by flow cytometry, after singlet discrimination by FSC-A/FSC-H and live cell discrimination by FSC-A/SSC-A. (A) Data refers to Figure 3.2B. (B) Data refers to Figure 3.2C. (C) Data refers to Figure 3.7B. (D) Data refers to Figure 3.7D. (E) Data refers to Figure 3.6C.



**Triple-replicon cells contribute to the pool of dual- and single-replicon cells over time.**

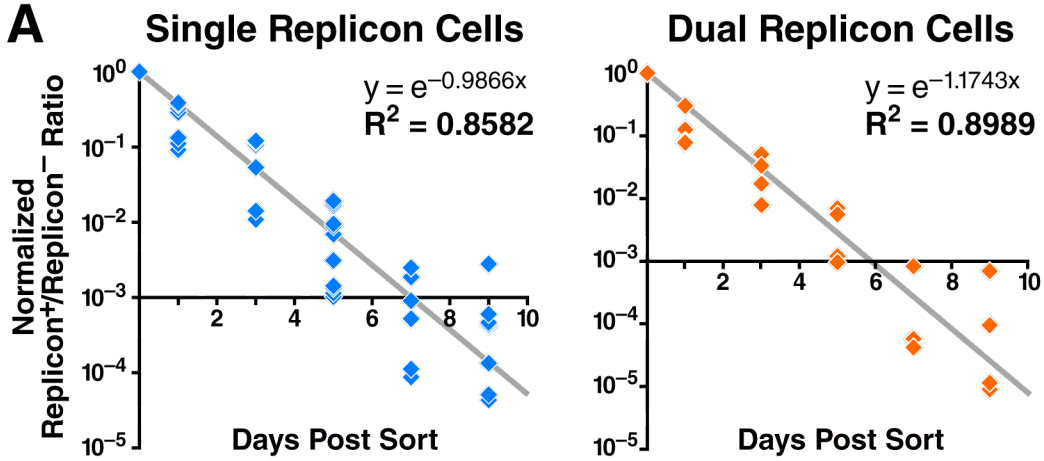
To explain the apparent transition of triple-replicon cells to dual-replicon and finally to single-replicon, we hypothesized that cells replicating fewer strains of HCV have a selective advantage. Hence, the small number of contaminating dual- and single-replicon cells in a population of isolated triple-replicon cells would come to dominate the pool of replicon-positive cells over time. In order to disprove this null hypothesis, we carried out modeling studies to predict the behavior of the contaminating dual- and single-replicon cells in the absence of any decay of triple-replicon cells.

Huh7.5 cells were transfected with a total of 10  $\mu\text{g}$  of Jc1/ $\Delta^{\text{GFP}}$  and Jc1/ $\Delta^{\text{mCherry}}$ , and single- (mCherry+GFP- / mCherry-GFP+) and dual-replicon (mCherry+GFP+) cells were isolated by flow cytometry two days later. The ratio of the replicon-positive cells to the contaminating replicon-negative cells was obtained by flow cytometric analysis at various time points post-sort. This ratio was normalized to 1 at the time point immediately following FACS isolation (as the number of replicon-negative cells varied between experiments). As shown in Supplemental Figure B.2, both the single-replicon:replicon-negative and dual-replicon:replicon-negative ratio decays exponentially over the time period analyzed, due to Jc1-mediated cytotoxicity and slowed cellular proliferation. Note that the exponential decay slope is steeper in dual-replicon:replicon-negative (-1.1743) compared to single-replicon:replicon-negative (-0.9866). As these decay curves were obtained in the absence of any triple-replicon cells, they can be used to predict the behavior of these populations



over time in the presence of triple-replicon cells, assuming that decay of triple-replicon cells is not contributing to their numbers.

The equation given in Supplemental Figure B.2 was used to model the behavior of the contaminating dual- and single-replicon cells in a population of isolated triple-replicon cells. Huh7.5 cells were transfected with a total of 10  $\mu\text{g}$  of Jc1/ $\Delta^{\text{GFP}}$ , Jc1/ $\Delta^{\text{mCherry}}$ , and Jc1/ $\Delta^{\text{mCherry}}$ , and triple-replicon (GFP+mCherry+EBFP2+) cells were isolated by flow cytometry two days later. Using the decay slopes obtained in Supplemental Figure B.2A, we could then model (1) the count of single-replicon, dual-replicon, and replicon-negative cells immediately following isolation, (2) the replicon-negative cell count at various time points post-isolation, and (3) the behavior of the dual- and single-replicon cells. As shown in Supplemental Figure B.2, there are far more single- and dual-replicon cells, both as a proportion of replicon-positive cells and as an overall percentage of the culture, than would be expected given their behavior in isolation (the absence of triple-replicon cells). Further note that the dual-replicon pool increases prior to the single-replicon pool of cells, consistent with the hypothesis that triple-replicon cells decay into dual- and finally single-replicon cells. This allows us to disprove the null hypothesis that the single- and dual-replicon cells prevail over triple-replicon cells due to a selective advantage.

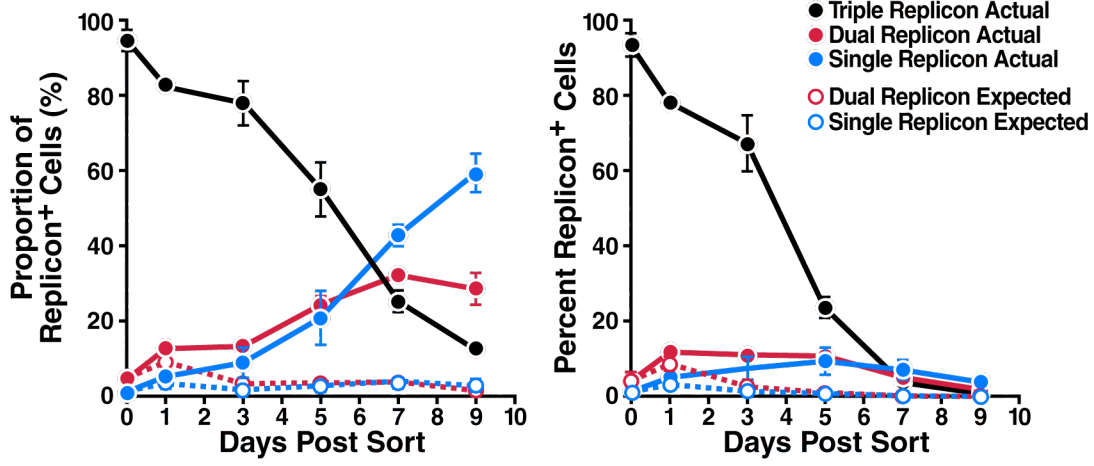


**B**

$$I_{Et} = e^{-\lambda t} (I_{A0}/U_{A0}) U_{At}$$

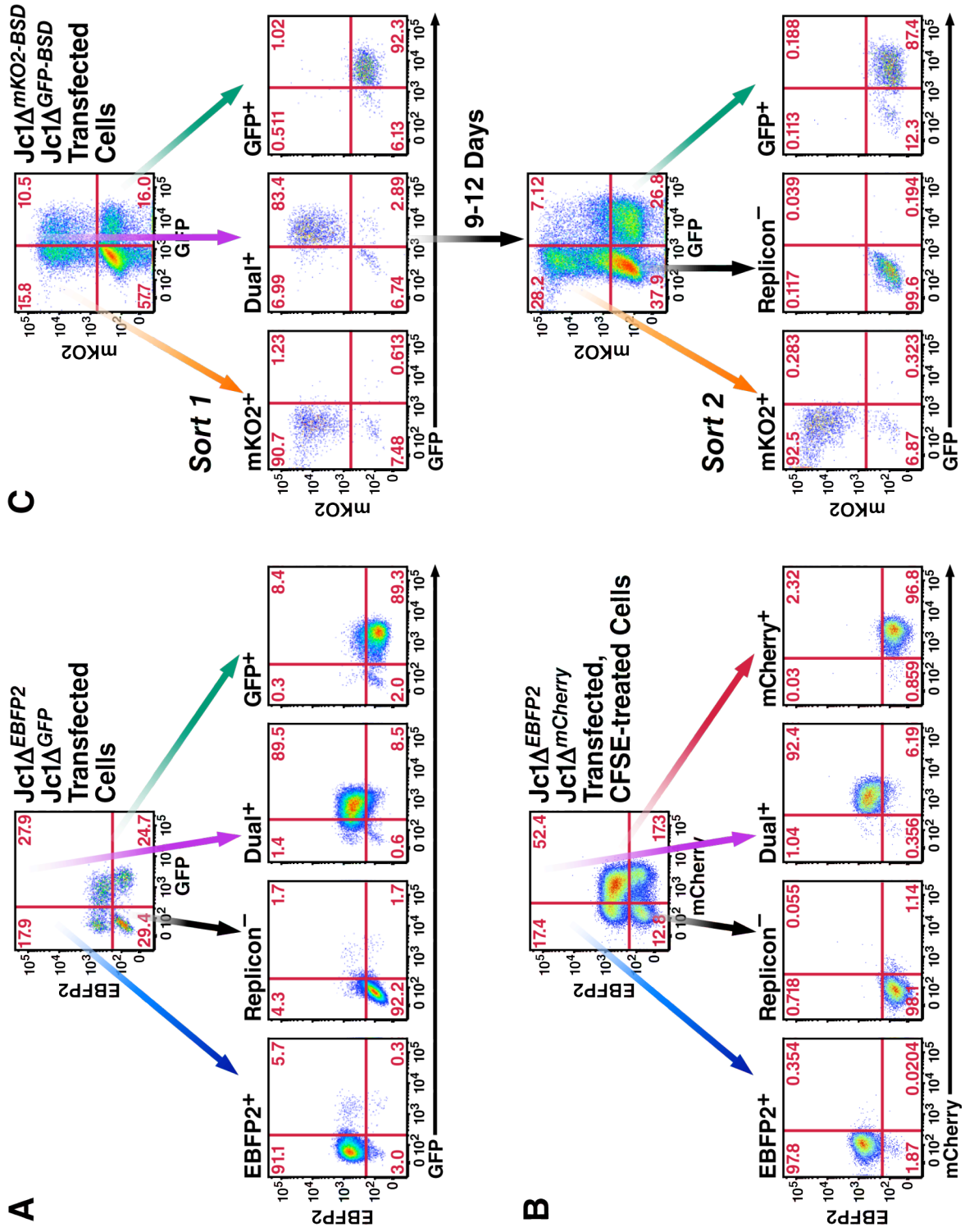
- $I_{Et}$     *Expected Replicon<sup>+</sup> cell count at time t*
- $\lambda$         *Decay rate*
- $t$          *Time*
- $I_{A0}$      *Actual Replicon<sup>+</sup> cell count at time 0*
- $U_{A0}$      *Actual Replicon<sup>-</sup> cell count at time 0*
- $U_{At}$      *Actual Replicon<sup>-</sup> cell count at time t*

$\lambda = 1.1743$  (Dual Replicon)  
 $\lambda = 0.9866$  (Single Replicon)



**Supplemental Figure B.2: Decay of dual- and single-replicon cells in the presence and absence of triple-replicon cells.**

(A) Huh7.5 cells were transfected with a total of 10  $\mu\text{g}$  of Jc1/ $\Delta^{\text{GFP}}$  and Jc1/ $\Delta^{\text{mCherry}}$  RNA, followed 48 hours later by FACS isolation of single- and dual-replicon cells. Cells were analyzed by flow cytometry for GFP/mCherry expression. The ratio of single- and dual-replicon cells to replicon-negative cells was normalized to 1 at 0 days post-isolation, and an exponential decay curve was fit to the data. ( $n=3$  independent experiments) (B) Huh7.5 cells were transfected with a total of 10  $\mu\text{g}$  of Jc1/ $\Delta^{\text{GFP}}$ , Jc1/ $\Delta^{\text{EBFP2}}$ , and Jc1/ $\Delta^{\text{mCherry}}$  RNA, followed 48 hours later by FACS isolation of triple-replicon cells. Cells were analyzed by flow cytometry for GFP/EBFP2/mCherry expression. The actual percentages of single-, dual-, and triple-replicon cells in this population are indicated by solid lines on the chart, with the chart at left indicating the proportion of replicon-positive cells, and the chart at right indicating the percentage of the culture (including replicon-negative cells). Further, the given equation was used to model the expected behavior of single- and dual-replicon cells in a population of isolated triple-replicon cells, according to the exponential decay curves in (A) (dashed lines on charts). Error bars indicate  $\pm\text{SEM}$ . ( $n=3$ ).



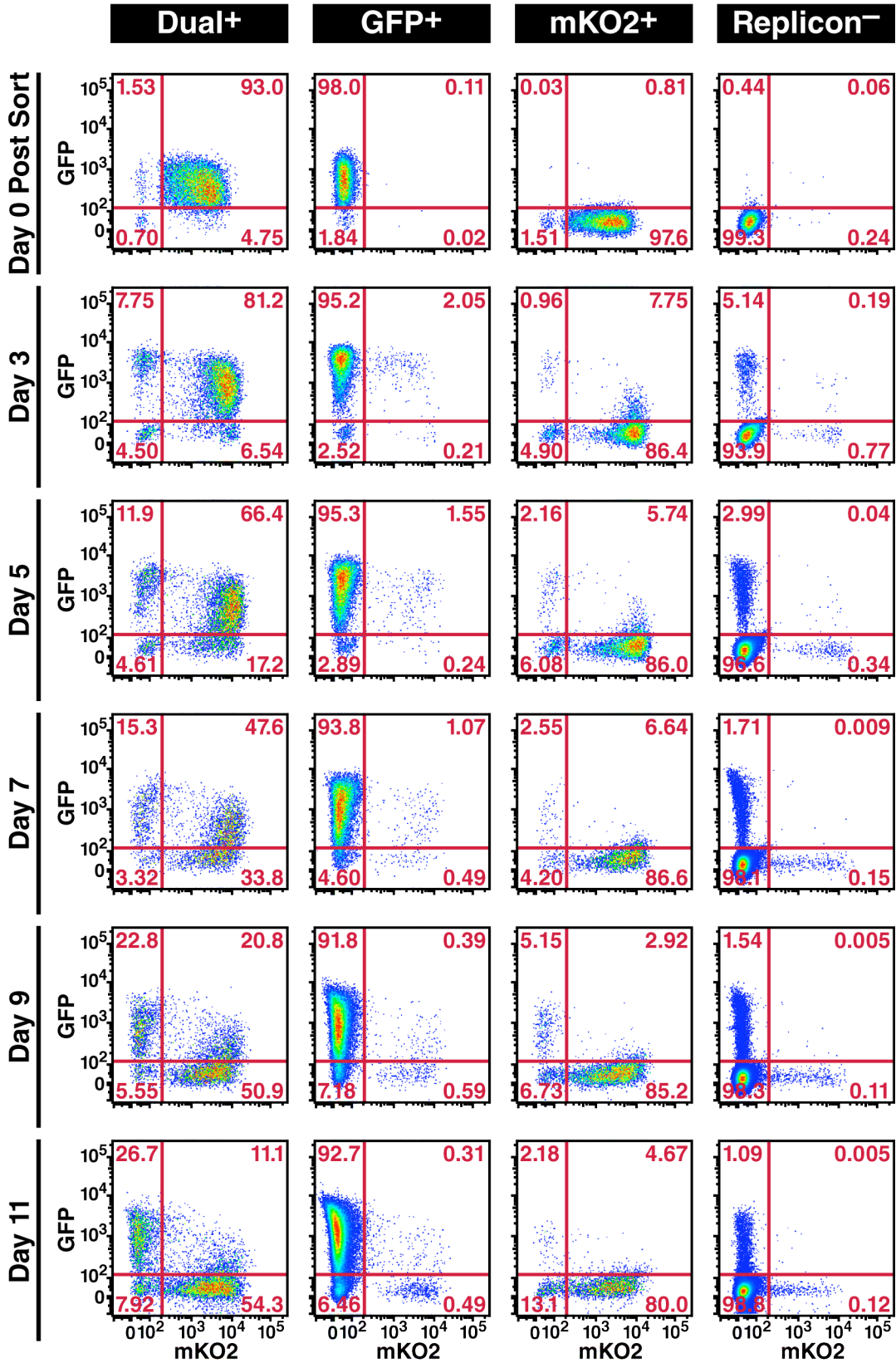
Supplemental Figure B.3. Sorting procedures.

(A) Flow cytometry plots refer to the cells described in Figure 3.3B, and their sorting strategy. (B) Flow cytometry plots refer to the cells described in Figure 3.4B, and their sorting strategy. (C) Flow cytometry plots refer to the cells described in Figure 3.8A & B, and their sorting strategy.

| <b>Transfection: Jc1/<math>\Delta</math>GFP &amp; Jc1/<math>\Delta</math>EBFP2</b> |              |               |                  |               |                  |                  |
|--|--------------|---------------|------------------|---------------|------------------|------------------|
| <b>Days</b>  | <b>Dual+</b> | <b>Dual+</b>  | <b>Dual+</b>     | <b>GFP+</b>   | <b>GFP+</b>      | <b>EBFP2+</b>    |
| <b>Post-</b>   | <b>vs.</b>   | <b>vs.</b>    | <b>vs.</b>       | <b>vs.</b>    | <b>vs.</b>       | <b>vs.</b>       |
| <b>Sort</b>  | <b>GFP+</b>  | <b>EBFP2+</b> | <b>Replicon-</b> | <b>EBFP2+</b> | <b>Replicon-</b> | <b>Replicon-</b> |
| <b>2</b>   | ns           | ns            | p<0.05           | ns            | ns               | p<0.05           |
| <b>3</b>   | ns           | ns            | p<0.0001         | ns            | p<0.05           | p<0.01           |
| <b>4</b>   | ns           | ns            | p<0.0001         | ns            | p<0.001          | p<0.0001         |
| <b>5</b>   | ns           | ns            | p<0.001          | ns            | p<0.05           | p<0.01           |
| <b>6</b>   | ns           | ns            | p<0.001          | ns            | p<0.01           | p<0.0001         |
| <b>7</b>   | ns           | ns            | p<0.05           | ns            | ns               | ns               |

**Supplemental Table B.2. Statistical significance of differences in apoptosis rates of dual-, single-, or replicon-negative cells<sup>a</sup>.**

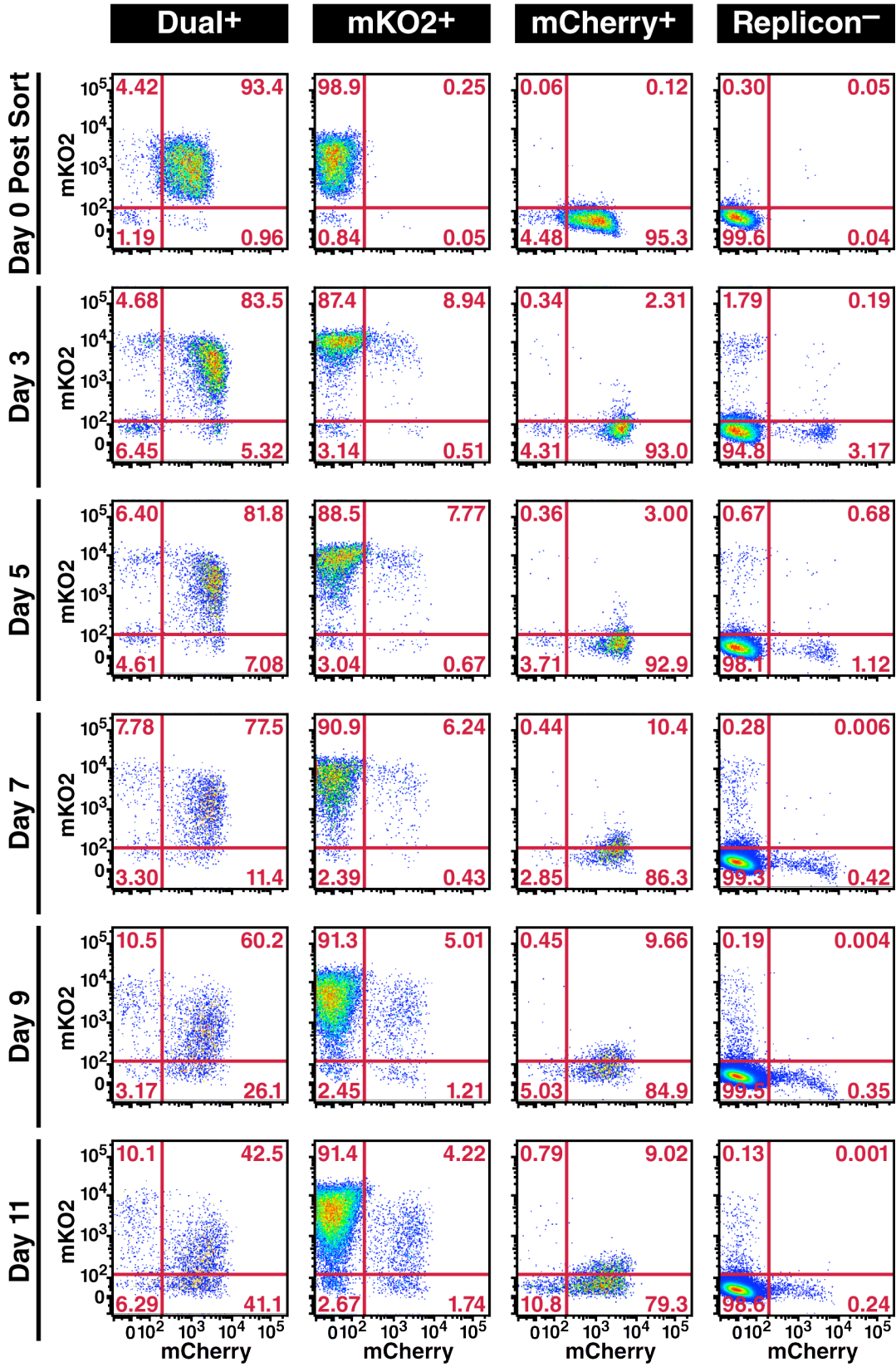
<sup>a</sup> Two-way ANOVA with Bonferroni multiple comparisons correction was used to analyze the difference in apoptosis rates of each replicon-positive cell population (ns: non-significant).



**Supplemental Figure B.4: Persistence of single-replicon cells and decay of dual-replicon cells in Jc1/ $\Delta^{XFP-BSD}$ -transfected cells.**

Cells were transfected with Jc1/ $\Delta^{GFP-BSD}$  & Jc1/ $\Delta^{mKO2-BSD}$ , followed by isolation of the indicated populations by FACS 2 days later. One representative experiment is shown, referring to the data shown in Figure 3.7B&E. All replicon-positive cultures were kept under 10  $\mu$ g/mL blasticidin selection throughout the culture. Note the bias in the decay of dual-replicon cells toward Jc1/ $\Delta^{mKO2-BSD}$  single-replicon cells.





**Supplemental Figure B.5: Persistence of single-replicon cells and decay of dual-replicon cells in Jc1/ $\Delta^{XFP-BSD}$ -transfected cells.**

Cells were transfected with Jc1/ $\Delta$ mCherry-BSD & Jc1/ $\Delta$ mKO2-BSD, followed by isolation of the indicated populations by FACS 2 days later. One representative experiment is shown, referring to the data shown in Figure 3.7D&F. All replicon-positive cultures were kept under 10  $\mu$ g/mL blasticidin selection throughout the culture. Note the bias in the decay of dual-replicon cells toward Jc1/ $\Delta$ mCherry-BSD single-replicon cells.

| Transfection: Jc1/ $\Delta$ GFP-BSD & Jc1/ $\Delta$ mKO2-BSD |           |                |     |                 |     |                |     |
|--|-----------|----------------|-----|-----------------|-----|----------------|-----|
| Days   | Post-Sort | Dual+ vs. GFP+ | vs. | Dual+ vs. mKO2+ | vs. | mKO2+ vs. GFP+ | vs. |
|  | 0         | p<0.0001       |     | p<0.0001        |     | ns             |     |
|  | 2         | p<0.0001       |     | p<0.0001        |     | ns             |     |
|  | 3         | p<0.0001       |     | p<0.0001        |     | ns             |     |
|  | 4         | p<0.0001       |     | p<0.0001        |     | ns             |     |
|  | 5         | p<0.0001       |     | p<0.0001        |     | p<0.05         |     |
|  | 6         | p<0.0001       |     | ns              |     | p<0.0001       |     |
|  | 7         | p<0.0001       |     | ns              |     | p<0.0001       |     |
|  | 8         | ns             |     | p<0.0001        |     | p<0.0001       |     |
|  | 9         | ns             |     | p<0.0001        |     | p<0.0001       |     |
|  | 10        | ns             |     | p<0.0001        |     | p<0.0001       |     |
|  | 11        | ns             |     | p<0.0001        |     | p<0.0001       |     |

**Supplemental Table B.3. Statistical significance of the differences in the proportions of replicon-positive cells in dual-replicon decay experiments<sup>a</sup>.**

<sup>a</sup> Two-way ANOVA with Bonferroni multiple comparisons correction was used to analyze the difference in proportions of each replicon-positive cell population (ns: non-significant).

| Transfection: Jc1/ $\Delta$ mKO2-BSD & Jc1/ $\Delta$ mCherry-BSD |                 |                    |                    |
|--|-----------------|--------------------|--------------------|
| Days Post-Sort   | Dual+ vs. mKO2+ | Dual+ vs. mCherry+ | mKO2+ vs. mCherry+ |
| 0  | p<0.0001        | p<0.0001           | ns                 |
| 2  | p<0.0001        | p<0.0001           | ns                 |
| 3  | p<0.0001        | p<0.0001           | ns                 |
| 4  | p<0.0001        | p<0.0001           | ns                 |
| 5  | p<0.0001        | p<0.0001           | ns                 |
| 6  | p<0.0001        | p<0.0001           | ns                 |
| 7  | p<0.0001        | p<0.0001           | ns                 |
| 8  | p<0.0001        | p<0.0001           | ns                 |
| 9  | p<0.0001        | p<0.0001           | ns                 |
| 10   | p<0.0001        | p<0.001            | p<0.01             |
| 11   | p<0.0001        | ns                 | p<0.05             |

**Supplemental Table B.4. Statistical significance of the differences in the proportions of replicon-positive cells in dual-replicon decay experiments<sup>a</sup>.**

<sup>a</sup> Two-way ANOVA with Bonferroni multiple comparisons correction was used to analyze the difference in proportions of each replicon-positive cell population (ns: non-significant).

| Transfection: Jc1/ $\Delta$ GFP-BSD & Jc1/ $\Delta$ mKO2-BSD |          |       |           |          |           |           |
|--|----------|-------|-----------|----------|-----------|-----------|
| Days   | Dual+    | Dual+ | Dual+     | GFP+     | GFP+      | mKO2+     |
| Post-  | vs.      | vs.   | vs.       | vs.      | vs.       | vs.       |
| Sort   | GFP+     | mKO2+ | Replicon- | mKO2+    | Replicon- | Replicon- |
| 2  | ns       | ns    | p<0.0001  | p<0.01   | ns        | p<0.0001  |
| 3  | p<0.05   | ns    | p<0.0001  | p<0.01   | ns        | p<0.0001  |
| 4  | p<0.001  | ns    | p<0.0001  | p<0.0001 | p<0.0001  | p<0.0001  |
| 5  | p<0.0001 | ns    | p<0.0001  | p<0.0001 | p<0.05    | p<0.0001  |
| 6  | p<0.001  | ns    | p<0.0001  | p<0.01   | p<0.01    | p<0.0001  |
| 7  | ns       | ns    | p<0.0001  | p<0.001  | p<0.01    | p<0.0001  |

**Supplemental Table B.5. Statistical significance of differences in apoptosis rates of dual-, single-, or replicon-negative cells<sup>a</sup>.**

<sup>a</sup> Two-way ANOVA with Bonferroni multiple comparisons correction was used to analyze the difference in apoptosis rates of each replicon-positive cell population (ns: non-significant).

| <b>Transfection: Jc1/<math>\Delta</math>mKO2-BSD &amp; Jc1/<math>\Delta</math>mCherry-BSD</b> |              |                 |                  |                 |                  |                  |
|---|--------------|-----------------|------------------|-----------------|------------------|------------------|
| <b>Days</b>   | <b>Dual+</b> | <b>Dual+</b>    | <b>Dual+</b>     | <b>mKO2+</b>    | <b>mKO2+</b>     | <b>mCherry+</b>  |
| <b>Post-</b>  | <b>vs.</b>   | <b>vs.</b>      | <b>vs.</b>       | <b>vs.</b>      | <b>vs.</b>       | <b>vs.</b>       |
| <b>Sort</b>   | <b>mKO2+</b> | <b>mCherry+</b> | <b>Replicon-</b> | <b>mCherry+</b> | <b>Replicon-</b> | <b>Replicon-</b> |
| <b>2</b>  | ns           | ns              | p<0.0001         | ns              | p<0.0001         | p<0.0001         |
| <b>3</b>  | ns           | ns              | p<0.0001         | ns              | p<0.0001         | p<0.0001         |
| <b>4</b>  | ns           | ns              | p<0.0001         | ns              | p<0.0001         | p<0.0001         |
| <b>5</b>  | ns           | ns              | p<0.0001         | ns              | p<0.0001         | p<0.0001         |
| <b>6</b>  | ns           | ns              | p<0.0001         | ns              | p<0.0001         | p<0.0001         |
| <b>7</b>  | ns           | ns              | p<0.0001         | ns              | p<0.0001         | p<0.0001         |

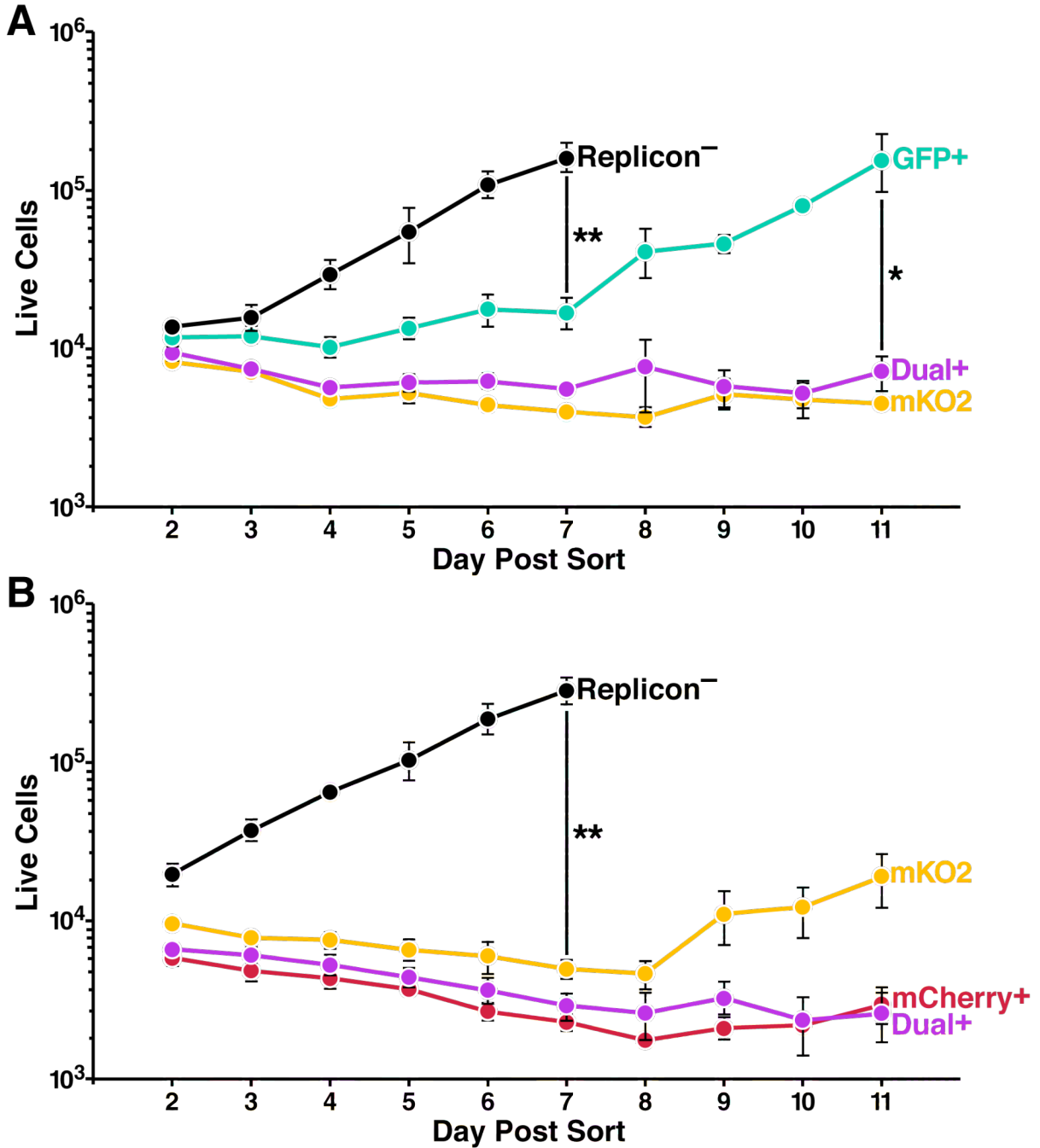
**Supplemental Table B.6. Statistical significance of differences in apoptosis rates of dual-, single-, or replicon-negative cells<sup>a</sup>.**

<sup>a</sup> Two-way ANOVA with Bonferroni multiple comparisons correction was used to analyze the difference in apoptosis rates of each replicon-positive cell population (ns: non-significant).

### **Live cell counts in isolated populations of Jc1/ $\Delta$ <sup>XFP-BSD</sup>-replicon-containing cells.**

To ensure that Jc1/ $\Delta$ <sup>XFP-BSD</sup> single-replicon-containing cells did not have a global increase in proliferation over dual-replicon cells, live cell counts (Fig S6; without singlet cell discrimination by forward scatter area/height) were obtained from the data presented in Figure 3.7. Due to the fast growth rate, replicon-negative cultures were terminated 7 days post-sort. The proliferation curves obtained were not amenable to accurate regression analysis to assess statistically significant differences in proliferation. Hence, the integrated area under the curve (AUC) was obtained for each independent experiment, and the AUCs were compared for statistically significant differences by one-way ANOVA with Bonferroni multiple comparisons correction (curves and analysis not shown). When comparing replicon-containing cell proliferation curves, only the Jc1/ $\Delta$ <sup>GFP-BSD</sup>-single-replicon curve was significantly different than Jc1/ $\Delta$ <sup>mKO2-BSD</sup>-single-replicon or dual-replicon curves.

Higher proliferation rates in single-replicon cells compared to dual-replicon cells should be reflected as a larger increase in the number of live cells over time. Of note, in each case where the single-replicon cells had an advantage in proliferation over dual-replicon cells (Jc1/ $\Delta$ <sup>GFP-BSD</sup> when comparing Jc1/ $\Delta$ <sup>GFP-BSD</sup> & Jc1/ $\Delta$ <sup>mKO2-BSD</sup>; Jc1/ $\Delta$ <sup>mKO2-BSD</sup> when comparing Jc1/ $\Delta$ <sup>mCherry-BSD</sup> & Jc1/ $\Delta$ <sup>mKO2-BSD</sup>), this same replicon was at a disadvantage in the decay process (Figure 3.7, Supplemental Figure B.4, and Supplemental Figure B.5).



**Supplemental Figure B.6:  $Jc1/\Delta^{XFP-BSD}$  single-replicon-positive cells that have an advantage in proliferation have a *disadvantage* in the decay process.**

Proliferation was assessed using flow cytometry to measure absolute cell counts of isolated dual-replicon, single-replicon, or replicon-negative populations after live cell



discrimination by FSC-A/SSC-A. All replicon-positive cultures were kept under 10  $\mu\text{g/mL}$  blasticidin selection throughout the culture. Replicon-negative cultures were terminated at 7 days post-isolation due to high growth rates. (A)  $\text{Jc1}/\Delta^{\text{GFP-BSD}}$  single-replicon cells have a significant proliferative advantage over  $\text{Jc1}/\Delta^{\text{mKO2-BSD}}$  and dual-replicon cells. Data refers to a subset of the experiments shown in Figure 3.7B & E (only experiments where all isolated replicon-positive populations were analyzed through day 11 post-sort are amenable to area under the curve (AUC) analysis,  $n=3$  independent experiments). (B)  $\text{Jc1}/\Delta^{\text{mKO2-BSD}}$  single-replicon cells may have a proliferative advantage over  $\text{Jc1}/\Delta^{\text{mCherry-BSD}}$  and dual-replicon cells, although this difference is not significant. Data refers to the experiments shown in Figure 3.7D & E ( $n=3$  independent experiments). Error bars indicate  $\pm$  SEM. Differences in proliferation were assessed by obtaining the integrated AUC for each independent experiment, followed by one-way ANOVA with Bonferroni multiple comparisons correction to assess statistically significant differences in AUC (\*: $p<0.05$ , \*\*: $p<0.01$

| Primer                     | Sequence   | Template                             |
|----------------------------|--|--------------------------------------|
| S6660                      | CAGGACTGACCACCTGACAATCTG                         | pBR322 Jc1                           |
| Alinker_XbaIPmeI_NS5Aaa383 | TTAAACCCAGGTC TAGAACCGCTCGAGGGGGCTGGCCAAAG       | pBR322 Jc1                           |
| Slinker_XbaIPmeI_NS5Aaa383 | TCTAGACCTGGGTTAAACGTGATGCAGGCTCGTCCACGGG         | pBR322 Jc1                           |
| A7759                      | CAGACTCCAGTCCGGATCTCCAGGC                        | pBR322 Jc1                           |
| GFP_Fw_XbaI_NS5A           | GTTTCTCTAGAAATGGTGAGCAAGGGCGAGGAG                | pIRES2 EGFP, pMCherry, pEBFP2-Nuc    |
| GFP_Rev_PmeI_NS5A          | GTTTCTGTTTAAACCCCTTGACAGCTCGTCCATGCC             | pIRES2 EGFP, pMCherry, pEBFP2-Nuc    |
| Jc1_567_KpnI_Fw            | GTTTCTGGTACCGCACCCCTGCCGTACTAGA                  | pBR322 Jc1                           |
| Jc1_865_KpnI_Rev           | GTTTCTGGTACCCACTCCTGAATCATGG                     | pBR322 Jc1                           |
| mKO2_Fw_XbaI_NS5A          | GTTTCTCTAGAGCCACCATGGTTCTGTGATCAAGCCCGAAA        | In vitro synthesized mKO2            |
| mKO2_Rev_Gly Linker        | CTTGCCACCACCACCCTCGGCTGTAGTGGGCCACGGCGTCT        | In vitro synthesized mKO2            |
| BSD_Fw_Gly Linker          | CGAGGTGGTGGTGGCAAGCTTGCATGGCCAAGCCTTTGTCTCAAGAAG | pcDNA6/myc-His A                     |
| BSD_Rev_PmeI_NS5A          | GTTTCTGTTTAAACCCGCCCTCCACACATAACAGAG             | pcDNA6/myc-His A                     |
| GFP_Fw                     | ATGGTGAGCAAGGGCGAGGAG                            | pIRES2 EGFP, pMCherry                |
| GFP_Rev_-stop              | CTTGACAGCTCGTCCATGCC                             | pIRES2 EGFP, pMCherry                |
| hGem_Fw_Gly Linker         | CGAGGTGGTGGTGGCAAGATGAATCCCAGTATGAAGCAGAAAACAA   | HeLa cDNA                            |
| hGem_Rev_EcoRI             | GTTTCTGAATTTCTACAGCGCCTTTCTCCGTTTCT              | HeLa cDNA                            |
| GFP_Fw_XbaI_Kozak          | GTTTCTCTAGAGCCACCATGGTGAGCAAGGGCGAGGAG           | pIRES2 EGFP, pEBFP2-Nuc              |
| GFP_Rev_Gly Linker         | CTTGCCACCACCACCCTCGCTTGACAGCTCGTCCATGCC          | pIRES2 EGFP, pEBFP2-Nuc, pMCherry    |
| H2B_Fw_NheI_Kozak          | GTTTCTGCTAGCGCCACCATGCCAGAGCCAGCAAGTCT           | HeLa cDNA                            |
| H2B_Rev_Gly Linker         | CTTGCCACCACCACCCTCGCTTGACAGCTGGTACTTGGTGAT       | HeLa cDNA                            |
| GFP_Fw_Gly Linker          | CGAGGTGGTGGTGGCAAGATGGTGAGCAAGGGCGAGGAG          | EBFP2-Nuc                            |
| GFP_Rev_+stop_PmeI         | GTTTCTGTTTAAACCCCTTACTGTACAGCTCGTCCATGCC         | EBFP2-Nuc                            |
| mKO2_1                     | ATGGTTCTGTGATCAAGCCCGAAATGAAGATGAGGTA            |                                      |
| mKO2_2                     | GACGCTGCCGCTCCATGTAGTACCTCATCTTCAATTCGGGC        |                                      |
| mKO2_3                     | CATGGACGCGAGCCTCAATGGACATGAGTTTACGATCGAA         |                                      |
| mKO2_4                     | TCGGCCGGTGCCCTCCCTTCGATCGTAAACTCATGTCCA          |                                      |
| mKO2_5                     | AGGGCACCGCCGACCCCTACGAGGGCCACCAGGAGATGAC         |                                      |
| mKO2_6                     | CTCTGCCATCGTCACCCTCAGGGTCATCTCTGGTGGCC           |                                      |
| mKO2_7                     | AGGGTGACGATGGCAGAGGGCGTCCCATGCCCTTCGCCT          |                                      |
| mKO2_8                     | AGAACCGTGGCTTACCAGTTCGAAGGCGAAGGGCATGGG          |                                      |
| mKO2_9                     | CTGGTAAGCCAGTGTCTGTGCTACGGCCACCGAGTGTCA          |                                      |
| mKO2_10                    | TGGGATCTCTCCGGGTATTTGTGAACACTCGGTGGCCG           |                                      |
| mKO2_11                    | ACCCGGAGGAGATCCAGACTACTTCAAGCAGGCTTTCC           |                                      |
| mKO2_12                    | TCTCCAGCTCAGCCCTCGGAAAGGCCTGCTTGAAGTA            |                                      |
| mKO2_13                    | GGGCTGAGCTGGGAGAGGAGCTGGAATTTGAGGACGGTG          |                                      |
| mKO2_14                    | GGGCGCTAACGCTAGCACTGCCACCGTCTCAAATCCAG           |                                      |
| mKO2_15                    | GCTAGCGTTAGCGCCACATCAGTCTGAGGGGCAACCT            |                                      |
| mKO2_16                    | GTGAAGTGTCTTGTGGTAAAGGTGTTGCCCTCAGAC             |                                      |
| mKO2_17                    | TTTACCACAAGAGCAAGTTCACTGGCGTTAATTCCCAGC          |                                      |
| mKO2_18                    | GTTCTGCATGATGGGGCTCCGCTGGGAAGTTAAGCCA            |                                      |
| mKO2_19                    | GGCCCCATATGCAGAACCAGAGCGTGGACTGGGAGCCCA          |                                      |
| mKO2_20                    | CGCTGGCGGTGATCTTCTCGTGTGGCTCCAGTCCAC             |                                      |
| mKO2_21                    | GAAGATCACGCCACGACGCGGTGCTGAAGGGCAGCTG            |                                      |
| mKO2_22                    | TCTTCCAGCTTCAGGTACATGGTACGCTCGCCCTTCAGC          |                                      |
| mKO2_23                    | TGTACTGAAGCTGGAAGGAGTGGCAACCATAAGTGCCA           |                                      |
| mKO2_24                    | GCCTTGTAGTGGTCTTTCATCTGGCACTTATGGTTGCCAC         |                                      |
| mKO2_25                    | GATGAAGACCCTTACAAGGCCGCCAAGGAGATTCTGGAG          |                                      |
| mKO2_26                    | AATATAGTGGTCTCCGGCATCTCCAGAATCTCTTGGCG           |                                      |
| mKO2_27                    | TGCCGGGAGACCACTATATTGGACACAGGCTGGTCCGAAA         |                                      |
| mKO2_28                    | TTCGGTGTGTACCTTTCAGTCTTCGGACCAAGCCTGTGT          |                                      |
| mKO2_29                    | ACTGAAGGTAACATCACCGAACAGGTGGAAGACGCCGTGG         |                                      |
| mKO2_30                    | GCTGTAGTGGGCCACGGCTCTTCCAC                       | Overlapping PCR-based gene synthesis |

**Supplemental Table B.7: Primer sequences used in plasmid construction.**

| Primer/Probe | Sequence                      |
|--------------|-------------------------------|
| Core Fw      | 5'-CGGGAGAGCCATAGTGG-3'       |
| Core Rev     | 5'-AGTACCACAAGGCCTTTCG-3'     |
| Core Probe   | 5'-CTGCGGAACCGGTGAGTACAC-3'   |
| GFP Fw       | 5'-CTGCTGCCCGACAACCA-3'       |
| GFP Rev      | 5'-GAACTCCAGCAGGACCATGTG-3'   |
| GFP Probe    | 5'-AAAGACCCCAACGAGAAGCGCGA-3' |
| mKO2 Fw      | 5'-GGAAGGAGGTGGCAACCATA-3'    |
| mKO2 Rev     | 5'-TCCTTGGCGGCCTTGTAG-3'      |
| mKO2 Probe   | 5'-TGCCAGATGAAGACCA-3'        |
| GAPDH Fw     | 5'-GAAGGTGAAGGTCGGAGTC-3'     |
| GAPDH Rev    | 5'-GAAGATGGTGATGGGATTTTC-3'   |
| GAPDH Probe  | 5'-CAAGCTTCCCGTTCTCAGCC-3'    |

**Supplemental Table B.8: Probe/primer sets used in quantitative real-time PCR.**

## **Appendix C. References**

1. Brown RS (2005) Hepatitis C and liver transplantation. *Nature* 436: 973-978.
2. Perz JF, Armstrong GL, Farrington LA, Hutin YJ, Bell BP (2006) The contributions of hepatitis B virus and hepatitis C virus infections to cirrhosis and primary liver cancer worldwide. *J Hepatol* 45: 529-538.
3. Irshad M, Ansari MA, Singh A, Nag P, Raghvendra L, et al. (2010) HCV-genotypes: a review on their origin, global status, assay system, pathogenicity and response to treatment. *Hepatogastroenterology* 57: 1529-1538.
4. Read SA, Douglas MW (2011) Hepatitis C Virus Genotypes. *Advanced Therapy for Hepatitis C: Wiley-Blackwell*. pp. 12-16.
5. McHutchison JG, Gordon SC, Schiff ER, Shiffman ML, Lee WM, et al. (1998) Interferon alfa-2b alone or in combination with ribavirin as initial treatment for chronic hepatitis C. Hepatitis Interventional Therapy Group. *N Engl J Med* 339: 1485-1492.
6. Tran TT (2012) A review of standard and newer treatment strategies in hepatitis C. *Am J Manag Care* 18: S340-349.
7. Mandell GL, Bennett JE, Dolin R (2009) *Mandell, Douglas, and Bennett's principles and practice of infectious diseases*. 7th ed. Philadelphia: Churchill Livingstone/Elsevier. pp. 2161.
8. Simmonds P (1995) Variability of hepatitis C virus. *Hepatology* 21: 570-583.
9. Suzuki T, Aizaki H, Murakami K, Shoji I, Wakita T (2007) Molecular biology of hepatitis C virus. *J Gastroenterol* 42: 411-423.
10. Blackard JT, Kemmer N, Sherman KE (2006) Extrahepatic replication of HCV: insights into clinical manifestations and biological consequences. *Hepatology* 44: 15-22.
11. Helle F, Dubuisson J (2008) Hepatitis C virus entry into host cells. *Cell Mol Life Sci* 65: 100-112.
12. Evans MJ, von Hahn T, Tscherne DM, Syder AJ, Panis M, et al. (2007) Claudin-1 is a hepatitis C virus co-receptor required for a late step in entry. *Nature* 446: 801-805.
13. Liu S, Yang W, Shen L, Turner JR, Coyne CB, et al. (2009) Tight junction proteins claudin-1 and occludin control hepatitis C virus entry and are downregulated during infection to prevent superinfection. *J Virol* 83: 2011-2014.
14. Egger D, Wolk B, Gosert R, Bianchi L, Blum HE, et al. (2002) Expression of hepatitis C virus proteins induces distinct membrane alterations including a candidate viral replication complex. *J Virol* 76: 5974-5984.
15. Sklan EH, Glenn JS (2006) HCV NS4B: From Obscurity to Central Stage.
16. Suzuki T (2010) Assembly of hepatitis C virus particles. *Microbiol Immunol* 55: 12-18.

17. Nielsen SU, Bassendine MF, Burt AD, Martin C, Pumeechockchai W, et al. (2006) Association between hepatitis C virus and very-low-density lipoprotein (VLDL)/LDL analyzed in iodixanol density gradients. *J Virol* 80: 2418-2428.
18. Tellinghuisen TL, Evans MJ, von Hahn T, You S, Rice CM (2007) Studying hepatitis C virus: making the best of a bad virus. *J Virol* 81: 8853-8867.
19. Nahmias Y, Goldwasser J, Casali M, van Poll D, Wakita T, et al. (2008) Apolipoprotein B-dependent hepatitis C virus secretion is inhibited by the grapefruit flavonoid naringenin. *Hepatology* 47: 1437-1445.
20. Herker E, Ott M (2011) Unique ties between hepatitis C virus replication and intracellular lipids. *Trends Endocrinol Metab* 22: 241-248.
21. Sheehy P, Mullan B, Moreau I, Kenny-Walsh E, Shanahan F, et al. (2007) In vitro replication models for the hepatitis C virus. *J Viral Hepat* 14: 2-10.
22. Duverlie G, Wychowski C (2007) Cell culture systems for the hepatitis C virus. *World J Gastroenterol* 13: 2442-2445.
23. McCaffrey AP, Ohashi K, Meuse L, Shen S, Lancaster AM, et al. (2002) Determinants of hepatitis C translational initiation in vitro, in cultured cells and mice. *Mol Ther* 5: 676-684.
24. Dubuisson J, Helle F, Cocquerel L (2008) Early steps of the hepatitis C virus life cycle. *Cell Microbiol* 10: 821-827.
25. Lindenbach BD, Evans MJ, Syder AJ, Wolk B, Tellinghuisen TL, et al. (2005) Complete replication of hepatitis C virus in cell culture. *Science* 309: 623-626.
26. Wakita T, Pietschmann T, Kato T, Date T, Miyamoto M, et al. (2005) Production of infectious hepatitis C virus in tissue culture from a cloned viral genome. *Nat Med* 11: 791-796.
27. Zhong J, Gastaminza P, Cheng G, Kapadia S, Kato T, et al. (2005) Robust hepatitis C virus infection in vitro. *Proc Natl Acad Sci U S A* 102: 9294-9299.
28. Kato T, Furusaka A, Miyamoto M, Date T, Yasui K, et al. (2001) Sequence analysis of hepatitis C virus isolated from a fulminant hepatitis patient. *J Med Virol* 64: 334-339.
29. Bartenschlager R, Sparacio S (2007) Hepatitis C virus molecular clones and their replication capacity in vivo and in cell culture. *Virus Res* 127: 195-207.
30. Smith JA, Aberle JH, Fleming VM, Ferenci P, Thomson EC, et al. (2010) Dynamic coinfection with multiple viral subtypes in acute hepatitis C. *J Infect Dis* 202: 1770-1779.
31. Blackard JT, Sherman KE (2007) Hepatitis C virus coinfection and superinfection. *J Infect Dis* 195: 519-524.
32. Bowden S, McCaw R, White PA, Crofts N, Aitken CK (2005) Detection of multiple hepatitis C virus genotypes in a cohort of injecting drug users. *J Viral Hepat* 12: 322-324.
33. Chen YD, Liu MY, Yu WL, Li JQ, Dai Q, et al. (2003) Mix-infections with different genotypes of HCV and with HCV plus other hepatitis viruses in patients with hepatitis C in China. *World J Gastroenterol* 9: 984-992.
34. Okamoto H, Mishiro S, Tokita H, Tsuda F, Miyakawa Y, et al. (1994) Superinfection of chimpanzees carrying hepatitis C virus of genotype II/1b with that of genotype III/2a or I/1a. *Hepatology* 20: 1131-1136.

35. Schroter M, Feucht HH, Zollner B, Schafer P, Laufs R (2003) Multiple infections with different HCV genotypes: prevalence and clinical impact. *J Clin Virol* 27: 200-204.
36. Kao JH, Chen PJ, Lai MY, Yang PM, Sheu JC, et al. (1994) Mixed infections of hepatitis C virus as a factor in acute exacerbations of chronic type C hepatitis. *J Infect Dis* 170: 1128-1133.
37. Bernardin F, Herring B, Page-Shafer K, Kuiken C, Delwart E (2006) Absence of HCV viral recombination following superinfection. *J Viral Hepat* 13: 532-537.
38. Zhou Y, Wang X, Hong G, Tan Z, Zhu Y, et al. (2010) Natural intragenotypic and intergenotypic HCV recombinants are rare in southwest China even among patients with multiple exposures. *J Clin Virol* 49: 272-276.
39. Viazov S, Ross SS, Kyuregyan KK, Timm J, Neumann-Haefelin C, et al. (2010) Hepatitis C virus recombinants are rare even among intravenous drug users. *J Med Virol* 82: 232-238.
40. Gonzalez-Candelas F, Lopez-Labrador FX, Bracho MA (2011) Recombination in hepatitis C virus. *Viruses* 3: 2006-2024.
41. Colina R, Casane D, Vasquez S, Garcia-Aguirre L, Chunga A, et al. (2004) Evidence of intratypic recombination in natural populations of hepatitis C virus. *J Gen Virol* 85: 31-37.
42. Kageyama S, Agdamag DM, Alesna ET, Leano PS, Heredia AM, et al. (2006) A natural inter-genotypic (2b/1b) recombinant of hepatitis C virus in the Philippines. *J Med Virol* 78: 1423-1428.
43. Kurbanov F, Tanaka Y, Avazova D, Khan A, Sugauchi F, et al. (2008) Detection of hepatitis C virus natural recombinant RF1\_2k/1b strain among intravenous drug users in Uzbekistan. *Hepatology* 38: 457-464.
44. Moreno P, Alvarez M, Lopez L, Moratorio G, Casane D, et al. (2009) Evidence of recombination in Hepatitis C Virus populations infecting a hemophiliac patient. *Virology* 396: 203.
45. Shi W, Freitas IT, Zhu C, Zheng W, Hall WW, et al. (2012) Recombination in hepatitis C virus: identification of four novel naturally occurring inter-subtype recombinants. *PLoS One* 7: e41997.
46. Moreau I, Hegarty S, Levis J, Sheehy P, Crosbie O, et al. (2006) Serendipitous identification of natural intergenotypic recombinants of hepatitis C in Ireland. *Virology* 347: 95.
47. Michel N, Allespach I, Venzke S, Fackler OT, Keppler OT (2005) The Nef protein of human immunodeficiency virus establishes superinfection immunity by a dual strategy to downregulate cell-surface CCR5 and CD4. *Curr Biol* 15: 714-723.
48. Adams RH, Brown DT (1985) BHK cells expressing Sindbis virus-induced homologous interference allow the translation of nonstructural genes of superinfecting virus. *J Virol* 54: 351-357.
49. Walters KA, Joyce MA, Addison WR, Fischer KP, Tyrrell DL (2004) Superinfection exclusion in duck hepatitis B virus infection is mediated by the large surface antigen. *J Virol* 78: 7925-7937.
50. Folimonova SY (2012) Superinfection exclusion is an active virus-controlled function that requires a specific viral protein. *J Virol* 86: 5554-5561.

51. Evans MJ, Rice CM, Goff SP (2004) Genetic interactions between hepatitis C virus replicons. *J Virol* 78: 12085-12089.
52. Tscherne DM, Evans MJ, von Hahn T, Jones CT, Stamataki Z, et al. (2007) Superinfection exclusion in cells infected with hepatitis C virus. *J Virol* 81: 3693-3703.
53. Schaller T, Appel N, Koutsoudakis G, Kallis S, Lohmann V, et al. (2007) Analysis of hepatitis C virus superinfection exclusion by using novel fluorochrome gene-tagged viral genomes. *J Virol* 81: 4591-4603.
54. Webster B, Wissing S, Herker E, Ott M, Greene WC (2013) Rapid intracellular competition between hepatitis C viral genomes as a result of mitosis. *J Virol* 87: 581-596.
55. Lee YM, Tscherne DM, Yun SI, Frolov I, Rice CM (2005) Dual mechanisms of pestiviral superinfection exclusion at entry and RNA replication. *J Virol* 79: 3231-3242.
56. Pietschmann T, Kaul A, Koutsoudakis G, Shavinskaya A, Kallis S, et al. (2006) Construction and characterization of infectious intragenotypic and intergenotypic hepatitis C virus chimeras. *Proc Natl Acad Sci U S A* 103: 7408-7413.
57. Gastaminza P, Kapadia SB, Chisari FV (2006) Differential biophysical properties of infectious intracellular and secreted hepatitis C virus particles. *J Virol* 80: 11074-11081.
58. Targett-Adams P, Boulant S, McLauchlan J (2008) Visualization of double-stranded RNA in cells supporting hepatitis C virus RNA replication. *J Virol* 82: 2182-2195.
59. Cheng G, Chan K, Yang H, Corsa A, Pokrovskii M, et al. (2011) Selection of clinically relevant protease inhibitor-resistant viruses using the genotype 2a hepatitis C virus infection system. *Antimicrob Agents Chemother* 55: 2197-2205.
60. Kolykhalov AA, Agapov EV, Rice CM (1994) Specificity of the hepatitis C virus NS3 serine protease: effects of substitutions at the 3/4A, 4A/4B, 4B/5A, and 5A/5B cleavage sites on polyprotein processing. *J Virol* 68: 7525-7533.
61. Li YP, Ramirez S, Gottwein JM, Scheel TK, Mikkelsen L, et al. (2012) Robust full-length hepatitis C virus genotype 2a and 2b infectious cultures using mutations identified by a systematic approach applicable to patient strains. *Proc Natl Acad Sci U S A* 109: E1101-1110.
62. Murayama A, Weng L, Date T, Akazawa D, Tian X, et al. (2010) RNA polymerase activity and specific RNA structure are required for efficient HCV replication in cultured cells. *PLoS Pathog* 6: e1000885.
63. Tardif KD, Mori K, Siddiqui A (2002) Hepatitis C virus subgenomic replicons induce endoplasmic reticulum stress activating an intracellular signaling pathway. *J Virol* 76: 7453-7459.
64. Krieger N, Lohmann V, Bartenschlager R (2001) Enhancement of hepatitis C virus RNA replication by cell culture-adaptive mutations. *J Virol* 75: 4614-4624.

65. Koutsoudakis G, Kaul A, Steinmann E, Kallis S, Lohmann V, et al. (2006) Characterization of the early steps of hepatitis C virus infection by using luciferase reporter viruses. *J Virol* 80: 5308-5320.
66. Horwitz JA, Dorner M, Friling T, Donovan BM, Vogt A, et al. (2013) Expression of heterologous proteins flanked by NS3-4A cleavage sites within the hepatitis C virus polyprotein. *Virology*.
67. Quinkert D, Bartenschlager R, Lohmann V (2005) Quantitative analysis of the hepatitis C virus replication complex. *J Virol* 79: 13594-13605.
68. Nakamuta M, Fujino T, Yada R, Aoyagi Y, Yasutake K, et al. (2011) Expression profiles of genes associated with viral entry in HCV-infected human liver. *J Med Virol* 83: 921-927.
69. Reynolds GM, Harris HJ, Jennings A, Hu K, Grove J, et al. (2008) Hepatitis C virus receptor expression in normal and diseased liver tissue. *Hepatology* 47: 418-427.
70. Sainz B, Jr., Barretto N, Martin DN, Hiraga N, Imamura M, et al. (2012) Identification of the Niemann-Pick C1-like 1 cholesterol absorption receptor as a new hepatitis C virus entry factor. *Nat Med* 18: 281-285.
71. Lohmann V, Hoffmann S, Herian U, Penin F, Bartenschlager R (2003) Viral and cellular determinants of hepatitis C virus RNA replication in cell culture. *J Virol* 77: 3007-3019.
72. von Wagner M, Huber M, Berg T, Hinrichsen H, Rasenack J, et al. (2005) Peginterferon-alpha-2a (40KD) and ribavirin for 16 or 24 weeks in patients with genotype 2 or 3 chronic hepatitis C. *Gastroenterology* 129: 522-527.
73. Rong L, Dahari H, Ribeiro RM, Perelson AS (2010) Rapid emergence of protease inhibitor resistance in hepatitis C virus. *Sci Transl Med* 2: 30ra32.
74. Blight KJ, McKeating JA, Rice CM (2002) Highly permissive cell lines for subgenomic and genomic hepatitis C virus RNA replication. *J Virol* 76: 13001-13014.
75. Herker E, Harris C, Hernandez C, Carpentier A, Kaehlcke K, et al. (2011) Efficient hepatitis C virus particle formation requires diacylglycerol acyltransferase-1. *Nat Med* 16: 1295-1298.
76. Wissing S, Montano M, Garcia-Perez JL, Moran JV, Greene WC (2011) Endogenous APOBEC3B restricts LINE-1 retrotransposition in transformed cells and human embryonic stem cells. *J Biol Chem* 286: 36427-36437.
77. Kato T, Date T, Murayama A, Morikawa K, Akazawa D, et al. (2006) Cell culture and infection system for hepatitis C virus. *Nat Protoc* 1: 2334-2339.
78. Boson B, Granio O, Bartenschlager R, Cosset FL (2011) A concerted action of hepatitis C virus p7 and nonstructural protein 2 regulates core localization at the endoplasmic reticulum and virus assembly. *PLoS Pathog* 7: e1002144.
79. Manna D, Aligo J, Xu C, Park WS, Koc H, et al. (2009) Endocytic Rab proteins are required for hepatitis C virus replication complex formation. *Virology* 398: 21-37.
80. Lauer GM, Walker BD (2001) Hepatitis C virus infection. *N Engl J Med* 345: 41-52.
81. Flamm SL (2003) Chronic hepatitis C virus infection. *Jama* 289: 2413-2417.



82. Gottwein JM, Scheel TK, Jensen TB, Lademann JB, Prentoe JC, et al. (2009) Development and characterization of hepatitis C virus genotype 1-7 cell culture systems: role of CD81 and scavenger receptor class B type I and effect of antiviral drugs. *Hepatology* 49: 364-377.
83. Dentzer TG, Lorenz IC, Evans MJ, Rice CM (2009) Determinants of the hepatitis C virus nonstructural protein 2 protease domain required for production of infectious virus. *J Virol* 83: 12702-12713.
84. Moradpour D, Evans MJ, Gosert R, Yuan Z, Blum HE, et al. (2004) Insertion of green fluorescent protein into nonstructural protein 5A allows direct visualization of functional hepatitis C virus replication complexes. *J Virol* 78: 7400-7409.
85. Appel N, Herian U, Bartenschlager R (2005) Efficient rescue of hepatitis C virus RNA replication by trans-complementation with nonstructural protein 5A. *J Virol* 79: 896-909.
86. Deng L, Adachi T, Kitayama K, Bungyoku Y, Kitazawa S, et al. (2008) Hepatitis C virus infection induces apoptosis through a Bax-triggered, mitochondrion-mediated, caspase 3-dependent pathway. *J Virol* 82: 10375-10385.
87. Mateu G, Donis RO, Wakita T, Bukh J, Grakoui A (2008) Intragenotypic JFH1 based recombinant hepatitis C virus produces high levels of infectious particles but causes increased cell death. *Virology* 376: 397-407.
88. Walters KA, Syder AJ, Lederer SL, Diamond DL, Paeper B, et al. (2009) Genomic analysis reveals a potential role for cell cycle perturbation in HCV-mediated apoptosis of cultured hepatocytes. *PLoS Pathog* 5: e1000269.
89. Blackham S, Baillie A, Al-Hababi F, Remlinger K, You S, et al. (2010) Gene expression profiling indicates the roles of host oxidative stress, apoptosis, lipid metabolism, and intracellular transport genes in the replication of hepatitis C virus. *J Virol* 84: 5404-5414.
90. vanEngeland M, Ramaekers FCS, Schutte B, Reutelingsperger CPM (1996) A novel assay to measure loss of plasma membrane asymmetry during apoptosis of adherent cells in culture. *Cytometry* 24: 131-139.
91. Kannan RP, Hensley LL, Evers LE, Lemon SM, McGivern DR (2011) Hepatitis C virus infection causes cell cycle arrest at the level of initiation of mitosis. *J Virol* 85: 7989-8001.
92. Lu L, Ladinsky MS, Kirchhausen T (2009) Cisternal organization of the endoplasmic reticulum during mitosis. *Mol Biol Cell* 20: 3471-3480.
93. Puhka M, Vihinen H, Joensuu M, Jokitalo E (2007) Endoplasmic reticulum remains continuous and undergoes sheet-to-tubule transformation during cell division in mammalian cells. *J Cell Biol* 179: 895-909.
94. Sainz B, Jr., Chisari FV (2006) Production of infectious hepatitis C virus by well-differentiated, growth-arrested human hepatoma-derived cells. *J Virol* 80: 10253-10257.
95. Sakaue-Sawano A, Kurokawa H, Morimura T, Hanyu A, Hama H, et al. (2008) Visualizing spatiotemporal dynamics of multicellular cell-cycle progression. *Cell* 132: 487-498.
96. Tada S (2007) Cdt1 and geminin: role during cell cycle progression and DNA damage in higher eukaryotes. *Front Biosci* 12: 1629-1641.

97. Wahl LM, Gerrish PJ (2001) The probability that beneficial mutations are lost in populations with periodic bottlenecks. *Evolution* 55: 2606-2610.
98. Edwards CT, Holmes EC, Wilson DJ, Viscidi RP, Abrams EJ, et al. (2006) Population genetic estimation of the loss of genetic diversity during horizontal transmission of HIV-1. *BMC Evol Biol* 6: 28.
99. Hartl DL, Clark AG (1997) Principles of population genetics. Sunderland, MA: Sinauer Associates. xiii, 542 p. p.
100. Kimura M, Ohta T (1969) The Average Number of Generations until Fixation of a Mutant Gene in a Finite Population. *Genetics* 61: 763-771.
101. Lindenbach BD (2011) Understanding how hepatitis C virus builds its unctuous home. *Cell Host Microbe* 9: 1-2.
102. Grassmann CW, Isken O, Tautz N, Behrens SE (2001) Genetic analysis of the pestivirus nonstructural coding region: defects in the NS5A unit can be complemented in trans. *J Virol* 75: 7791-7802.
103. Fridell RA, Qiu D, Valera L, Wang C, Rose RE, et al. (2011) Distinct functions of NS5A in hepatitis C virus RNA replication uncovered by studies with the NS5A inhibitor BMS-790052. *J Virol* 85: 7312-7320.
104. Jones DM, Patel AH, Targett-Adams P, McLauchlan J (2009) The hepatitis C virus NS4B protein can trans-complement viral RNA replication and modulates production of infectious virus. *J Virol* 83: 2163-2177.
105. Mottola G, Cardinali G, Ceccacci A, Trozzi C, Bartholomew L, et al. (2002) Hepatitis C virus nonstructural proteins are localized in a modified endoplasmic reticulum of cells expressing viral subgenomic replicons. *Virology* 293: 31-43.
106. Mannova P, Fang R, Wang H, Deng B, McIntosh MW, et al. (2006) Modification of host lipid raft proteome upon hepatitis C virus replication. *Mol Cell Proteomics* 5: 2319-2325.
107. Gao L, Aizaki H, He JW, Lai MM (2004) Interactions between viral nonstructural proteins and host protein hVAP-33 mediate the formation of hepatitis C virus RNA replication complex on lipid raft. *J Virol* 78: 3480-3488.
108. Aizaki H, Lee KJ, Sung VM, Ishiko H, Lai MM (2004) Characterization of the hepatitis C virus RNA replication complex associated with lipid rafts. *Virology* 324: 450-461.
109. Shi ST, Lee KJ, Aizaki H, Hwang SB, Lai MM (2003) Hepatitis C virus RNA replication occurs on a detergent-resistant membrane that cofractionates with caveolin-2. *J Virol* 77: 4160-4168.
110. Heng YW, Koh CG (2010) Actin cytoskeleton dynamics and the cell division cycle. *Int J Biochem Cell Biol* 42: 1622-1633.
111. Bost AG, Venable D, Liu L, Heinz BA (2003) Cytoskeletal requirements for hepatitis C virus (HCV) RNA synthesis in the HCV replicon cell culture system. *J Virol* 77: 4401-4408.
112. Lai CK, Jeng KS, Machida K, Lai MM (2008) Association of hepatitis C virus replication complexes with microtubules and actin filaments is dependent on the interaction of NS3 and NS5A. *J Virol* 82: 8838-8848.

113. Legrand-Abrevanel F, Claudinon J, Nicot F, Dubois M, Chapuy-Regaud S, et al. (2007) New natural intergenotypic (2/5) recombinant of hepatitis C virus. *J Virol* 81: 4357-4362.
114. Ramirez S, Perez-del-Pulgar S, Carrion JA, Coto-Llerena M, Mensa L, et al. (2010) Hepatitis C virus superinfection of liver grafts: a detailed analysis of early exclusion of non-dominant virus strains. *J Gen Virol* 91: 1183-1188.
115. Nelson HB, Tang H (2006) Effect of cell growth on hepatitis C virus (HCV) replication and a mechanism of cell confluence-based inhibition of HCV RNA and protein expression. *J Virol* 80: 1181-1190.
116. Scholle F, Li K, Bodola F, Ikeda M, Luxon BA, et al. (2004) Virus-host cell interactions during hepatitis C virus RNA replication: impact of polyprotein expression on the cellular transcriptome and cell cycle association with viral RNA synthesis. *J Virol* 78: 1513-1524.
117. Kronenberger B, Ruster B, Lee JH, Sarrazin C, Roth WK, et al. (2000) Hepatocellular proliferation in patients with chronic hepatitis C and persistently normal or abnormal aminotransferase levels. *J Hepatol* 33: 640-647.
118. Wilfredo Canchis P, Gonzalez SA, Isabel Fiel M, Chiriboga L, Yee H, et al. (2004) Hepatocyte proliferation in chronic hepatitis C: correlation with degree of liver disease and serum alpha-fetoprotein. *Liver Int* 24: 198-203.
119. Levrero M (2006) Viral hepatitis and liver cancer: the case of hepatitis C. *Oncogene* 25: 3834-3847.
120. Kung JW, Currie IS, Forbes SJ, Ross JA (2010) Liver development, regeneration, and carcinogenesis. *J Biomed Biotechnol* 2010: 984248.
121. Sarfraz S, Hamid S, Ali S, Jafri W, Siddiqui AA (2009) Modulations of cell cycle checkpoints during HCV associated disease. *BMC Infect Dis* 9: 125.
122. Lake-Bakaar G, Mazzocchi V, Ruffini L (2002) Digital image analysis of the distribution of proliferating cell nuclear antigen in hepatitis C virus-related chronic hepatitis, cirrhosis, and hepatocellular carcinoma. *Dig Dis Sci* 47: 1644-1648.
123. Farinati F, Cardin R, D'Errico A, De Maria N, Naccarato R, et al. (1996) Hepatocyte proliferative activity in chronic liver damage as assessed by the monoclonal antibody MIB1 Ki67 in archival material: the role of etiology, disease activity, iron, and lipid peroxidation. *Hepatology* 23: 1468-1475.
124. Freeman A, Hamid S, Morris L, Vowler S, Rushbrook S, et al. (2003) Improved detection of hepatocyte proliferation using antibody to the pre-replication complex: an association with hepatic fibrosis and viral replication in chronic hepatitis C virus infection. *J Viral Hepat* 10: 345-350.
125. Sangfelt O, Erickson S, Castro J, Heiden T, Gustafsson A, et al. (1999) Molecular mechanisms underlying interferon-alpha-induced G0/G1 arrest: CKI-mediated regulation of G1 Cdk-complexes and activation of pocket proteins. *Oncogene* 18: 2798-2810.
126. Matsuoka M, Tani K, Asano S (1998) Interferon-alpha-induced G1 phase arrest through up-regulated expression of CDK inhibitors, p19Ink4D and p21Cip1 in mouse macrophages. *Oncogene* 16: 2075-2086.

127. Hoover DM, Lubkowski J (2002) DNAWorks: an automated method for designing oligonucleotides for PCR-based gene synthesis. *Nucleic Acids Res* 30: e43.
128. Naldini L, Blomer U, Gallay P, Ory D, Mulligan R, et al. (1996) In vivo gene delivery and stable transduction of nondividing cells by a lentiviral vector. *Science* 272: 263-267.
129. Parsley TB, Chen B, Geletka LM, Nuss DL (2002) Differential modulation of cellular signaling pathways by mild and severe hypovirus strains. *Eukaryot Cell* 1: 401-413.
130. Reiter J, Perez-Vilaro G, Scheller N, Mina LB, Diez J, et al. (2011) Hepatitis C virus RNA recombination in cell culture. *J Hepatol* 55: 777-783.


## Appendix D. Publishing Release

### **Publishing Agreement**

*It is the policy of the University to encourage the distribution of all theses, dissertations, and manuscripts. Copies of all UCSF theses, dissertations, and manuscripts will be routed to the library via the Graduate Division. The library will make all theses, dissertations, and manuscripts accessible to the public and will preserve these to the best of their abilities, in perpetuity.*

### **Please sign the following statement:**

*I hereby grant permission to the Graduate Division of the University of California, San Francisco to release copies of my thesis, dissertation, or manuscript to the Campus Library to provide access and preservation, in whole or in part, in perpetuity.*

  
 \_\_\_\_\_  
 Author Signature

4/21/13  
 \_\_\_\_\_  
 Date